



GEORG-AUGUST-UNIVERSITÄT  
GÖTTINGEN

**AntisenseRNA mediated gene regulation via double  
stranded RNA formation**

**Dissertation**

for the award of the degree  
“Doctor rerum naturalium” (Dr.rer.nat.)  
of the Georg-August-Universität Göttingen

within the doctoral program „Biology”  
of the Georg-August University School of Science (GAUSS)

submitted by

**Cesur Ivo Coban**

from Berlin  
Göttingen, 2022

## **Thesis Committee**

Prof. Dr. Heike Krebber  
Molecular Genetics, Institute for Microbiology and Genetics  
Georg-August Universität Göttingen

Prof. Dr. Jörg Großhans  
Developmental Genetics, Department of Biology  
Phillips-Universität Marburg

Prof. Dr. Ralf Ficner  
Molecular Structural Biology, Institute for Microbiology and genetics  
Georg-August Universität Göttingen

## **Members of the examination board**

Reviewer: Prof. Dr. Heike Krebber  
Molecular Genetics, Institute for Microbiology and Genetics  
Georg-August Universität Göttingen

2<sup>nd</sup> Reviewer: Prof. Dr. Jörg Großhans  
Developmental Genetics, Department of Biology  
Phillips-Universität Marburg

3<sup>rd</sup> reviewer: Prof. Dr. Ralf Ficner  
Molecular Structural Biology, Institute for Microbiology and Genetics  
Georg-August Universität Göttingen

Further members of the Examination Board:

Prof. Dr. Ralph Kehlenbach  
Molecular Biology, University Medical Center Göttingen  
Georg-August-Universität Göttingen

Prof. Dr. Kai Heimel  
Molecular Microbiology and Genetics; Institute for Microbiology and Genetics  
Georg-August-Universität Göttingen

PD Dr. Wilfried Kramer  
Molecular Genetics, Institute for Microbiology and Genetics  
Georg-August Universität Göttingen

Date of the oral examination: 01.03.2022

## **Affidavit**

I hereby declare that this doctoral thesis entitled “AntisenseRNA mediated gene regulation via double stranded RNA formation” has been written independently with no other sources and aids than quoted.

Göttingen, January 2022

---

Cesur Ivo Coban

# Table of contents

<b>1. Abstract .....</b>	<b>1</b>
<b>2. Introduction .....</b>	<b>2</b>
2.1 Nuclear mRNA maturation and RNP assembling .....	3
2.2 RNA transport .....	5
2.3 Cytoplasmic RNA surveillance and translation .....	7
2.4 The classification of lncRNAs .....	8
2.5 Additional classification of lncRNAs in yeast.....	8
2.6 lncRNAs in higher eukaryotes .....	11
2.7 The functionality of lncRNAs.....	12
2.8 asRNAs .....	14
2.8.1 <i>asRNAs repress basal transcription of sense genes under non-inducing conditions</i> .....	14
2.8.2 <i>asRNAs can form double stranded (ds)RNA with their mRNA counterpart to carry             out posttranscriptional functions.....</i>	15
2.9 Gene expression changes in adaption and stress response.....	16
2.9.1 <i>Adaption to nutrient availability.....</i>	16
2.9.2 <i>Osmotic stress response.....</i>	17
2.9.3 <i>Iron homeostasis.....</i>	18
2.10 Aim of the Study .....	20
<b>3. Material and Methods.....</b>	<b>21</b>
3.1 Material.....	21
3.2 Cultivation .....	28
3.2.1 <i>Media and plates .....</i>	28
3.2.2 <i>Cultivation of S. cerevisiae .....</i>	29
3.3 DNA Cloning.....	30
3.3.1 <i>Polymerase Chain Reaction (PCR) .....</i>	30

3.3.2	<i>Agarose gel electrophoresis</i> .....	31
3.3.3	<i>DNA extraction from agarose gels</i> .....	32
3.3.4	<i>Restriction Free (RF-)Cloning</i> .....	32
3.3.5	<i>Gibson assembly</i> .....	32
3.3.6	<i>Transformation of electro competent E. coli</i> .....	33
3.3.7	<i>Heat shock transformation of competent E. coli</i> .....	33
3.3.8	<i>Sequencing</i> .....	33
3.4	<i>Cell biological methods</i> .....	33
3.4.1	<i>Creation of the haploid dbp2Δ strain</i> .....	33
3.4.2	<i>Lithium acetate transformation of S. cerevisiae</i> .....	34
3.4.3	<i>Drop dilution analysis</i> .....	35
3.4.4	<i>Fe<sup>2+</sup> measurement by BPS absorption</i> .....	35
3.5	<i>Biochemical methods</i> .....	36
3.5.1	<i>J2-RNA co-immunoprecipitation experiments</i> .....	36
3.5.2	<i>Cytoplasmic fractionation</i> .....	37
3.5.3	<i>Export release assay</i> .....	37
3.5.4	<i>RNA-Isolation using Trizol</i> .....	38
3.5.5	<i>RNA-Isolation using NucleoSpin® RNA from Machery-Nagel</i> .....	38
3.5.6	<i>Strand specific cDNA synthesis</i> .....	39
3.5.7	<i>qPCR</i> .....	39
3.5.8	<i>SDS-PAGE</i> .....	40
3.5.9	<i>Western blot analysis</i> .....	40
3.6	<i>In vitro binding studies</i> .....	41
3.6.1	<i>Protein isolation and purification</i> .....	41
3.6.2	<i>Electrophoretic mobility shift assay (EMSA)</i> .....	41
3.7	<i>Microscopic studies</i> .....	42
3.7.1	<i>Fluorescent in situ hybridization experiments (FISH)</i> .....	42
3.7.2	<i>Immunofluorescence (IF)</i> .....	43
3.7.3	<i>GFP-microscopy</i> .....	43
3.8	<i>Bioinformatics</i> .....	44
3.8.1	<i>RNA-sequencing</i> .....	44
3.8.2	<i>Accession number</i> .....	44
3.8.3	<i>Gene ontology analysis</i> .....	45
3.8.4	<i>Quantification</i> .....	45

<b>4. Results .....</b>	<b>46</b>
4.1 The loss of <i>NPL3</i> leads to alterations in the cellular RNA composition of all classes of RNAs based on their type, abundance, and half-life.....	46
4.2 Cytoplasmic fractionation RNA-seq analysis identifies properties of RNAs influencing their nucleo-cytoplasmic distribution .....	48
4.2.1 <i>Cytoplasmic fractionation experiment and subsequent RNA-seq analysis unravels the nucleo-cytoplasmic distribution of RNAs .....</i>	48
4.2.2 <i>dsRNAs are enriched in the cytoplasmic fraction.....</i>	50
4.2.3 <i>The cytoplasmic distribution of dsRNA is asRNA mediated.....</i>	51
4.2.4 <i>A rather nuclear distribution of mRNAs is caused by a reduced export rate and affects highly expressed genes.....</i>	52
4.3 dsRNA are preferentially exported mediated by Mex67 .....	54
4.3.1 <i>The nuclear export block in mex67-5 xpo1-1 retains ssRNAs and dsRNA .....</i>	54
4.3.2 <i>dsRNAs are exported through Mex67 and Xpo1 and are detached during translation.....</i>	55
4.3.3 <i>dsRNAs are preferentially exported compared to ssRNA.....</i>	57
4.3.4 <i>Mex67 preferentially binds to dsRNA which possess a higher capacity for Mex67 attachment compared to ssRNA.....</i>	59
4.4 dsRNA formation is essential for cells particularly during adaptation to environmental change like stress conditions .....	61
4.4.1 <i>dsRNAs are essential for cells.....</i>	61
4.4.2 <i>Stress associated SRATs can form dsRNA structures leading to the cytoplasmic enrichment of their mRNA .....</i>	62
4.4.3 <i>The general asRNA level is increased under stress conditions leading to more dsRNA formation.....</i>	64
4.4.4 <i>dsRNA formation is advantageous for stress response.....</i>	65
4.5 The helicase Dbp2 plays a key role in dsRNA formation.....	66
4.5.1 <i>Dbp2 interacts with dsRNA and its loss leads to reduced dsRNA amounts.....</i>	66
4.5.2 <i>The asRNA mediated preferential export is lost in the dbp2Δ mutant.....</i>	67
4.6 asRNAs can have multiple conditional functions on different levels of gene expression .....	69
4.6.1 <i>The stability of the FRE5 mRNA relies on asRNA SUT802.....</i>	69
4.6.2 <i>SUT802 and FRE5 levels depend on iron .....</i>	70
4.6.3 <i>SUT802 prevents FRE5 expression in the presence of high iron levels .....</i>	71
4.6.4 <i>SUT802 recruits Hek2 to prevent FRE5 translation .....</i>	72

<b>5. Discussion .....</b>	<b>74</b>
5.1 Model of the preferential mRNA export.....	74
5.2 The limiting amounts of RBPs represent an evolutionary concept on the molecular level.....	75
5.3 The function of asRNA depends on the transcription state of the sense gene .....	76
5.4 asRNAs are localized to the cytoplasm .....	77
5.5 The relevance and commonness of dsRNA formation.....	79
5.6 dsRNA formation and biogenesis.....	80
5.7 Hybridization of dsRNA in the nucleus is accomplished by Dbp2 and Yra1 .....	81
5.8 Mex67-Mtr2 binding mediates the preferential export .....	82
5.9 Export is the key factor for the nucleo-cytoplasmic distribution and half-life of RNAs	83
5.10 A longer cytoplasmic lifespan of dsRNAs could be implicated .....	84
5.11 dsRNAs are involved in stress response.....	85
5.12 dsRNA formation and preferential expression could be a reason for cancer .....	87
5.13 <i>SUT802</i> inhibits <i>FRE5</i> translation under high iron levels and thus highlights the multifunctional properties of asRNAs.....	88
<b>6. Concluding remarks.....</b>	<b>90</b>
<b>7. References .....</b>	<b>91</b>

## Table of figures

Figure 1 lncRNA classification by their genomic position..	9
Figure 2 Processing of lncRNAs compared to mRNAs.....	10
Figure 3 lncRNAs carry out diverse functions (adapted from Villegas et al., 2016).....	13
Figure 4 Reductive high affinity uptake of iron (adapted from Judith Weyergraf).....	19
Figure 5 <i>npl3Δ</i> RNA-seq shows different alterations in the RNA level.....	47
Figure 6 Cytoplasmic fractionation followed by RNA-seq shows the nucleo-cytoplasmic distribution of RNAs (together with Anna Greta Hirsch and Orr Shomroni). ....	49
Figure 7 Gene ontology (GO-)analysis of cytoplasmic fractionation RNA-seq shows terms of RNAs enriched or decreased in the cytoplasmic fraction. ....	50
Figure 8 dsRNAs are enriched in the cytoplasmic fraction. ....	51
Figure 9 Overexpression of <i>asPHO85</i> ( <i>SUT412</i> ) leads to a cytoplasmic shift of the corresponding mRNA <i>PHO85</i> .....	52
Figure 10 The nucleo-cytoplasmic distribution correlates with the half-life, the level of expression and the length of transcripts. ....	53
Figure 11 In the double mutant <i>mex67-5 xpo1-1</i> most RNAs are retained in the nucleus.....	55
Figure 12 J2-immunoprecipitation validates dsRNA targets and shows their accumulation upon nuclear export block. ....	56
Figure 13 dsRNAs are formed in the nucleus and detached at the ribosomes.....	57
Figure 14 dsRNAs reach ribosomes first after export release compared to ssRNA targets....	58
Figure 15 Mex67 preferentially binds to dsRNA and dsRNA shows a higher capacity for Mex67 compared to ssRNA. ....	60
Figure 16 Nuclear RNaseIII expression is toxic to cells. ....	61
Figure 17 Higher concentration of SRATs in <i>set2Δ</i> form dsRNA with their mRNA counterpart and are exported. ....	63
Figure 18 Increased levels of <i>asSEG2</i> in <i>set2Δ</i> leads to a cytoplasmic shift of its mRNA <i>SEG2</i> . ....	64
Figure 19 asRNA and dsRNA take part in stress response. ....	65
Figure 20 Restriction of dsRNAs during stress leads to a growth defect of cells. ....	66
Figure 21 Dbp2 is involved in dsRNA hybridization. ....	67
Figure 22 Loss of <i>DBP2</i> negates the preferential export effect of <i>PHO85</i> mRNA after <i>asPHO85</i> ( <i>SUT412</i> ) overexpression. ....	68
Figure 23 <i>FRE5</i> mRNA stability depends on its asRNA <i>SUT802</i> (together with Judith Aylin Weyergraf). ....	69
Figure 24 <i>FRE5</i> and <i>SUT802</i> levels anticorrelate at different iron concentrations (together with Judith Aylin Weyergraf). ....	70
Figure 25 <i>FRE5</i> overexpression is toxic under high Fe <sup>3+</sup> due to cellular accumulation of Fe <sup>2+</sup> . ....	71



Figure 26 Hek2 binds to <i>SUT802</i> .....	73
Figure 27 Model for the preferential gene expression of dsRNAs.....	74
Figure 28 ssRNAs and dsRNAs spend different amounts of time in the nucleus and in the cytoplasm.....	85
Figure 29 <i>SUT802</i> prevents translation of its mRNA <i>FRE5</i> under high iron levels. ....	89

## 1. Abstract

The flow of genetic information in eukaryotic cells is established through transcription from the nuclear DNA into messenger (m)RNA, which travels into the cytoplasm for translation into proteins, the functional units of cells. With the discovery of the manifold existence of long non-coding (lnc)RNAs, which amounts exceed the ones of mRNAs, the established dogma (DNA:RNA:Protein) has been challenged. Still, the general functionality of most lncRNAs is debated, and mostly individual functions have been unraveled so far. Especially, antisense (as)RNAs exist in a high number. Although the majority of asRNAs is degraded by translation associated nonsense-mediated decay and the cytoplasmic exonuclease Xrn1, their attributed functions in *S. cerevisiae* are so far restricted to the nucleus and transcriptional regulation, leaving their journey into the cytoplasm out of sight. Here, we identify a new mechanism, in which asRNAs accelerate the export of their mRNA counterparts by forming double stranded RNAs (dsRNA). dsRNAs have a higher affinity and capacity for the nuclear export heterodimer Mex67-Mtr2 than single stranded mRNAs, which results in a faster export. This preferential export represents a major and essential advantage for cells to adapt to new necessities through the rapid establishment of new gene expression programs. Furthermore, we unravel a specific function of the asRNA *SUT802* in translation inhibition of its corresponding mRNA *FRE5*. *SUT802* recruits the translational repressor Hek2 to the *SUT802-FRE5* dsRNA under repressing conditions. Thereby, it enables the possibility of even tighter regulation of gene expression in iron homeostasis. Together, these unraveled novel mechanisms highlight the multifunctionality of asRNA in modulating mRNA gene expression.

## 2. Introduction

Eukaryotic cells are divided mainly into a nucleus and the cytoplasm, the latter of which contains several organelles such as mitochondria. The separation of the cell into different compartments is an essential element of complex life. The genome of an organism is located in the nucleus in the form of DNA. It is organized in genes, that can be transcribed into RNA. In the case of protein coding genes, the resulting messenger (m)RNAs transport the genetic information of the DNA to the ribosomes, where they are translated into proteins. The genome of higher eukaryotes consists only of a small number of protein coding genes. In human this is estimated to be only ~2% of the DNA. For a long time, only protein coding genes and genes coding for housekeeping RNAs were known to be transcribed from the DNA. Therefore, the remaining DNA and thus most parts were argued to be “junk DNA”, with no functional information (Comings, 1972; Hüttenhofer et al., 2005; Ohno, 1972). However, first discoveries of RNAs, which are involved in chromatin regulation have demonstrated the existence of unknown long non-coding (lnc)RNAs (Brown et al., 1991; Wutz et al., 2002). With the progress in sequencing methods, next generation sequencing has finally unraveled the manifold existence of unknown RNA classes. It is now broadly understood that the genome of eukaryotes is widely transcribed. This results in a variety of non-coding RNAs, which do not possess any protein coding potential (Carninci et al., 2005; David et al., 2006; Li et al., 2006; Stolc et al., 2004). While mRNAs harbor an open reading frame and are thereby translated into proteins, ncRNAs rather have diverse functions. They are divided into different groups by size and function. Regarding their size, they are divided into small non-coding RNAs (sncRNA) and long non-coding RNAs (lncRNA). sncRNAs are shorter than 200 nucleotides (nts) and include small nuclear RNAs (snRNA) and small nucleolar RNAs (snoRNA), which participate in RNA processing (Dupuis-Sandoval et al., 2015; Wahl et al., 2009). Additional sncRNAs are transfer RNAs (tRNA) and ribosomal RNAs (rRNA), required for translation (Fernández-Pevida et al., 2015). lncRNAs are defined by being longer than 200 nts (Kapranov et al., 2007). This broad definition entails, that lncRNAs comprise a highly diverse heterogeneous class of RNAs with differences in biogenesis, localization, and function (reviewed in Statello et al., 2020). With increasing insights, lncRNAs were found to be involved in many regulatory mechanisms, making them a dignified study object. As they are factors in neural development, cell division and many more cellular processes, the dysfunctionality of lncRNAs is responsible for

neurodegenerative diseases and cancer (Arun et al., 2016; Grelet et al., 2017; Huarte et al., 2010; Kim et al., 2015; Wei et al., 2018).

## 2.1 Nuclear mRNA maturation and RNP assembly

In their lifetime, RNAs undergo certain steps of processing and remodeling, carried out by different RNA binding proteins (RBPs), that form ribonucleotide protein complexes (RNPs) with their bound RNAs. RBPs do not only process their RNA targets, but also control the RNA quality and rightful processing, in the end leading to the stabilization or degradation of RNAs. Current research suggests, that lncRNAs are similarly processed as mRNAs. They are capped and polyadenylated and mRNP associated proteins have been shown to also interact with lncRNAs (Tuck & Tollervey, 2013). The binding of RBPs in a fixed order ensures the integrity of mRNAs, which eventually leads to nuclear export (Figure 2).

In *S. cerevisiae*, mRNAs and lncRNAs are transcribed by RNA polymerase II (RNAP II) (Cramer et al., 2008). It consists of 12 proteins, of which Rbp1 comprises its catalytic activity. Further, RNAP II mediates co-transcriptional loading of factors involved in mRNA maturation through its C-terminal domain (CTD). Thereby, the order of processing steps is regulated by the phosphorylation state of the CTD (Hsin & Manley, 2012). First, mRNAs are capped with an N<sup>7</sup>-methylated guanosine at their 5' ends. It is linked through a triphosphate linker by the triphosphatase Cet1, the guanyl transferase Ceg1 and the methyltransferase Abd1 (Martinez-Rucobo et al., 2015). The cap stabilizes RNAs and prevents their 5' degradation (Jiao et al., 2010; Schwer et al., 1998). It is further covered by the cap binding complex (CBC), which consists of Cbp20 and Cbp80. Early during transcription, Npl3 and Dbp2 are loaded onto the RNA. Npl3 interacts with the cap binding complex and probably controls proper formation of the cap and thereby stabilizes RNAs (Baejen et al., 2014; Shen et al., 2000). It is a highly abundant RBP and further involved in transcription elongation, splicing and 3' end formation (Bucheli & Buratowski, 2005; Kress et al., 2008; Wong et al., 2010). The deletion of Npl3 causes 3' elongated transcripts resulting from a prominent termination readthrough phenotype (Holmes et al., 2015). Consequentially, Npl3 is found on all classes of RNAs (Windgassen et al., 2004). Dbp2 is a DEAD box helicase that resolves intramolecular dsRNA structures. It is suggested to linearize the transcribed RNA to support loading of further RBPs such as Yra1. While interacting with Yra1, Dbp2 is repressed in its helicase function and regains its high affinity to dsRNA (Ma et al., 2013, 2016).

## INTRODUCTION

During transcription elongation, intron containing RNAs are spliced by the spliceosome, which removes the intron and ligates the resulting ends of exons. In higher eukaryotes splicing of mRNAs and lncRNAs is omnipresent. *S. cerevisiae*, on the other hand, possesses only few intron containing mRNAs and so far, no intron containing lncRNA have described in yeast (Davis et al., 2000; Spingola et al., 1999). Ongoing transcription further leads to the recruitment of the THO complex, which includes Tho2, Thp2, Mft1 and Hpr1. Together with Yra1 and Sub2, the THO complex forms the TREX complex. This complex seems to be a requirement for RNA export, as the deletion of *YRA1*, *SUB2* and *HPR1* leads to the accumulation of polyadenylated RNAs in the nucleus (Jensen, Boulay, et al., 2001; Jensen, Patricio, et al., 2001; Zenklusen et al., 2002). Thus, the TREX-complex connects mRNA processing with export. In addition, the SR-rich proteins and quality control factors Gbp2 and Hrb1 are found on mRNAs interacting with the THO/TREX complex (Häcker & Krebber, 2004; Hurt et al., 2004; Martínez-Lumbreras et al., 2016). Gbp2 and Hrb1 control efficient and correct splicing of RNAs, as their deletion leads to leakage of unspliced RNAs into the cytoplasm (Hackmann et al., 2014). Like Npl3, Gbp2 is found on diverse classes of RNAs including lncRNAs (Tuck & Tollervey, 2013).

Transcription termination occurs once a poly(A) termination signal is reached. The further 3' end processing of most mRNAs and lncRNAs depends on the cleavage factor (CF)/cleavage and polyadenylation factor (CPF). The RNA gets cleaved, and the complex progressively adds a poly(A) to the 3' end of the premature RNA, which contributes to its stability (Porrúa & Libri, 2015; van Dijk et al., 2011). The poly(A) tail is an important hallmark of mRNAs and lncRNAs and plays a role in processing, export, and translation (Goss & Kleiman, 2013; Lemay et al., 2010). There are two essential poly(A)-binding proteins in *S. cerevisiae* that maintain the integrity of the poly(A) tail. Nab2 is mostly localized to the nucleus and Pab1 is distributed within the cytoplasm. Interestingly, both shuttle between nucleus and cytoplasm and their functions overlap (Brune et al., 2005). After loss of *NAB2*, nuclear RNA gets rapidly degraded (Schmid et al., 2015), elucidating how RBPs protect RNAs from degradation in the nucleus. Strikingly, the additional deletion of *RRP6*, a part of the nuclear exosome, rescues this phenotype (González-Aguilera et al., 2011; Zander et al., 2016). In that case, RNAs are not degraded, although not protected by Nab2, but instead exported and translated into functional proteins.

Npl3 and Nab2 together with Gbp2 and Hrb1 are adapter proteins for the export receptor Mex67, which mediates mRNA export through the nuclear pore complex (NPC) together with Xpo1 (Hackmann et al., 2014; Huang & Steitz, 2005; Tutucci & Stutz, 2011; Wu et al., 2014). The potential to recruit Mex67 gives these RBPs a decisive role in nuclear export. If RNAs are faulty, Mex67 is not recruited, and the RNA is degraded (Porrua & Libri, 2013). Aberrant RNAs are actively marked for degradation. Therefore, the TRAMP complex is recruited, which tags RNAs with a short poly(A) tail at their 3' end and directs them to the nuclear exosome for elimination (Houseley et al., 2006; LaCava et al., 2005).

The TRAMP complex consists of the poly(A) polymerase Trf4/5, Air1/Air2, and Mtr4. The TRAMP5 (Trf5, Air1, Mtr4) is primarily involved in rRNA processing and the TRAMP4 (Tr4, Air2, Mtr4) in quality control and degradation of aberrant RNAs and mRNA maturation byproducts like spliced out introns (Falk et al., 2014). Mtr4 is a DExH helicase and unwinds secondary RNA structures, while the poly(A) polymerases add a short poly(A)-tail to the RNA, which serves for the initial binding of Rrp6 and the exosome (Callahan & Butler, 2010). In *S. cerevisiae*, the exosome complex comprises two active exonuclease subunits, Rrp6 and Dis3 (Chlebowski et al., 2013). Rrp6 initiates degradation of the RNA and incorporates it into the center of the exosome, where Dis3 continues to degrade the RNA.

Recent research suggests that cells maintain a steady cellular RNA amount by connecting transcription with decay (Das et al., 2017). During cellular transition, the alteration of gene expression leads to the transcription of new sets of genes. Meanwhile, the simultaneous degradation of previous RNAs maintains RNA homeostasis and accelerates the transition. The opposing roles of nuclear RBPs in producing stable mRNPs or mediating degradation is thus common and not restricted to faulty RNAs. Consequently, the limiting amounts of RBPs are crucial for maintaining RNA homeostasis. (Haimovich et al., 2013; Sun et al., 2013) Nuclear-retained RNA is generally turned over, which is evidenced by the highly unstable nature of pervasive transcripts in both yeast and human nuclei (Preker et al., 2008; Wyers et al., 2005). Nuclear mRNA decay is countered by nuclear export, which in turn relies on efficient mRNP assembly.

## **2.2 RNA transport**

Transcription in the nucleus and translation in the cytoplasm are separated by the nuclear envelope. Therefore, the transport of RNPs is channeled through the nuclear pore complex

## INTRODUCTION

(NPC), that connects the nucleoplasm with the cytoplasm (Wente & Rout, 2010). The export of mRNAs is coupled to their upstream processing steps. As soon as all processing steps are successfully accomplished, the RNP is bound by export receptors, which interact with the nucleoporins (NUP) of the NPC (Niño et al., 2013). Due to their size, sufficient coverage with export receptors is essential for the export of mRNAs and lncRNAs (Soheilypour & Mofrad, 2018). In *S. cerevisiae*, these export receptors are the heterodimer Mex67-Mtr2 (NXF1-p15 in human) and Xpo1 (Crm1 in human) (Segref et al., 1997; Wu et al., 2014). Although Mex67-Mtr2 contains an RNA binding motif (RBM), it binds to adapter proteins instead of RNAs directly (Zander et al., 2016). In that way, the adapter and quality control factors ensure the export of proper mRNPs. Only under heat stress conditions has Mex67 been shown to directly bind heat shock response mRNAs for selective export, as they are not quality controlled within the nucleus (Zander et al., 2016). Xpo1, on the other hand, binds to the CBC (Becker et al., 2019).

A mature nuclear mRNP moves in a Brownian motion until it randomly finds an NPC (Grünwald & Singer, 2010). Even if the transcription site is localized at the nuclear envelope, mRNPs disperse in the entire nucleoplasm before export (Vargas et al., 2005). While nuclear diffusion takes up to several minutes, the export process itself, which consists of docking, transport and release, only takes 180 +/- 10 ms (Grünwald & Singer, 2010).

Along with the export, mRNPs are further remodeled. Some factors are removed prior to export, like Yra1 and Dbp2. Mex67 and Nab2, on the other hand, disassemble on the cytoplasmic side of the NPC. Here, the interaction with the NUP Gle1 activates the helicase Dbp5, which leads to the release of the mRNP into the cytoplasm and the relocation of the shuttling proteins back into the nucleus (Hodge et al., 1999; Lund & Guthrie, 2005; Tran et al., 2007). The successive Mex67 removal enables the directionality of nucleo-cytoplasmic transport and exposes RNA binding sites for cytoplasmic regulation factors, which for instance are involved in translation (Gromadzka et al., 2016).

Upon arrival in the cytoplasm, mRNPs can undergo further transportation steps. This is common for mRNAs of membrane associated proteins, which are directly translated at the membrane to be co-translationally incorporated. In contrast to the nuclear movement, the cytoplasmic transport can be directional. Therefore, cytoplasmic mRNPs are bound by motor proteins that mediate cytoplasmic transport via actin fibers (Hocine et al., 2010). *ASH1* mRNA, for instance, which encodes a mating type switch preventing protein, is bound by the She-

complex that recruits Myo4 to the RNP. Myo4 subsequently contacts the actin filaments for movement. To ensure translation only at the end of cytoplasmic transport, Hek2, which is part of the She-complex, inhibits binding of the small ribosomal subunit. Thus, mRNAs are only translated at the place of function of their encoding protein (R. M. Long et al., 2000).

### **2.3 Cytoplasmic RNA surveillance and translation**

Modulation of gene expression is continued in the cytoplasm. Previous studies have shown that nuclear and cytoplasmic quality control are connected (Grosse et al., 2021), and although they may escape nuclear control, exported faulty RNAs can still be recognized in the cytoplasm, resulting in their subsequent degradation. This additional layer prevents the production of faulty and thus harmful proteins.

Cytoplasmic quality control is tightly associated with translation (Beißel et al., 2019; Grosse et al., 2021). While nuclear surveillance controls correct processing of RNAs regarding capping, polyadenylation and splicing, cytoplasmic surveillance verifies the integrity of the open reading frame (ORF) (Soheilypour & Mofrad, 2018; Tutucci & Stutz, 2011). The ORF of an mRNA is defined by a start and a stop codon. Both can be affected by an altered sequence of the mRNA. If an mRNA has lost its start or stop codon because of changes in its sequence, the transcripts are recognized and eliminated either by the no-go decay (NGD) or no-stop decay (NSG) (Beißel et al., 2020; Lykke-Andersen & Bennett, 2014). Additionally, a faulty sequence can also contain a premature stop codon, which leads to nonsense-mediated decay (NMD). The key player of NMD is Upf1 in association with Upf2 and Upf3 (Dehecq et al., 2018; Maquat & Serin, 2001). There are different possibilities and hypotheses assuming how NMD recognizes a premature stop codon (PTC). In the long 3'UTR model, the distance of the stop codon to the poly(A)<sup>+</sup> tail and the poly(A)<sup>+</sup> associated protein Pab1 identifies a possible PTC (Brojna & Wen, 2009; Kurosaki et al., 2019). Regularly, the interaction of Pab1 and the termination factor eRF3 directs termination of translation and displaces the Upf complex. This interaction is prevented at a PTC due to the long distance of eRF3 to the poly(A)<sup>+</sup> tail bound Pab1. Thus, the Upf complex can form and initiate NMD.

NMD does not only play a role in quality control and degradation of faulty mRNAs but also in gene regulation of natural NMD targets like lncRNAs (Wery et al., 2016). Further, 5-10 % of mRNAs in *S. cerevisiae* are mis-regulated if NMD is disturbed (He et al., 2003). Certain mRNAs possess NMD-targeting features and are only degraded under defined conditions (Kebaara &



Atkin, 2009; Peccarelli et al., 2019b). The degradation of these mRNA targets via NMD seems to be affected by the environmental condition (Murtha et al., 2019; Peccarelli et al., 2016). One example is the *FRE2* mRNA that naturally has a long 3'UTR. *FRE2* is involved in ensuring steady cellular iron levels. Under high iron conditions the *FRE2* mRNA is degraded via NMD, whereas the mRNA is stabilized and translated under low iron conditions (Peccarelli et al., 2019).

#### **2.4 The classification of lncRNAs**

Around 85 % of the *S. cerevisiae* genome is transcribed into RNA (David et al., 2006; Nagalakshmi et al., 2008), the majority being non-coding RNAs. Early statistics from Human GENCODE have suggested that the human genome contains more than 16.000 lncRNA genes, but other more detailed evaluations exceed 100.000 human lncRNAs, which is still considered to be underestimated (Fang et al., 2018; Uszczynska-Ratajczak et al., 2018). However, compared to 20.000 protein coding genes, the amount and diversity of ncRNAs impressively exceeds that of mRNAs in human cells.

Known RNA classes are named by their localization, like snRNAs and snoRNAs, their function, like mRNAs and siRNAs, or their associated complex, like rRNAs and *TLC1*. However, the class of lncRNAs is so far rather classified by their genomic localization. Relative to protein coding genes, lncRNAs are divided into distinct groups (Kung et al., 2013). Intergenic lncRNAs (lincRNA) are transcribed as distinct genes. They do not overlap noticeably with other features of the genome. Sense or intronic lncRNAs, on the other hand, comprise partially sequences of protein coding genes, either of the exon or the intron. Additionally, there are antisense lncRNAs (asRNAs) or natural antisense transcripts (NAT), which are transcribed from the opposite complementary DNA strand of protein coding genes (Figure 1).

#### **2.5 Additional classification of lncRNAs in yeast**

In *S. cerevisiae*, the first identification and evaluation of lncRNAs concentrated on their stability and degradation, hence leading to another possible nomenclature. In that case, parts of several RNA degradation and processing pathways were deleted, followed by RNA-sequencing and analysis.



**Figure 1 lincRNA classification by their genomic position.** lincRNAs that are transcribed between two protein coding genes are called intergenic lincRNA (*lincRNA*; 1.). If a lincRNA overlaps with the intron or exon of a gene in sense orientation, they are either called intronic lincRNA (2.) or sense lincRNA (3.). *asRNAs* are lincRNAs transcribed from the opposite complementary DNA strand of a protein coding gene (4.).

lincRNAs detectable in wild type cells are called stable unannotated transcripts (SUT) (Xu et al., 2009). Transcripts accumulating in the nuclear exosome mutant *rrp6Δ* are referred to as cryptic unstable transcripts (CUT) (Xu et al., 2009), while targets enriched in the deletion mutant of *XRN1*, encoding a cytoplasmic exonuclease, are *Xrn1*-sensitive unstable transcripts (XUT) (van Dijk et al., 2011; Figure 2). Since Rrp6 is a nuclear and *Xrn1* a cytoplasmic nuclease, CUTs are seen as mainly nuclear and XUTs as exported transcripts. The great majority of XUTs are transcribed from the opposite strand of a protein coding gene. Thus, these transcripts are mostly *asRNAs*. Further, there are *Nrd1*-sensitive unterminated transcripts (NUT), *Dcr1*-sensitive unstable transcripts (DUT) and *Set2*-repressed antisense transcripts (SRAT) enriching in the respective mutant strains *nrd1-FRB*, *dcr1Δ* and *set2Δ* (Schulz et al., 2013; Szachnowski et al., 2019; Venkatesh et al., 2016). *Nrd1* is part of the NNS-transcription termination complex (Steinmetz et al., 2001). *Dcr1* is involved in the RNAi system and *Set2* is a methyltransferase acting on histones to influence the chromatin state (Ji, 2008; B. Li et al., 2003). Because lincRNAs can combine several of these features, a distinct classification based on them is not preferable. DUTs, for instance, are still mainly degraded by *Xrn1* and only upon deletion of *XRN1* does the additional deletion of *DCR1* lead to a further accumulation of DUTs (Szachnowski et al., 2019). NUTs are also degraded by the nuclear exosome, therefore they could be assigned to CUTs. Similarly, SRATs are degraded by *Xrn1* and thus could be classified as XUTs (Venkatesh et al., 2016). And yet, SUTs have shown enrichment in *rrp6Δ* and in *xrn1Δ* to an even higher degree than XUTs (Wery et al., 2016).

In some cases, the stability of lincRNAs has been shown to be condition-dependent. The *asRNA* of *PHO84*, for instance, which is degraded by Rrp6, gets stabilized depending on the age of

cells. The stabilization of the asRNA in turn represses *PHO84* expression by mediating H3K18 deacetylation at the *PHO84* promoter through the Hda1/2/3 deacetylase complex (Camblong et al., 2007). How this influences aging of cells is not known but highlights the condition-dependent regulation of the stability of lncRNAs. Thus, the nomenclature of lncRNAs regarding their degradation pathways is questionable as it is variable. However, these studies have begun to reveal distinct processes of lncRNA biogenesis in connection with their cellular fates, localization, and functions. Remarkably, approximately 70% of the 1.781 identified XUTs are NMD sensitive, pointing to the nuclear export and cytoplasmic localization of the majority of XUTs (Wery et al., 2016), suggesting that these transcripts are involved in processes connected to their localization (Figure 2).

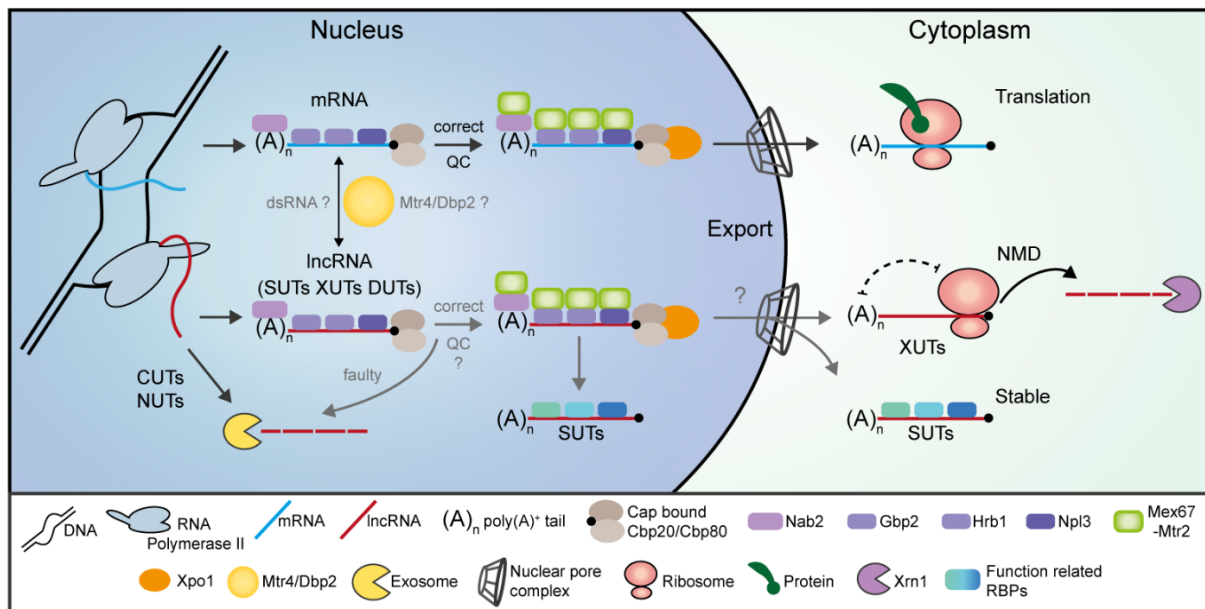


**Figure 2 Processing of lncRNAs compared to mRNAs.** After transcription by RNA polymerase II, mRNAs and lncRNAs are capped and polyadenylated. These processes are controlled by the guard proteins Npl3, Gbp2, Hrb1 and Nab2. Whether lncRNAs are quality controlled like mRNAs is not completely understood. CUTs and NUTs are regarded as unstable transcripts, which are immediately degraded by the exosome after transcription. The possible dsRNA formation of asRNAs and mRNAs is described to be resolved by the nuclear helicases Dbp2 and Mtr4. After correct processing, the quality control factors recruit the export heterodimer Mex67-Mtr2. Together with Xpo1, which is bound to the cap binding complex, Mex67 initiates and mediates the nuclear export of RNAs. Nuclear SUTs are thought to stay in the nucleus to carry out different functions, e.g. by binding specific function related RBPs. After their export, mRNAs are translated. lncRNAs, which do not possess any coding potential, still engage ribosomes. However, after a first round of translation, they are degraded through Xrn1 in the NMD. Therefore, most cytoplasmic lncRNAs are called XUTs. Cytoplasmic SUTs escape cytoplasmic degradation by binding of function related RBPs or factors, that inhibit binding of the small ribosomal subunit.

## 2.6 lncRNAs in higher eukaryotes

In multicellular eukaryotes, functionally identified lncRNAs are either temporally restricted in development or locally to tissues and organs (Jiang et al., 2016). Single cell RNA-seq analysis of neural cells in the larval brain of *Drosophila melanogaster* and the human neocortex has shown a highly specific expression of lncRNAs even between cells of the same tissue (Avalos et al., 2019; Liu et al., 2016). These lncRNAs seem to be key regulators in the fate of neural cells. Their expression level in single cells reaches the ones of mRNAs, challenging the assumption of lncRNAs being generally low expressed, but rather specifically expressed. This may be transferable to other tissues and organs. Compared to mRNAs, lncRNAs are less evolutionary conserved. Thus, they are seen as evolutionary young genes. Interestingly, even conserved lncRNAs in sequence and genetic position can still have differences in function and cellular localization between species. The lincRNA *FAST* exists in human and murine embryonic stem cells. Although the human *hFAST* is localized in the cytoplasm and promotes WNT signaling, which is needed for the pluripotency of stem cells, the processing of the murine *mFast* is repressed leading to a nuclear localization (Guo et al., 2020). The different expression of lncRNAs in development and between tissues and species, indicates their diverse role in establishing the high complexity of multicellular organisms.

Like mRNAs, lncRNAs of higher eukaryotes possess introns, but to a much smaller extent. Thereby, they consequently have fewer exons, which are in turn longer than the ones of mRNAs. On the one hand it was shown that introns of lncRNAs are less efficiently spliced, which to some extent leads to nuclear retention (Melé et al., 2017; Zuckerman & Ulitsky, 2019). On the other hand, RNAs with fewer exons like lncRNAs have been shown to preferentially use the export pathway of the nuclear RNA export receptor factor 1 (NXF1; *MEX67* in yeast). Deletion of NFX1 in human breast cancer MCF7 cells affects the localization of lncRNAs far more than that of mRNAs by shifting them to a more nuclear localization (Zuckerman et al., 2020). However, the deletion of members of the TREX complex affects the nucleo-cytoplasmic localization of both mRNAs and lncRNAs to a similar extent. This already indicates that lncRNAs are exported from the nucleus in human cells and is supported by other studies (Carlevaro-Fita et al., 2016; van Heesch et al., 2014). In the human leukemia cell line K562 ~54 % of the 637 filtered lncRNA transcripts were found to be cytoplasmic. Approximately 70 % were associated with ribosomes and about 30 % were found in the free

cytoplasmic fraction (Carlevaro-Fita et al., 2016). This shows that a huge part of stable asRNAs and lncRNAs are exported in human cells.

## 2.7 The functionality of lncRNAs

Although it has been shown that lncRNAs are processed and matured like mRNAs, the number of functional lncRNAs is still debated. The rapid production and degradation of lncRNAs was argued to be a sign for their non-functionality (Struhl, 2007). However, these attributes rather seem to be well suited for fine-tuning of gene expression, without the need of additional translation (Xu et al., 2011). This especially meets the need of cells that must adapt to changing requirements. The number of documentations about the important cellular functions of lncRNAs is growing, still, evidence is lacking to support the functionality of most lncRNAs. (Villegas et al., 2016; Fig. 3). Known lncRNAs play key roles in gene regulation at different points of expression, both negatively and positively. Thus, they are connected to a variety of cellular processes. They modulate transcription by interference with polymerase elongation and chromatin modification or alternative splicing, stability, and translation, the latter of which occurs through accelerating or inhibiting recruitment of ribosomes (Statello et al., 2020) (Figure 3). All lncRNAs have in common, that they mainly act through their ability to establish interactions with proteins and nucleic acids. Thereby, they function as scaffold RNAs, that bring together certain factors.

The first identified lncRNAs have been shown to act in chromatin remodeling and transcription repression (Quinodoz & Guttman, 2014). The well-studied lncRNA *XIST* was found to be the key regulator of X-chromosome inactivation (Brown et al., 1991; Wutz et al., 2002). By recruiting the polycomb repressive complex along the in the future inactivated X-chromosome, *XIST* enriches repressive chromatin modifications at the chromosome (Colognori et al., 2019; Pintacuda et al., 2017). In *S. cerevisiae*, the *GAL10* asRNA prevents leakage of the *GAL* cluster under growth on glucose by interfering with transcription in sense direction (Geisler et al., 2012). Furthermore, lncRNAs have nuclear functions beyond transcription regulation. The originally cancer associated lncRNA metastasis-associated lung adenocarcinoma transcript 1 (*MALAT1*) influences the distribution of SR-proteins in the nucleus by regulating their phosphorylation levels (Tripathi et al., 2010). Thus, by regulating SR-protein modifications, *MALAT1* has been shown to affect alternative splicing and possibly nuclear export or NMD (J. C. Long & Cáceres, 2009; Stamm, 2008).

Cytoplasmic functions of lncRNAs are regulating stability and translation of mRNAs and have so far only been identified in higher eukaryotes. The stability modulation is based on interfering with miRNAs. So called competing endogenous RNAs (ceRNAs) can protect mRNAs by acting as a sponge for miRNAs, which would also target the mRNA. Thereby, ceRNAs increase the stability of mRNAs (Cheng & Lin, 2013; Denzler et al., 2014). The antisense transcript of *BACE1* has a similar stabilization effect by masking the miRNA binding site of *BACE1* mRNA (Faghihi et al., 2008, 2010).

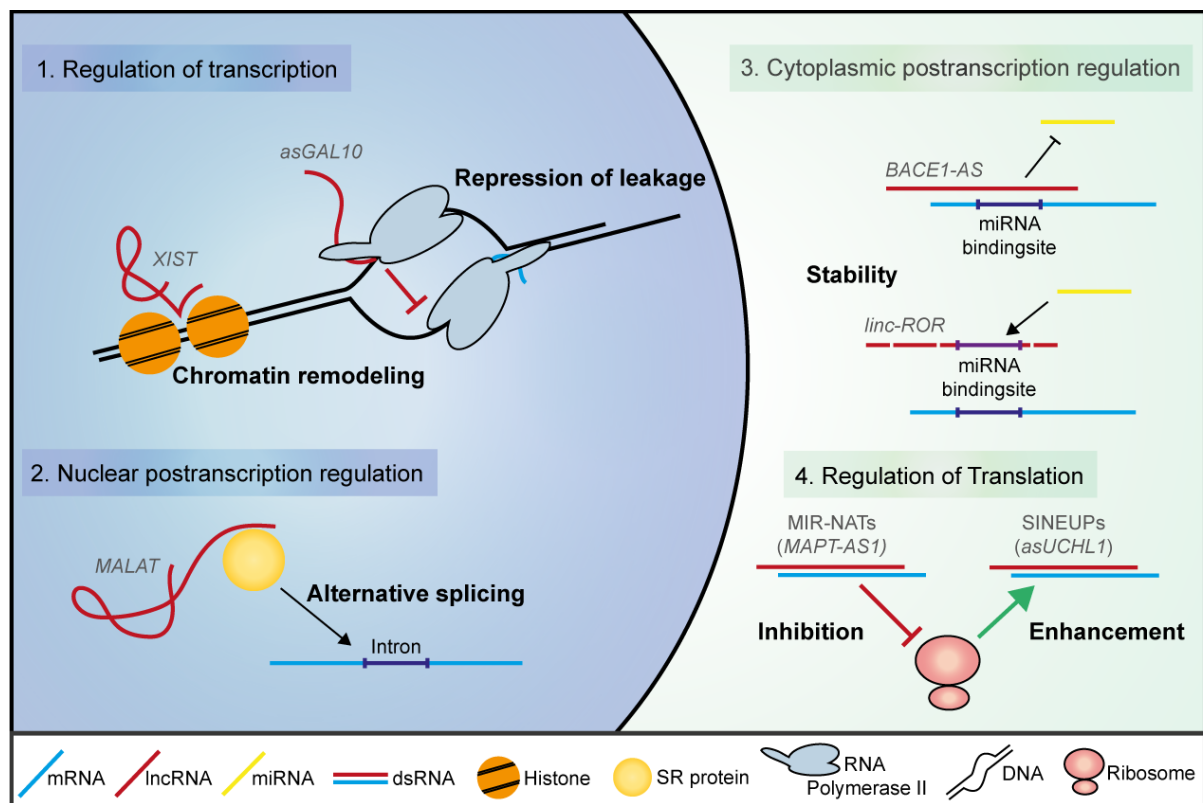


**Figure 3 lncRNAs carry out diverse functions (adapted from Villegas et al., 2016).** Since the discovery of lncRNAs, different and diverse functions were identified for them in modulating gene expression. At the level of transcription (1.), they modulate the chromatin state (*XIST*) or repress the transcription of protein coding genes via transcriptional interference (*asGAL10*). Further, *MALAT1* influences alternative splicing by modifying the phosphorylation state of SR proteins (2.). In the cytoplasm, lncRNAs stabilize mRNAs, for instance by interfering with miRNA binding to mRNAs (3.). *BACE1-AS* covers the miRNA binding site of *BACE1* mRNA and *linc-ROR* acts as a sponge for miRNAs. Additionally, two sets of asRNAs have been shown to modulate translation of their mRNA counterpart (4.). MIR-NATs repress translation by interfering with the binding of ribosomes and SINEUPs upregulate translation by recruiting polysomes.

lncRNA mediated translation regulation of mRNAs is carried out by asRNAs and dsRNA formation. SINEUPs are a class of asRNAs that increase translation efficiency of their mRNA by inducing the association with heavy polysomes for extended translation. They are named by

their functional domain, the SINEB2 element (Carrieri et al., 2012; Zucchelli et al., 2015). Another class comprises a set of asRNAs that represses translation of their mRNA by interfering with its ribosomal RNA pairing at the internal ribosome entry site. These asRNAs are called MIR-NATS. Noticeably, MIR-NATS possess an embedded mammalian-wide interspersed repeat (MIR) as their functional domain (Simone et al., 2021).

## 2.8 asRNAs

A specific type of lncRNAs are asRNAs. They are transcribed from the opposite strand of a protein coding gene, which transcript is thus called senseRNA. According to their orientation, a pair of sense and antisense genes can fully overlap if their sequence is completely covered by each other. Additionally, they can have 3' or 5' overhangs, thereby being called tail-to-tail or head-to-head, respectively (Villegas & Zaphiropoulos, 2015). In *S. cerevisiae*, most asRNAs were shown to be degraded by the cytoplasmic exonuclease Xrn1 (van Dijk et al., 2011). Further, they show stabilization after deletion of *DCP1* and *UPF1* (Wery et al., 2016). Because both are factors in NMD, it indicates the association of asRNAs with ribosomes and suggests their cytoplasmic degradation to occur via NMD. Consequently, a noticeable number of asRNAs contain small open reading frames (smORFs) on their 5' end, which probably mediates the degradation via NMD (Smith et al., 2014). However, few examples exist where these peptides carry out functions, for example in the leg development of *Drosophila melanogaster* (Pueyo & Couso, 2008). Whether the resulting small peptides carry out functions in general or are just byproducts of degradation is still discussed. However, most results hint to them not being functionally relevant and just being part of the degradation (Guerra-Almeida & Nunes-da-Fonseca, 2020).

### 2.8.1 asRNAs repress basal transcription of sense genes under non-inducing conditions

Whole transcriptome studies have shown that asRNA transcription in *S. cerevisiae* is highly enriched for stress responsive genes and plasma membrane genes, which are involved in sensing and responding to environmental cues. On the one hand, the minimum transcript level of genes with antisense transcripts is lower than that of genes without an asRNA transcript. On the other hand, the range between their minimum and maximum expression level is larger, which consequently leads to a higher variability in protein abundance. This indicates the high regulation of genes with asRNAs (Xu et al., 2011). If a gene is not actively transcribed, the

transcription of its asRNA seems to be able to repress the basal transcription, for instance by pervasive transcription of the gene. Thereby, asRNA transcription can lead to the complete shutdown of a gene. Huber and colleagues have measured protein abundance under different growth conditions and have found that the expression of 13 out of a small subset of 41 genes has been completely turned off under at least one condition. They argued that the majority of asRNAs are unlikely to be functional and only a subset prevents leakage of their sense transcription, thus, challenging the idea of a global function of antisense transcripts, but suggesting gene-specific mechanisms (Huber et al., 2016). In the case of *GAL10*, *IME4* and *PHO84*, blocking the transcription of the asRNA leads to an increase of sense transcription, supporting the idea of transcription repression (Camblong et al., 2007; Hongay et al., 2006; Houseley et al., 2008). However, this is only the case if the gene is not actively transcribed. In the case of transcription by an active promoter, asRNAs have shown no general repressive impact on their sense gene (Xu et al., 2011).

### **2.8.2 asRNAs can form dsRNA with their mRNA counterpart to carry out posttranscriptional functions**

One dogma of biology is that eukaryotes transcribe their double stranded DNA into single stranded RNA. It is agreed that these RNAs can form secondary structures, thereby forming intramolecular dsRNAs, but the possibility of eukaryotic intermolecular dsRNAs is not as known. Recent studies have enlightened the dsRNA formation in eukaryotes. In *S. cerevisiae* an RNAi based system has been used to identify dsRNA structures. For this, the RNAi key enzymes *DICER* and *ARGO* have been introduced into *S. cerevisiae*, which has lost the RNAi system during evolution (Drinnenberg et al., 2009). The dsRNase Dicer cuts dsRNA into 23 nt long products, which were isolated, sequenced via RNA-seq and compared to that of wild type cells without the RNAi system. (Wery et al., 2016) Approximately 80% of the identified 1.781 XUTs were shown to be engaged in dsRNA structures. However, the authors argued that dsRNAs are resolved by Mtr4 or Dbp2 in the nucleus prior to export and that mRNA and asRNA engage the ribosome separately. The work of Wery and colleagues has revealed the existence of intermolecular dsRNAs in *S. cerevisiae*, but also displays the controversial debate about asRNA functionality.

In mammalian cells, two major asRNA classes have been found to modulate the translation of their mRNA by forming a double strand: SINEUPs and MIR-NATs (Carrieri et al., 2012; Simone



et al., 2021; Zucchelli et al., 2015). It is noticeable that both types of asRNA do overlap with their mRNA at the 5' end and have a 3' end overhang. Their functional domains, the SINEB2 or MIR element, are embedded in the 3' overhang, whereas the 5' overlapping sequence ensures specificity for their sense mRNA. The overlap represents only a small part of the complete sequence of the asRNAs. The SINEUP *asUCHL1* is thought to be exported from the nucleus separately upon activation of stress signaling pathways. In the cytoplasm, the asRNA undergoes base pairing with its mRNA to enhance the translation (Carrieri et al., 2012).

Protein coding genes do not only overlap with non-coding genes, also two protein coding genes can overlap with each other. In *S. cerevisiae*, it was shown that the dsRNA formation between two mRNAs can inhibit each other's translation by mediating NGD (Sinturel et al., 2015).

## **2.9 Gene expression changes in adaptation and stress response**

A variety of lncRNA mediated gene regulation in *S. cerevisiae* is connected to cellular processes and adaptation to environmental changes, for instance in adaptation to nutrient availability and during osmotic stress. Thereby, lncRNAs regulate the transition between distinct expression patterns (Beck et al., 2016; Pelechano & Steinmetz, 2013).

### **2.9.1 Adaptation to nutrient availability**

*S. cerevisiae* has adapted to an environment with a diverse composition of carbon sources. Depending on the accessibility of these carbon sources, cells must change their metabolic profile and thus expression of metabolic genes (Vadkertiová et al., 2012). Up to 40 % of protein coding genes have been shown to be differentially expressed at growth on a carbon source other than glucose (Zaman et al., 2008).

A major factor in the switch between glucose and galactose metabolism is the *GAL* gene cluster including *GAL1*, *GAL10* and *GAL7*, which are involved in metabolizing galactose. The regulation of this cluster was extensively studied, and recent research has identified the asRNA *asGAL10* as a key element regulating that cluster (Houseley et al., 2008; van Dijk et al., 2011). The *GAL* cluster can be situated in three different states: repressed, induced and derepressed (Johnston et al., 1994). Under growth in glucose, the transcription of the *GAL* cluster is repressed by the glucose-dependent transcription factors Nrg1 and Mig1 (Zhou & Winston, 2001). On galactose, the needed *GAL* genes are induced through binding of the transcription

factor Gal4 to their promoter regions (Traven et al., 2006). Further, the glucose-dependent transcription factors dissociate, releasing the repression. If neither glucose nor galactose is available for the cell, for instance during growth on raffinose, the *GAL* cluster is neither induced nor repressed and therefore situated in the derepressed state (Johnston et al., 1994). Depending on the conditional state, the *asGAL10* exhibits different regulatory functions. When the widespread transcription of asRNAs was discovered, they were found to be present on gene loci of repressed genes, including the *asGAL10* (van Dijk et al., 2011). Further single molecule microscopy experiments have shown, that during growth in glucose *asGAL10* can prevent leakage of its sense genes, when these are not needed and thus would interfere with the glucose metabolism (Lenstra et al., 2015). However, the *asGAL10* is not the main repressor. Its transcription rather helps to shut down the unspecific pervasive transcription of the *GAL* cluster by interfering with sense transcription. Strikingly, under inducing conditions, the *asGAL10* expression represents an advantage for cells during the switch from glucose to galactose. Cells expressing *asGAL10* are able to induce the expression of *GAL* genes faster than cells lacking the lncRNA. In that case, the authors suggested an acceleration of transcription through asRNA mediated R-loop formation (Cloutier et al., 2016). R-loops are DNA:RNA hybrids, which open up the DNA double helix. The *asGAL10* is thereby an impressive example for the multifunctional properties of asRNAs (Beck et al., 2016).

### **2.9.2 Osmotic stress response**

Cells have evolved to fit in specific surrounding including the range of pH or temperature, salt concentration or availability of metabolites. The change of these conditions to suboptimal parameters is considered as stress. Multicellular and unicellular organisms are constantly exposed to changing requirements. Depending on the difference between optimal and shifted suboptimal condition, cells must adapt. At drastic changes, cellular response must be immediate (de Nadal et al., 2011). Unicellular organisms are continuously exposed to a fluctuating environment. Complex multicellular organisms have evolved to establish an internal homeostasis for their cells and can buffer external changes. Cells of specific tissues are still exposed to external changes and thus must adapt. For instance, shortage of water accessibility can increase osmolarity differences in roots of plants compared to their surroundings. Also, in mammalian renal cells, high urea concentrations force cells to adapt.

In *S. cerevisiae*, stress response is regulated by the high osmolarity glycerol (HOG) signal transduction pathway (Saito & Posas, 2012). It induces the decrease of growth and biomass associated proteins like ribosomal proteins and upregulates stress responsive genes. Upon osmotic stress, RNAPII dissociates from the DNA, resulting in an overall reduction of transcription (Proft & Struhl, 2004). Meanwhile, Hog1 gets phosphorylated and recruits RNAPII to early responding genes. It directly binds to the chromatin and recruits the transcription factors Hot1, Sko1, Msn2/Msn4 and Msn1 and RNAPII to stress responsive genes (Alepez et al., 2001; Nadal-Ribelles et al., 2012). Hog1 does not only bind to promoter regions but also to the coding region, suggesting an additional role in transcription elongation.

In *S. cerevisiae*, between 200 and 400 stress responsive protein coding genes are upregulated by Hog1, depending on the intensity of the applied stress, and threshold, regarding their minimum level of change. In addition, it has been shown that Hog1 also directly upregulates lncRNAs upon osmotic stress. After the addition of 0.4 M NaCl and 1.2 M NaCl, Hog1 upregulates 173 or 216 lncRNAs, respectively. However, only 20 % of the overall upregulated genes are Hog1 dependent, suggesting five-time higher numbers in upregulated protein coding genes and lncRNAs upon osmotic stress (Nadal-Ribelles et al., 2014).

The majority of upregulated lncRNA transcripts are asRNAs and 37% of the upregulated asRNAs have a positive correlation with their sense gene. In these cases, sense and antisense RNAs are simultaneously increased. Astonishingly, if the transcription of the stress induced asRNA *asCDC28* is inhibited, the induction of *CDC28* upon osmotic stress itself is impaired. *CDC28* has been shown to be needed for cells to re-enter the cell cycle after its arrest. Cells without the *asCDC28* have re-entered the cell cycle approximately 20 min later upon stress. This indicates the involvement of antisense transcripts in stress response (Nadal-Ribelles et al., 2014).

### **2.9.3 Iron homeostasis**

Iron homeostasis represents a highly regulated and adaptive system to ensure steady cellular iron levels. Iron is an essential nutrient of every known organism. In the aerobic environment, iron exists in its oxidative Fe(III) form, which is poorly bioavailable. However, iron in its reduced ferrous form Fe(II) participates as a redox factor in a variety of cellular processes and is therefore considered to be an essential metal (Sigel & Sigel, 1998). Consequently, limitation of iron is harmful for cells. However, high cellular concentrations of iron are toxic since it

participates in Fenton reactions, which results in reactive oxygen radicals. Therefore, the uptake and localization of iron in a cell is tightly controlled, which clearly requires fine tuning (Li and Ward, 2018).

Microorganisms have found different ways to take up iron. One major pathway in *S. cerevisiae* is the reduction mediated iron uptake (Figure 4). In this case, the siderophore-bound Fe(III) has to be dissociated and reduced to Fe(II) by the plasma membrane associated iron reductases of the *FRE1-7* family (Dancis, 1998). The reduction of extracellular Fe(III) is catalysed by Fre1 and Fre2, the most studied members of the iron reductases. Cells with deletions of *FRE1* and *FRE2* fail to grow in iron poor surroundings (Yun et al., 2001). The reduced Fe(II) is imported across the plasma membrane by the high affinity iron permease Ftr1. Ftr1 is in complex with intracellular Fet3, which again oxidates Fe(II) to Fe(III) after import (Askwith et al., 1994; Stearman et al., 1996). The Fe(III) is not bioactive, thus, its renewed oxidation prevents its engagement in toxic Fenton reactions. The incorporation of iron into proteins takes place in the mitochondria. To get there, Fe(III) again has to be reduced at the mitochondrial membrane. In mass spec analysis of mitochondrial proteins, Fre5, Ftr1 and Fet3 were found. Thus, Fre5 is presumably the member of the *FRE* family to reduce Fe(III) for the reduction mediated mitochondrial uptake (Sickmann et al., 2003).

Genes involved in iron homeostasis are under control of the transcription factors Aft1 and Aft2. Both, on the one hand, sense cellular iron amounts and, on the other hand, act as a transcription factor to induce transcription of the iron regulon genes *FRE1-6*, *FTR1* and *FET3* (Rutherford et al., 2003). Aft1 and Aft2 do not sense Fe(II) or Fe(III) directly, but rather through the mitochondrial formed iron-sulphur cluster Fe<sub>2</sub>S<sub>2</sub>, which is delivered to Aft1 and Aft2 that reside in the nucleus (Lindahl, 2019).

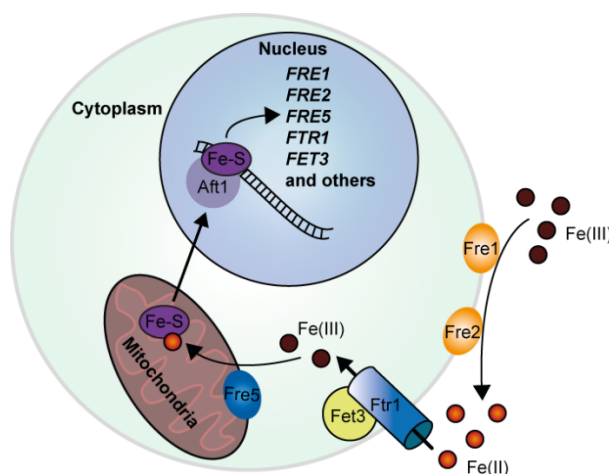


**Figure 4 Reductive high affinity uptake of iron (adapted from Judith Weyergraf).** In the environment, iron exists in its oxidative Fe(III) form. For uptake, it is reduced by the membrane associated reductases Fre1 and Fre2. The reduced Fe(II) is imported via the iron permease Ftr1 and again oxidized by Fet3. After cellular uptake, the cellular Fe(III) can probably be reduced by Fre5 for mitochondrial uptake and be incorporated into Fe-S-clusters. Fe-S-clusters act as an indicator of cellular iron amounts for the transcription factor Aft1, which regulates genes involved in iron homeostasis based on its binding to Fe-S.

### 2.10 Aim of the Study

lncRNAs have become a center of attention in molecular biology, as they are omnipresent and have been discovered to be involved in major regulatory mechanisms (Statello et al., 2020; Villegas & Zaphiropoulos, 2015). Their malfunction leads to cancer, neurodegenerative diseases, or faulty development of organisms (Arun et al., 2016; Grelet et al., 2017; Huarte et al., 2010; Kim et al., 2015; Wei et al., 2018). However, the enlightenment of their diverse functions has just started. Thus, elementary information about lncRNAs is still lacking and contradicting assessments about their function, processing, localization, and degradation exist.

Here, we want to unravel the nucleo-cytoplasmic distribution of all RNAs in the model system *S. cerevisiae*, while empathizing lncRNAs and asRNAs, as their up to date assigned function and degradation pathway seems to be inconsistent (van Dijk et al., 2011; Wery et al., 2016; Xu et al., 2011). So far, the general existence of asRNAs is explained by transcriptional repression of their sense genes to prevent leakage under non-inducing conditions. However, this disregards their obvious export and association with ribosomes in yeast and human cells in disregard. An export only for degradation seems like a waste of resources. The localization of other ncRNAs like rRNAs and snoRNAs shows their place of function (Dupuis-Sandoval et al., 2015; Fernández-Pevida et al., 2015). Therefore, with unraveling the localization of lncRNAs, we want to get insights into their cellular functions.

Further, cells have developed different mechanisms to change their expression pattern and thus adapt to changing requirements (de Nadal et al., 2011). During heat stress, this is accomplished by dissociation of adapter proteins from housekeeping mRNAs, among other things (Zander et al., 2016). However, recent studies showed that lncRNAs are also involved in gene expression adaptation (Nadal-Ribelles et al., 2014; Xu et al., 2011). The attributes of lncRNAs, as they are rapidly accessible and low in energy cost, are well suited for fast adaptation and fine-tuning of gene expression. To study processes in gene expression adaptation, model organisms like *S. cerevisiae* have shown to be highly advantageous. Changing requirements are easily inducible by altering their growth conditions. With the addition of stress factors like higher osmolarity or reduction of essential nutrients like iron, *S. cerevisiae* cells are immediately exposed to new requirements. By applying these methods, we are confident to broaden the understanding of the mechanisms of lncRNA mediated adaptation in gene expression.

### 3. Material and Methods

#### 3.1 Material

**Table 1: Hardware**

Hardware	Source
Äkta Prime plus	GE Healthcare
Leica AF6000 microscope	Leica
Primo Star light microscope	Zeiss
Eclipse E400 tetrad microscope	Nikon
Fast-Prep 24	MP Biomedicals
Electro Blotter PerfectBlue Semi-Dry, Sedec M	Peqlab
Heraeus Fresco 21	Thermo Fisher Scientific
Heraeus Pico 21	Thermo Fisher Scientific
Heraeus Multifuge X3	Thermo Fisher Scientific
Intas UV-System	INTAS GmbH
qPCR Cycler CFX Connect	BioRad
T100™ Thermocycler	BioRad
Bio-Link 254 UV-crosslinking chamber	Vilber
Water Purification Milli-Q	Millipore
Nano Drop 2000 spectrophotometer	Peqlab
Fusion FX7 Edge 18.06c	Vilber
Improved Neubauer counting chamber	Carl Roth
<i>E. coli</i> pulser	BioRad

## MATERIAL AND METHODS

**Table 2: Software**

Software	Source
Adobe Illustrator CS 6	Adobe
Adobe Photoshop CS 6	Adobe
Fiji 1.48s	W. Rasband (NIH/USA)
Microsoft Office 2013/2019	Microsoft
Microscopy LAS AF 1.6.2	Leica
SnapGene Viewer 5.2.1	GSL Biotech
APE v2.0.61	M. Wayne Davis (University of Utah/USA)
Integrated Genome Browser 9.1.8	Freese NH et al. (2016)
GraphPad Prism 7	GraphPad Software
Silverfast® AI V 6.6	LaserSoft Imaging AG Gernamny
Evolution-Capture Edge Software	Vilber

**Table 3: Chemicals and Consumables**

Chemical or consumable	Source
Agarose NEEO Ultra-Qualität	Carl-Roth
Amersham™ Protran™ 0.45 µm nitrocellulose membrane	GE Healthcare
cOmplete™, EDTA-free protease inhibitor cocktail	Roche
dNTPs	Invitrogen / Thermo Fisher Scientific
Formaldehyde 37%	Carl Roth
RiboLock™ RNase Inhibitor	Thermo Fisher Scientific
Rotiphorese Gel 30 (37.5:1) acrylamide	Carl-Roth
Salmon Sperm DNA	Sigma-Aldrich
Trizol™ Reagent	Thermo Fisher Scientific
Whatmann Blotting Paper 0.8 mm	Hahnemühle
tRNA	Sigma-Aldrich
GFP Selector beads	NanoTag Biotechnologies

## MATERIAL AND METHODS

Poly-L-lysine solution	Sigma-Aldrich
IgG Glutathion Sepharose 4B Beads	GE Healthcare
HDGreen™ Plus DNA Stain	Intas Science Imaging
Lambda DNA/EcoRI HindIII Marker	Thermo Fisher Scientific
PageRuler™ Prestained Protein Ladder	Thermo Fisher Scientific
GlycoBlue™	Thermo Fisher Scientific

**Table 4: Enzymes and master mixes**

Antibody	Source
DreamTaq DNA polymerase	Thermo Fisher Scientific
Q5® DNA polymerase	New England Biolabs
qPCRBIO SyGreen Mix Lo-ROX	Nippon Genetics
Restriction Enzymes	Nippon Genetics/ Thermo Fisher Scientific/ New England Biolabs
RNaseIII	New England Biolabs
RNase-Free DNase I	Qiagen
Zymolyase 20T	Zymo Research

**Table 5: Kits**

Kit	Source
NucleoSpin® Gel and PCR Clean-up	Macherey-Nagel
NucleoSpin® Plasmid	Macherey-Nagel
NucleoSpin® RNA	Macherey-Nagel
Westernbright™ Quantum™ HRP substrate	Advansta
FastGene® Scriptase II cDNA Kit	Nippon Genetics



## MATERIAL AND METHODS

**Table 6: Antibodies**

Antibody	Organism	Dilution	Application	Source
J2 anti-dsRNA	mouse	1:200/1:250	IF/IP	Scicons
Anti-GFP	rabbit	1:1000	WB	Chromotek
Anti-Myc	rabbit	1:1000	WB	Santa Cruz
Anti-Aco1	rabbit	1:2000	WB	Prof. Dr. Mühlenhoff (Marburg/Germany)
Anti-Hem15	rabbit	1:5000	WB	Prof. Dr. Mühlenhoff (Marburg/Germany)
Anti-Mex67	rabbit	1:10000	WB	Selfmade (David Biotechnologie)
Anti-Nop1	mouse	1:4000	WB	Santa Cruz
Anti-Zwf1	rabbit	1:4000	WB	Prof. Dr. Mühlenhoff (Marburg/Germany)
Anti-mouse IgG-HRP	goat	1:20000	WB	Dianova
Anti-rabbit IgG-HRP	goat	1:20000	WB	Dianova
Anti-mouse Cy3	goat	1:200	IF	Dianova

IF = Immunofluorescence, IP = Immunoprecipitation, WB = Western blot

**Table 7: Yeast strains**

Strain number	Genotype	Source
HKY314	<i>MAT<math>\alpha</math> his3<math>\Delta</math>1 leu2<math>\Delta</math>0 met15<math>\Delta</math>0 ura3<math>\Delta</math>0</i>	Euroscarf
HKY703	<i>MAT<math>\alpha</math> nmd3::kanMX4 his3<math>\Delta</math>1 leu2<math>\Delta</math> lys2<math>\Delta</math> ura3<math>\Delta</math> pNMD3</i>	(Brune et al., 2005)
HKY682	<i>MAT<math>\alpha</math> npl3::kanMX4 his3<math>\Delta</math>1 leu2<math>\Delta</math>0 ura3<math>\Delta</math>0</i>	
HKY863	<i>MAT<math>\alpha</math> rpl10::kanMX4 his3<math>\Delta</math>1 leu2<math>\Delta</math>0 ura3<math>\Delta</math>0 lys2<math>\Delta</math>0 prpl10(G161D)-GFP</i>	(Baierlein et al., 2013)
HKY1353	<i>MAT<math>\alpha</math> mex67::HIS3 xpo1::TRP1 ura3<math>\Delta</math>0 pmex67-5 pxpo1-1</i>	(Gadal et al., 2001)
HKY1898	<i>MAT<math>\alpha</math> set2::kanMX ura3<math>\Delta</math>0 leu2<math>\Delta</math>0 his3<math>\Delta</math>1 met15<math>\Delta</math>0</i>	Euroscarf
HKY1899	<i>MAT<math>\alpha</math> fre5::kanMX ura3<math>\Delta</math>0 leu2<math>\Delta</math>0 his3<math>\Delta</math>1 met15<math>\Delta</math>0</i>	Euroscarf
HKY2012	<i>leu2-3 trp1-1 can1-100 ura3-1::EGFP::kanMX6 ade2-1his3- 11</i>	(Drinnenberg et al., 2009)

## MATERIAL AND METHODS

HKY2013	<i>leu2-3 trp1-1 can1-100 ura3-1::EGFP::kanMX6 ade2-1his3-11 pP<sub>TEF</sub>:DCR1(Scas) pP<sub>TEF</sub>:AGO1(Scas)</i>	(Drinneberg et al., 2009)
HKY2065	<i>MAT<math>\alpha</math>/Mata DBP2/dbp2::kanMX4 ura3<math>\Delta</math>0/ura3<math>\Delta</math>0 leu2<math>\Delta</math>0/leu2<math>\Delta</math>0 his3<math>\Delta</math>1/his3<math>\Delta</math>1 LYS2/lys2<math>\Delta</math>0</i>	Euroscarf
HKY2067	<i>MAT<math>\alpha</math> dbp2::kanMX4 ura3<math>\Delta</math>0 leu2<math>\Delta</math>0 his3<math>\Delta</math>1 lys2<math>\Delta</math>0</i>	This study

**Table 8: E.coli**

Strain number	Genotype	Usage
Dh5 $\alpha$	F- $\Phi$ 80lacZ $\Delta$ M15 $\Delta$ (lacZYA-argF) U169 recA1 endA1 hsdR17 (rK-, mK+) phoA supE44 $\lambda$ - thi-1 gyrA96 relA1	Plasmid amplification
Rosetta 2	F- ompT gal dcm lon hsdSB (rB-,mB-) $\lambda$ (DE3) pRARE2(CamR)	Protein expression

**Table 9: Plasmids**

Plasmid number	Genotype	Source
pHK87	<i>CEN LEU2</i>	(Sikorski & Hieter, 1989)
pHK88	<i>CEN URA3</i>	(Sikorski & Hieter, 1989)
pHK697	<i>CEN URA3 RPS2-GFP</i>	(Milkereit et al., 2003)
pHK1669	<i>CEN URA3 P<sub>GAL1</sub>:SUT802</i>	This study
pHK1716	<i>CEN URA3 P<sub>GAL1</sub>:SUT412</i>	This study
pHK1717	<i>CEN URA3 P<sub>GAL1</sub>:MYC-DBP2</i>	(Grosse et al., 2021)
pHK1812	<i>CEN LEU2 P<sub>GAL1</sub>:RNaseIII-NES-GFP</i>	This study
pHK1813	<i>CEN LEU2 P<sub>GAL1</sub>:RNaseIII-NLS-GFP</i>	This study
pHK1814	<i>CEN LEU2 P<sub>GAL1</sub>:RNaseIII-NES-NLS-GFP</i>	This study
pHK1815	<i>CEN LEU2 P<sub>ADH1</sub>:RNaseIII-NES-GFP-GFP</i>	This study

MATERIAL AND METHODS

**Table 10: Oligos**

Oligo number	Sequence	Gene/Probe
HK842	5'-CCAAGAACGTTTCTTGTTACAGACC-3'	<i>RPS6A</i> forward
HK843	5'-CGTCATCTTCCTTGGACAAACC-3'	<i>RPS6A</i> reverse
HK1002	5'-TGCTAAGGCTGTCGGTAAGG-3'	<i>TDH1</i> forward
HK1003	5'-TCAGAGGAGACAACGGCATC-3'	<i>TDH1</i> reverse
HK1024	5'-CAAGATTGCTGGTTACACCACC-3'	<i>RPS17A</i> forward
HK1025	5'-GTCTGTCTCTTTGGGCAGAAACG-3'	<i>RPS17A</i> reverse
HK2868	5'-AGCACTAGTTGCGGTGAC-3'	<i>HPF1</i> reverse
HK2870	5'-TGAAGCCACAACCACTACTG-3'	<i>HFP1</i> forward
HK2871	5'-AGTTGTGGTGGTAGCTTCAG-3'	<i>CSS1</i> reverse
HK2909	5'-GCTGTATATGTCAGATGCGACTG-3'	<i>FRE5</i> reverse
HK2911	5'-CCTTCACTGCACACCACTAC-3'	<i>FRE5</i> forward
HK2919	5'-ACGTTAGTACATCAACCGGTG-3'	<i>CSS1</i> forward
HK3001	5'-ATTGTCGGTTGGACTAGCTG-3'	<i>PRY3</i> reverse
HK3002	5'-ACGCCATTACATCCGAGC-3'	<i>PRY3</i> forward
HK3056	5'-TGAGTATCAAGCCACTGAGGTC-3'	<i>HEM15</i> forward
HK3057	5'-ACTGCCTTCTTCACGCCATC-3'	<i>HEM15</i> reverse
HK3151	5'-6FAM-UUUUUUUUAUUGCCUGGUUGCCUGGUUAUUUCUAUU-3'	N125_RNA_FA
HK3285	5'-AAUAGAAUAACCAGGCAACCAGGCAAUAAAAAAAA-3'	N125_RNA_compl
HK3923	5'-Cy5-UUAUAUGUCUUGUUCUCUUGUAUCUGUUCUUGUUGU-3'	CY5-labeled RNA
HK3989	5'-TCAAGTATCATTGGAAAGTAAAGAAC-3'	<i>PHO85</i> intron forward
HK3990	5'-TTCTTTCATTAGGGAGATCTCAC-3'	<i>PHO85</i> intron reverse
HK3991	5'-ACATTTTCAAGCGAAGTCG-3'	<i>PHO85</i> forward
HK3992	5'-CTGGATATTTGGGTTGATTTG-3'	<i>PHO85</i> reverse
HK4178	5'-TGGAGGATGAGACTGGTAGTG-3'	<i>SEG2</i> forward
HK4179	5'-CCGGATCTCTCATTATCACG-3'	<i>SEG2</i> reverse

\*Oligos were ordered and synthesized at Sigma-Aldrich

MATERIAL AND METHODS

**Table 11: Oligos used for cloning**

Oligo number	Sequence	Amplificate	Target plasmid	Resulting construct
3850	AGCTATACCAAGCATACAATAAGCATCGATATGAACCCC ATCGTAATTAA	<i>RNaseIII</i>	pHK252 pHK1361	pHK1812 pHK1814 pHK1815
3851	TCTCTCTTTTTTGGAGGAGCACCCATCGATTCCAGCTCC AGTTTTTT	<i>RNaseIII</i>	pHK1361	pHK1814
3853	GAGTTCTTCTCCTTTGCTAGCCATGAATTCTCCAGCTCC AGTTTTTT	<i>RNaseIII</i>	pHK252 pHK1361	pHK1812 pHK1815
4012	GGAGCTCCACCGCGGTGGCGGCCGCTCTAGCGGATTAG AAGCCGCC	<i>GAL1</i> promoter	pHK1361	pHK1812 pHK1813 pHK1814
4013	CCGATTAATTACGATGGGGTTCATTGCTTACTCCTTGACG TTAAAGTATAGAG	<i>GAL1</i> promoter	pHK1361	pHK1812 pHK1813 pHK1814
4041	GAAGAGAAAGGTAGCTGGTATCAATAAAGACATCCCCG GGATGGCTAGCAAAGGAGAAGAAGCTTCACTGGAGTT GTCC	-	pHK1814	pHK1813
3122	CTCTATACTTTAACGTCAAGGAGAAAAAACTATATCTAG AAATGAAGAAAAGTGGCAACTTTG	<i>SUT802</i>	pHK1479	pHK1669
3123	GTAAGCGTGACATAACTAATTACATGATGCGGCCCTCGA GGTTCGAACATTCATATTACCTCCT	<i>SUT802</i>	pHK1479	pHK1669
4218	GGTCGACGGTATCGATAAGCTTGATATCGAATTCCCGGG GAGAAAGGTTTTCG	<i>FRE5</i> 3'UTR	pHK1572	
4217	ATTTACCTTCCCGAAAAGCATTCTTCGAAGCTGCAGTTCT TTCTGCCATTCATCTC	<i>FRE5</i> 3'UTR	pHK1572	
3888	CTCTATACTTTAACGTCAAGGAGAAAAAACTATA <sup>t</sup> TAGTA GTGTATTATAGATGATTATTATCATTATATATACATGGCT ACG	<i>SUT412</i>	pHK1479	pHK1716
3889	GTAAGCGTGACATAACTAATTACATGATGCGGCCCTTTT GAATTCATGGACAACGATTTAAAG	<i>SUT412</i>	pHK1479	pHK1716

\*Oligos were ordered and synthesized at Sigma-Aldrich

### 3.2 Cultivation

#### 3.2.1 Media and plates

Standard full medium YPD or synthetic selective media for *S. cerevisiae* was prepared as described earlier (Rose et al., 1990; Sherman & Hicks, 1991).

**Table 12: YP**

Reagent	Amount
Peptone	2 %
Yeast extract	1 %
Agar-agar for plates	1.8 %

**Table 13: YPD**

Reagent	Amount
Peptone	2 %
Yeast extract	1 %
Glucose	2 %
Agar-agar for plates	1.8 %

**Table 14: Selective media**

Reagent	Amount
Nitrogen base	0.17 %
Ammonium sulphate	0.51 %
Drop out mix (amino acids)	0.2 %
Glucose / Galactose	2 %
Agar-agar for plates	1.8 %

**Table 15: FOA plates**

Reagent	Amount
Nitrogen base	0.17 %
Ammonium sulphate	0.51 %
Drop out mix (amino acids)	0.2 %
Glucose / Galactose	2 %
Agar-agar	1.8 %
5-Fluoroortic acid (FOA)	0.1 %

**Table 16: LB-medium**

Reagent	Amount
Tryptone	1 %
Yeast extract	0.5 %
NaCl	0.5 %
Ampicillin	100 µg/ml
Agar-agar for plates	1.5 %

All amounts, except ampicillin, are given as weight per volume in percent. For selective plates the carbon source was autoclaved separately (20 % in ddH<sub>2</sub>O) and added before pouring the plates respectively using liquid media. Before adding ampicillin or FOA, the medium was cooled down to at least 60 °C.

### 3.2.2 Cultivation of *S. cerevisiae*

Yeast cells were long time stored at -80°C in 50% glycerol. Before use, cells were streaked out onto a YPD plate for growth at 30°C for on average of 2 days and further stored at 4°C (short time storage). Strain HKY2067 was cultivated at 37°C. Before an experiment, the corresponding strains were taken from their plates and incubated in liquid media. According to the experiment and needed volume, either Erlenmeyer flasks or tubes were taken for incubation. Plasmid containing strains were grown in selective media, missing amino acids suitably to the marker gen on the plasmid. If not stated otherwise, 2% glucose was added as the carbon source. To induce transcription of genes under the control of the *GAL1* promoter, 2% galactose was added instead of 2% glucose. Cells were harvested in their logarithmic stage

between  $0.5 \times 10^7$  cells/ml and  $4 \times 10^7$  cells/ml and after they had at least doubled in amount since previous counting and dilution.

### 3.3 DNA Cloning

#### 3.3.1 Polymerase Chain Reaction (PCR)

To amplify DNA, Polymerase Chain Reaction (PCR) was conducted. Regarding the purpose, either the Q5-Polymerase (NEB) or the DreamTaq polymerase (Thermo Fisher Scientific) was used. The Q5 is a proofreading polymerase and was thereby used to amplify inserts for cloning. The Dream Taq was used for colony PCR or other analytic PCRs. The pipetting scheme and PCR cycles were based on the suppliers' handouts and are depicted in tables 17 to 20. Subsequently, the PCR products were analyzed via gel electrophoresis and detected with the Intas UV system (INTAS GmbH).

**Table 17: DreamTaq pipetting scheme**

Reagent	Amount
10x DreamTaq Buffer	0.1 $\mu\text{l}/\mu\text{l}$
dNTP Mix	0.2 mM each
Forward primer	0.5 $\mu\text{M}$
Reverse primer	0.5 $\mu\text{M}$
Template DNA	100 ng -1 $\mu\text{g}$
DreamTaq DNA Polymerase	0.025 U/ $\mu\text{l}$

**Table 18: DreamTaq PCR cycle**

Step	Temperature	Time	Repetition
Initial denaturation	95 °C	3 min	
Denaturation	95 °C	30 sec	↑ 34x
Annealing	50-60 °C	30 sec	
Elongation	72 °C	1min/kb	
Final Elongation	72 °C	10 min	

**Table 19: Q5 pipetting scheme**

Reagent	Amount
5x Q5 Reaction Buffer	0.2 $\mu\text{l}/\mu\text{l}$
dNTP Mix	0.2 mM each
Forward primer	0.5 $\mu\text{M}$
Reverse primer	0.5 $\mu\text{M}$
Template DNA	100 ng -1 $\mu\text{g}$
Q5 DNA Polymerase	0.02 U/ $\mu\text{l}$

**Table 20: Q5 PCR cycle**

Step	Temperature	Time	Repetition
Initial denaturation	98 °C	30 sec	
Denaturation	98 °C	10 sec	↑ 34x
Annealing	50-60 °C	30 sec	
Elongation	72 °C	30 sec/kb	
Final Elongation	72 °C	2 min	

### 3.3.2 Agarose gel electrophoresis

To separate DNA according to its size, electrophoresis using agarose gels was conducted. For the gel, 1 % agarose was added to 1x TAE buffer (40 mM Tris base, 0.1% (v/v) Acetic acid, 1mM EDTA). The mixture was heated in a microwave until boiling and afterwards cooled down while stirring. After the suspension reached a temperature below 60 °C, HDGreen™ Plus DNA Stain (Intas Science Imaging) was added (5  $\mu\text{l}$  per 100 ml) and poured in a prepared gel chamber, followed by inserting a comb. The gel was further cooled down until it became solid and stored at 4 °C until use. For usage, the gel was placed in a running chamber filled with 1 x TAE buffer and the comb was removed. The samples and DNA ladder were loaded into the wells, created by the comb, and exposed to a 120 V current for about 45 min. The visualization was carried out with the Intas UV-System (INTAS GmbH).



### 3.3.3 DNA extraction from agarose gels

To extract DNA from the agarose gel, the NucleoSpin® Gel and PCR Clean-up kit (Macherey-Nagel) was used by following the suppliers' manual. In the end, the DNA was eluted in 20 µl of ddH<sub>2</sub>O.

### 3.3.4 Restriction Free (RF-)Cloning

To implement new inserts into plasmids, PCR based restriction free cloning was conducted. The insert was amplified with primers overlapping with the 3' and 5' sequence neighboring the point of desired insertion. Thereby, the amplified insert acts as a Megaprimer from where the polymerase starts to amplify the rest of the plasmid. Thus, instead of using a forward and reverse primer, only the mega primer was added to the template plasmid. For the amplification, the Q5-polymerase and the corresponding protocol (Table 19) were used.

**Table 21: PCR of Restriction Free Cloning**

Step	Temperature	Time	Repetition
Initial denaturation	98 °C	30 sec	
Denaturation	98 °C	10 sec	↑ 20x
Annealing	65 °C	30 sec	
Elongation	72 °C	3-5 min	
Final Elongation	72 °C	10 min	

Following PCR, the template plasmid was digested with DpnI for 4 h at 37°C and DpnI was inactivated through an incubation at 80°C for 20 min.

### 3.3.5 Gibson assembly

Gibson assembly was used for plasmid 1669. pHK1479 was first linearized with restriction enzymes XhoI and XbaI in 2x Tango buffer. Similar to RF-cloning the inserts for Gibson assembly were amplified with primer overlapping with the 3' and 5' sequence neighboring the point of desired insertion and respective restriction sites. 100 ng of the linearized plasmid and the amplified insert (1:3) were added to 15 µl of the Gibson assembly master mix (100 mM Tris-HCl pH 7.5; 10 mM MgCl<sub>2</sub>; 0.2 mM dATP; 0.2 mM dTTP; 0.2 mM dCTP; 0.2 mM dGTP; 10 mM DTT; 5 % PEG-8000; 1 mM NAD<sup>+</sup>; 4 U/µl Taq DNA Ligase; 4 U/ml T5 Exonuclease; 25 U/ml

Q5 Hi-Fi DNA Polymerase) to a final volume of 20  $\mu$ l and incubated at 50 °C for 30 min. After incubation and cooling down on ice, *E. coli* was transformed with 10  $\mu$ l of the samples.

### 3.3.6 Transformation of electrocompetent *E. coli*

First, samples from cloning were dialyzed on a 0.025  $\mu$ m MCE membrane with a diameter of 13 mm (Millipore) floating on sterile water in a Petri dish for 30 min and transferred into a new 1.5 ml reaction tube. Next, 10  $\mu$ l of the dialyzed sample was added to 40  $\mu$ l thawed competent DH5 $\alpha$  *E. coli* and mixed by pipetting up and down. The mixture was then transferred into an ice-cold sterile 0.1 cm cuvette and a pulse (150-ohm, 1500 V, 50  $\mu$ F) was applied with the help of an electroporator. The cells were immediately resuspended in 1 ml LB medium, transferred into a 15 ml falcon, and recovered in a rotator at 37 °C for 60 min. Finally, the suspension was plated on LB-plates containing 0.1 mg/ml ampicillin. LB-plates were then again incubated at 37 °C overnight. Grown colonies were subsequently analyzed by colony PCR.

### 3.3.7 Heat shock transformation of competent *E. coli*

10  $\mu$ l of cloning product or 100 ng of plasmid was added to 100  $\mu$ l of thawed, chemical competent DH5 $\alpha$  cells. After mixing gently, the cells were exposed to a heat shock at 42 °C for 2 min followed by immediate cool down on ice. For a better survival, cells were recovered at 37 °C for 60 min in 1 ml LB medium. Finally, they were pelleted at 6 krpm and 4 °C for 5 min, resuspended in 200  $\mu$ l ddH<sub>2</sub>O and plated on ampicillin containing LB-plates.

### 3.3.8 Sequencing

Cloned constructs were sequenced for the respective inserts by LGC Genomics, using Sanger sequencing.

## 3.4 Cell biological methods

### 3.4.1 Creation of the haploid *dbp2 $\Delta$* strain

To create the haploid *dbp2 $\Delta$*  strain (HKY2067), we inoculated the diploid *DBP2/dbp2 $\Delta$*  strain (HKY2065) in 2 ml of sporulation medium (Table 22) for 5 days at 25 °C. Thereby, the formation of tetrads was induced, which was controlled by using a light microscope. Next, 100  $\mu$ l of the

culture was centrifuged at 12 krpm for 1 min at 4 °C. Hereinafter, the pellet was washed once in 1 ml sterile water and resuspended in 50 µl P-solution (0.1 M phosphate buffer pH 6.5; 1.2 M sorbitol). Further, the ascus wall of the tetrads was digested. Therefore, 1 µg/µl of Zymolyase (Zymo Research) was added and incubated for 7 min at 25 °C. After digestion, the tetrads were washed once in P-Solution and resuspended in 200 µl P-Solution. Of the resulting cell suspension, 2 µl was transferred to 100 µl sterile water, which was again transferred onto a YPD plate. Here, only one third of the plate was covered. The tetrads were picked with the help of a tetrad microscope and incubated at 37 °C, as the *dbp2Δ* strain was shown to only grow at a temperature of at least 35 °C. Next, the spores were restreaked on two different YPD plates. One was again incubated at 37 °C and the other was incubated at 25 °C. A spore that did not grow at 25 °C should have inherited the *dbp2::KanMX4*, and was further tested on a YPD plate with 100 µl of geneticin (40 µg/µl).

**Table 22: Sporulation medium**

Reagent	Amount
Yeast extract	0.25 %
Glucose	0.05 %
Potassium acetate	150 mM
Uracil	40 mg/ml
Adenine	40 mg/ml
Tyrosine	40 mg/ml
Histidine	20 mg/ml
Leucine	20 mg/ml
Lysine	20 mg/ml
Tryptophan	20 mg/ml
Methionine	20 mg/ml
Arginine	20 mg/ml
Phenylalanine	100 mg/ml
Threonine	350 mg/ml

### 3.4.2 Lithium acetate transformation of *S. cerevisiae*

Essentially, transformation of yeast cells was carried out as described in Gietz et al., 1992. First, cells were grown to log phase in 5 ml media. Cells were then harvested through centrifugation at 4 krpm and 4 °C for 3 min, washing once with TE/LiOAc (10 mM Tris pH7.0;

1 mM EDTA; 100 mM LiOAc) and resuspending in 50  $\mu$ l TE/LiOAc. Next, 50  $\mu$ g preboiled ssDNA and 500 ng plasmid was added and mixed by pipetting up and down, followed by adding 300  $\mu$ l PEG4000/LiOAc/TE (10 mM Tris pH7.0; 1 mM EDTA; 100 mM LiOAc, 40% PEG 4000) and vortexing. Finally, cells were incubated at 25°C while rotating for 30min, heat shocked at 37 °C for 15 min, washed once in 1 ml sterile water and plated onto a suitable selective plate. The strain HKY2067 was incubated at 37 °C for 30 min before heat shock.

### **3.4.3 Drop dilution analysis**

Cells were grown to log phase ( $0.5-2 \times 10^7$  cells/ml) and diluted to  $1 \times 10^6$  cells/ml. 10-fold serial dilutions to  $1 \times 10^3$  cells/ml were prepared and 8  $\mu$ l of each dilution was spotted onto a respective plate. Each plate was incubated for 3 days at the indicated temperatures and conditions like addition of NaCl, BPS (Bathophenanthrolinedisulfonic acid) or FeCl<sub>3</sub>. Pictures were taken after 2 and 3 days with the Intelli Scan 1600 (Quanto technology) and the SilverFast Ai program.

### **3.4.4 Fe<sup>2+</sup> measurement by BPS absorption**

Bathophenanthrolinedisulfonic acid (4,7-diphenyl-1,10-phenanthrolinedisulfonic acid), in short, BPS, is a chelator of Fe<sup>2+</sup>. Its colour changes to red by binding Fe<sup>2+</sup> and thus, its light absorption at 535 nm can be used to measure the Fe<sup>2+</sup> content in cells.

First, cells were grown in 5 ml selective media until log phase before adding 5 mM FeCl<sub>3</sub> for 4h. Next, cells were centrifuged at 4 krpm and 4 °C for 5 min, washed once in 1 ml ddH<sub>2</sub>O and lysed with 300  $\mu$ l Tris-buffer (25 mM Tris HCl pH 7.5, 150 mM NaCl, 2 mM MgCl<sub>2</sub>, 0.5 % (v/v) Triton X-100) and glass beads by using the Fast-Prep 24 (MP Biomedicals) three times at 5 m/s for 30 sec. Between each repetition, the samples were cooled on ice for about 5 min. After centrifugation at 12 krpm and 4°C for 5 min, 8  $\mu$ l of the lysate was supplemented with 2  $\mu$ l of 1 mM BPS resulting in a total of 200  $\mu$ M/ $\mu$ l BPS. Finally, the absorbance of light at 535 nm was measured with the Nano Drop 2000 (Peglab) blanked with 200  $\mu$ M BPS in ddH<sub>2</sub>O.

### 3.5 Biochemical methods

#### 3.5.1 J2-RNA co-immunoprecipitation experiments

Yeast strains were grown to mid log phase ( $2 \times 10^7$  cells/ml) in 800 ml media. For the RNA-co-IP (RIP) experiment depicted in Figure 12b, the cells were additionally shifted to 37°C for 2 h. After harvest, the cells were resuspended in 20 ml media, transferred into a 25 cm diameter petri dish and UV-crosslinked at 254 nm for 7min. During crosslinking, the petri dish was placed on a cooling block. After the first 3.30 min, the Petri dish was carefully shaken to counteract the settling of cells. The cell suspension was then transferred into a 50 ml falcon and centrifuged at 4 krpm for 3 min, washed once in 5 ml sterile water and again transferred into a 15 ml falcon. After centrifugation at 4 krpm for 3 min, the supernatant was taken off and the cell pellet frozen in liquid nitrogen. Next, cells were lysed in equal amounts of about 2 ml RIP buffer (25 mM Tris HCl pH 7.5, 150 mM NaCl, 2 mM MgCl<sub>2</sub> 0.5 % (v/v) Triton X-100, 0.2 mM PMSF, 0.5 mM DTT, 10 U RiboLock™ RNase Inhibitor (Thermo Fisher Scientific) and protease inhibitor (Roche)) and glass beads by using the FastPrep®-24 machine (MP Biomedicals) 3-times for 30 sec at 5.5 m/s. In between, the samples were cooled down on ice for about 5 min. After a first centrifugation at 4 krpm and 4 °C for 3min, the lysate was transferred into 1.5 ml tubes and again centrifuged at 12 krpm and 4 °C for 5 min. 30 µl of the resulting cleared lysate was taken as input control and the remaining lysate was split equally and either incubated with or without 3 µl of the J2-antibody (1 µg/µl) from Scicons (Schonborn et al., 1991) for 30 min at 4 °C. After the first incubation the lysates were transferred to 5 times prewashed G-sepharose beads with RIP-buffer and incubated for another 90min at 4°C. The beads were then again washed 5-times with RIP buffer (0.25% Triton). For the experiments in Figure 15a and 21a, the supernatant was removed and SDS loading dye (125 mM Tris pH 6.8, 2% SDS, 10% glycerol, 5% 2-mercaptoethanol, bromphenolblue) was added, heated to 95°C for 5min and loaded onto an SDS-Polyacrylamide gel followed by western blot. For the J2-immunoprecipitations in Figure 12, the RNA was purified from the lysates and eluates via Trizol-chloroform (Ambion® RNA by Life technologies™) extraction followed by strand specific cDNA-synthesis and qPCR.

### 3.5.2 Cytoplasmic fractionation

For detection of RNAs in the cytoplasm, 200 ml cellcultures were grown to mid log-phase ( $2 \times 10^7$  cells/ml), harvested at 4 krpm and 4 °C for 3 min and washed once with 1 ml YPD/ 1 M Sorbitol/ 2 mM DTT. Following the washing step, the pellet was resuspended in YPD/ 1 M Sorbitol/ 1 mM DTT and cells were spheroplasted by adding 10 µl zymolyase (100 mg/ml) for about 10 min. For the cytoplasmic fractionation experiment followed by RNA seq (by Anna Greta Hirsch; Figure 6), the spheroplasted cells were recovered in 50 ml YPD/ 1 M Sorbitol for 30 min at 25 °C before they were shifted to 37 °C for 1 h. Next, one fifth of the cell suspension was separated for the analysis of the total RNA control and protein, and the remainder was used for the cytoplasmic fraction. For this, the cells were centrifuged at 2 krpm and 4 °C for 10 min and the pellet was resuspended in 500 µl Ficoll buffer (18 % Ficoll 400, 10 mM HEPES pH 6.0), followed by addition of 1 ml buffer A (50 mM NaCl, 1 mM MgCl<sub>2</sub>, 10 mM HEPES pH 6.0) and 1 µl Ribolock™ RNase Inhibitor (Thermo Fisher Scientific). The suspension was vortexed for about 5 sec and centrifuged for 10 min at 2 krpm. The resulting supernatant was used for the analysis of the cytoplasmic fraction. Here, 600 µl was taken for RNA isolation (Nucleo-Spin RNA® Kit) and 50 µl supplemented with 2 x SDS buffer (125 mM Tris pH 6.8; 2 % SDS; 10 % glycerol; 5 % 2-mercaptoethonal; bromphenolblue) for SDS-PAGE and western blot. The cell control (total) was lysed with 300 µl of the RIP buffer (25 mM Tris HCl pH 7.5, 150 mM NaCl, 2 mM MgCl<sub>2</sub> 0.5 % (v/v) Triton X-100, 0.2 mM PMSF, 0.5 mM DTT, 10 U RiboLock™ RNase Inhibitor (Thermo Fisher Scientific) and protease inhibitor (Roche)) and glass beads by using the Fast-Prep 24 (MP Biomedicals) three times at 5 m/s for 30 sec. After lysis and centrifugation at 12 krpm and 4 °C for 5 min, 250 µl of the supernatant was used for RNA isolation (Nucleo-Spin RNA® Kit) and 50 µl supplemented with 2 x SDS buffer for SDS-PAGE and western blot. To verify correct fractionation, samples were analyzed in western blots for the presence of the cytoplasmic Zwf1 and the nucleolar Nop1 proteins. RNA was isolated using the Nucleo-Spin RNA Kit (Macherey and Nagel).

### 3.5.3 Export release assay

Essentially, 2.8 L of the *mex67-5 xpo1-1 RPS2-GFP* strain was grown to mid log phase ( $2 \times 10^7$  cells/ml) and shifted to 37 °C for 2 h. 400 ml of cells were harvested before shifting to 37 °C, directly after shifting for 2 h (0min) and after shifting them back to 25 °C for 5 min, 10 min, 15 min, 30 min and 60 min. The cell pellets were frozen in liquid nitrogen and subsequent RIP

experiments were carried out as described in 2.5.1, with the exception that GFP Trap beads were used and no antibody was added. After the final washing step, the beads were split in half for RNA isolation with Trizol and subsequent qRT-PCRs and for SDS-PAGE and western blot analysis. For qPCR measurements, the single stranded RNAs (*RPS17A*, *RPS6A* and *HEM15*) and the dsRNA (*FRE5*, *HPF1* and *PRY3*) were analyzed. dsRNA targets were chosen based on three criteria: First, they showed an enrichment in RNAi.seq (Wery et al., 2016). Second, their asRNA had a higher RPKM than the mRNA and third, they showed an enrichment after J2-pulldown.

#### **3.5.4 RNA-Isolation using Trizol**

RNA-Isolation after immunoprecipitation was done with the Trizol reagent (Thermo Fisher Scientific). For this purpose, 1 ml Trizol was added to the washed beads and the lysate control taken beforehand. Subsequently, the samples were incubated at 65 °C and 1200 rpm for 10 min, supplemented with 200 µl chloroform, inverted several times and finally collected by centrifugation at 12 krpm for 15 min at room temperature. To precipitate the isolated RNA, 400 µl of the upper aqueous phase was transferred to 500 µl of isopropanol and 1 µl glycogen. After vortexing, the RNA was stored at -20 °C overnight. On the following day, the samples were centrifuged at 12 krpm and 4 °C for 30 min, followed by two washing steps with 1 ml of 70 % ethanol, that included centrifugation at 12 krpm and 4 °C for 15 min. Next, the pelleted RNA was dried at 65 °C for 10 min and resuspended in 20-100 µl RNase free H<sub>2</sub>O.

#### **3.5.5 RNA-Isolation using NucleoSpin® RNA from Machery-Nagel**

Direct RNA-isolation of cell lysates or after cytoplasmic fractionation was done with the NucleoSpin® RNA kit from Machery-Nagel by following the suppliers' instructions. Prior to RNA isolation, cells were either shifted to 37 °C for 1 h (Figure 5), to 2 % galactose overnight (Figure 23a), or treated with 100 µM BPS (by Judith Aylin Weyergraf, Figure 24a) or 5 mM FeCl<sub>3</sub> (by Judith Weyergraf, Figure 24b). Samples from the cytoplasmic fractionation experiments (3.5.2) were treated with the following exceptions. 250 µl of the total cell lysate was supplemented with 100 µl RA1 buffer before filtration. In the case of the cytoplasmic fraction, 310 µl of RA1 buffer and 490 µl of 100 % EtOH was added to the 600 µl lysate, resulting in a total volume of 1400 µl. The lysate was not filtrated on the violet column but immediately loaded twice in succession onto the blue column.

The isolated RNA was then reverse transcribed into cDNA. The samples of Figure 5 and Figure 6 were handed to the NIG (NGS-Serviceeinrichtung für integrative Genomik) for RNA-seq.

### 3.5.6 Strand specific cDNA synthesis

cDNA synthesis was done with the FastGene® Scriptase II cDNA Kit (Nippon genetics) by following the suppliers' manual. To exclusively measure either mRNA or asRNA in qPCR, gene specific primers were used in cDNA synthesis. Additionally, actinomycin D was added together with the reverse transcriptase, as it prevents unspecific transcription from DNA and thereby secures strand specific transcription as previously described (Xie et al., 2019; Perocchi et al., 2007). For the negative control, the same amount of RNA was treated without the reverse transcriptase.

### 3.5.7 qPCR

To quantify the RNA amounts, qPCR was carried out using cDNA from previously conducted reverse transcription. First, a master mix without the template DNA was made (Table 22). Of this master mix, 8  $\mu$ l was pipetted into wells of a 96 well plate, followed by the addition of 2  $\mu$ l template DNA. Each DNA sample was pipetted into three wells to create a triplet. For the following evaluation, the average of the triplet was taken. The negative control was only added to one well. For the calculations, the average of the subsequent Cq-values was used.

**Table 23: qPCR pipetting scheme**

Reagent	Amount
2x qPCR Master mix (Nippon Genetics)	5 $\mu$ l
RNase free H <sub>2</sub> O	2.6 $\mu$ l
Primer forward (10 $\mu$ M)	0.2 $\mu$ l
Primer reverse (10 $\mu$ M)	0.2 $\mu$ l
Template cDNA (1 ng/ $\mu$ l)	2 $\mu$ l



### 3.5.8 SDS-PAGE

To separate proteins from one sample, SDS-PAGE was conducted. For this purpose, an SDS-gel was poured consisting of a resolving gel (375 mM Tris pH 8.8; 0.1 % SDS; 10 % acrylamide mix; 0.1 % ammonium persulfate (APS), 0.04 % TEMED) below a stacking gel (125 mM Tris pH 6.8; 0.1 % SDS; 5 % acrylamide mix; 0.1 % ammonium persulfate (APS); 0,1 % TEMED). In this process, APS and TEMED were added just before pouring the respective part of the gel. First, two glass plates were separated by spacers, where the resolving gel was poured and covered with 2-propanol. After polymerization, the 2-propanol was removed, and the stacking gel was added, followed by placing a comb. After the polymerization of the stacking gel, the comb and the lower spacer were removed, and the gel was placed in a gel-run chamber. In the used system, the gel connects two chambers with SDS running buffer (25 mM Tris Base, 0.1% SDS, 190 mM glycine) and, respectively, two opposite electrodes. Finally, the samples mixed with 2x SDS loading buffer (125 mM Tris pH 6.8; 2 % SDS; 10 % glycerol; 5 % 2-mercaptoethonal; bromphenolblue) and a prestained protein marker (PageRuler™ Prestained Protein Ladder, Thermo Fisher Scientific) were loaded into the pockets formed by the comb. The SDS-PAGE was then running at 8 mA for about 16 h.

### 3.5.9 Western blot analysis

After SDS-PAGE, the proteins were transferred onto a nitro cellulose membrane by semi-dry western blotting. For this, the membrane and two slightly bigger Whatman papers were soaked in blotting buffer (25 mM Tris base, 192 mM glycine, 20 % methanol) and placed onto the anode plate in the following order: Whatman paper, membrane, SDS-Gel and Whatman paper. Air bubbles were removed, and blotting buffer was again added on top. The lid was attached and a current of approximately  $1.2 \text{ mA/cm}^2$  applied for 1 h 30 min. Thereafter, the blotting buffer was washed off the membrane with TBS-T (50 mM Tris base, 150 mM NaCl, 0.1 % Tween 20) for 5 min. Next, the membrane was blocked with 5 % milk powder in TBS-T for 60 min, followed by incubation with the primary antibody (table 6) in 1 % milk powder in TBS-T overnight at 4 °C. The membrane was then washed three times in TBS-T for 10 min, before the secondary antibody in 1 % milk powder in TBST-T (table 6) was added and incubated for 1 h at room temperature. Again, the antibody was removed, and the membrane washed three times in TBST-T for 10 min. Finally, the membrane was rinsed with water several

times and covered with ECL solution (Westernbright™ Quantum™ HRP substrate). Detection was carried out with the Fusion FX7 Edge 18.06c and Evolution-Capt. Edge Software.

### 3.6 *In vitro* binding studies

#### 3.6.1 Protein isolation and purification

Transformed Rosetta 2 *E. coli* cells were grown in 200 ml LB medium with ampicillin (100 µg/ml) and chloramphenicol (25 µg/ml) overnight, diluted to OD<sub>600</sub> = 0.1 in 1200 ml terrific both media (28.8 g yeast extract, 24 g Trypton, 9 ml 50 % glycerin, 17 mM KH<sub>2</sub>PO<sub>4</sub>, 72 mM K<sub>2</sub>HPO<sub>4</sub>) and 100 µg/ml ampicillin. The diluted cells were incubated at 32 °C and 130 rpm for 3 hours, followed by 37 °C and 130 rpm for 1 hour. 1.2 ml of 1M IPTG was added for protein induction and the culture was further incubated at 16°C and 130 rpm overnight. After induction, cells were washed in 200 ml IMAC loading buffer (50 mM NaH<sub>2</sub>PO<sub>4</sub>, 500 mM NaCl, 10 mM Imidazol, pH 7.8) and finally resuspended in 75 ml IMAC loading buffer with Roche complete Protease inhibitor (1 tablet/50 ml). Cells were lysed by using a microfluidizer with the setting 3-times at 700 bar. Thereafter, the lysate was centrifuged at 15,000 x g for 90 min. Cleared lysate was loaded onto a 5 ml HisFF column and subsequently washed with IMAC exchange buffer, then 1 M LiCl, again with IMAC exchange buffer and finally with IMAC loading buffer. The proteins were eluted with IMAC elution buffer (50 mM NaH<sub>2</sub>PO<sub>4</sub>, 500 mM NaCl, 400 mM Imidazol, pH 7.8) and dialyzed against heparin base buffer (40 mM HEPES KOH, 100 mM KCL, pH 7.5) overnight. After dialysis, the eluate was loaded onto a heparin column and again eluted with heparin elution buffer (40 mM HEPES-KOH, 100 mM KCl, 2 M NaCl, pH 7.5). Finally, the eluate was dialyzed in dialysis buffer (30 mM HEPES-KOH, 160 mM KCl, pH 7.6) for 2 days. Protein concentration was determined by measuring the OD at 280 nm.

#### 3.6.2 Electrophoretic mobility shift assay (EMSA)

The EMSA was used to analyze protein-RNA interactions. For this purpose, purified Mex67-Mtr2 (2.6.1) and either ordered FAB- or CY3-labeled RNAs (Sigma; Table 11) were used. For the binding assay (by Oliver Giesbrecht; Figure 15b), only the FAB-labeled RNA was utilized. dsRNAs were formed by incubating 20 µM of the labeled and 20.5 µM of the complementary non-labeled RNA in dialysis buffer (30 mM HEPES-KOH, 160 mM, KCl pH 7.6) in a total volume of 100 µl at 65°C for 5 min and immediate subsequent cool down on ice. The non-labeled RNA

oligo was added in excess to make sure, that all labeled and therefore visible RNAs are in a dsRNA structure. Next, dsRNAs or ssRNAs and Mex67-Mtr2 were incubated in the given molarity with 2  $\mu$ l Ribolock™ RNase Inhibitor (Thermo Fisher Scientific) in dialysis buffer and a total volume of 20  $\mu$ l at 30 °C for 15 min. For the competition assay, the FAB-labeled dsRNA, generated as mentioned above, and the CY3-labeled ssRNA was used (Figure 15c). Hereby, the respective competitor RNA was added after the first incubation of the substrate with Mex67-Mtr2 and further incubated at 30 °C for 15 min. Finally, a 6x loading dye (10 mM Tris pH 7.6, 60 % glycerol, 60 mM EDTA, 0.03 % bromophenol blue) was added to the samples and loaded onto a 0.5% agarose gel with 1xTAE (40 mM Tris, 1 mM EDTA, 0.1 % Acidic acid) pH 9.5. Complexes were separated by running the gel at 300 V for 40 min. In gel detection was carried out with the Fusion FX7 Edge 18.06c (Vilber) using the filter F-595 YR and Epi-Light module C530 or filter F-710 and Epi-Light module C640 together with the Evolution-Capt. Edge Software.

### 3.7 Microscopic studies

#### 3.7.1 Fluorescent *in situ* hybridization experiments (FISH)

To detect poly(A)<sup>+</sup> RNA, a Cy3-labeled oligo d(T)<sub>50</sub> probe (Sigma) was used. A 10 ml cell culture was grown to mid log phase ( $2 \times 10^7$  cells/ml). Depending on the experiment, cells were shifted to 0.7M NaCl or 10 % EtOH for the indicated time (Figure 19b, 20a), from 25 °C to 37 °C for 1h (Figure 13), from 37 °C to 25 °C for 2 h (Figure 21b, Figure 21c), to 2 % galactose for 6 h (Figure 16c) or fixed without shifting (Figure 17a, Figure 17b). Cell suspensions were fixed by transferring them into a falcon tube prepared with formaldehyde to reach a final concentration of 4 %. The mixture was incubated for 40 min at room temperature. If the cells were shifted to 37 °C beforehand, the first 10 min of fixation were conducted at 37 °C. After fixation, cells were collected by centrifugation at 4 krpm for 3 min. Afterwards, they were washed with 0.1 M potassium phosphate buffer pH 6.5, followed by washing twice with P-Solution (0.1 M potassium phosphate buffer pH 6.5, 1.2 M sorbitol). To remove their cell wall, cells were next spheroplasted by adding zymoylase (final 1 mM). After 7 min, the digestion was controlled under a light microscope. If 50-70 % of the cells appeared dark, the digestion was stopped by washing twice in P-Solution and a final resuspension in 300  $\mu$ l P-Solution. While washing, a slide was coated with polylysine and rinsed once with DEPC water before

20 µl of the cells were added to the wells. After settling for 20 min at room temperature, the cells were subsequently permeabilized in P-Solution with 0.5 % Triton® X-100 (10 min), rinsed once with P-Solution, equilibrated in 0.1 M TEA pH 8.0 (2 min), blocked with 0.25 % acetic anhydride in 0.1 M TEA (10 min) and pre-hybridized with Hybmix (50 % deionized formamide, 5× SSC, 1x Denhardtts, 500 µg/ml tRNA, 500 µg/ml salmon sperm DNA, 50 µg/ml heparin, 2.5 mM EDTA pH 8.0, 0.1 % Tween® 20, 10 % dextran sulfate) for 1 h at 37 °C. Hereinafter, the Cy3-labeled oligo d(T)<sub>50</sub> probe (1:200) was hybridized in Hybmix overnight at 37 °C. For this step, a Whatman paper was soaked with H<sub>2</sub>O and placed into a closed chamber together with the slide to prevent drying. After hybridization, cells were washed with 2x SSC and 1x SSC at room temperature, each for 1 h and 0.5x SSC at 37 °C and room temperature, each for 30 min. DNA was stained with DAPI (Sigma) in PBS (1:10000) for 2 min and washed once with 0.5 % Tween in 1x PBS and twice with 1x PBS each for 5 min. After the last washing step, the PBS was completely aspirated off and mounting medium was added. The slide was covered with a covering slide and sealed with nail polish. Microscopy studies were carried out with the Leica AF6000 microscope and pictures were obtained by using the LEICA DFC360FX camera and the LAS AF 2.7.3.9 software (Leica) and quantified by using the Fiji-software.

### **3.7.2 Immunofluorescence (IF)**

Cells were grown, harvested, and treated as described in the FISH experiment. After permeabilization, cells were rinsed once in P-Solution and blocked in ABB (0.1M Tris pH 9.0, 0.2 M NaCl, 5 % FCS, 0.3 % Tween, 500 µg/ml tRNA) for 1 h at 37 °C, followed by ABB with the addition of 1/200µl of the J2-antibody (1 µg/µl) from Scicons (Schonborn et al., 1991) and 0.2 % Triton for 2 h at 37 °C. Subsequently, cells were washed with 0.5 % Triton in 1x PBS for 15 min, twice with 1x PBS for 15 min and finally blocked again with ABB for 30 min. The secondary Cy3-conjugated anti-mouse antibody in ABB (1:200) was then incubated for 1 h at room temperature. Thereafter, the cells were washed with 0.5 % Tween in 1x PBS for 10 min and twice in 1x PBS for 10 min. Nuclei were stained with DAPI (Sigma) and mounting was carried out as described in FISH.

### **3.7.3 GFP-microscopy**

Cells were grown in glucose (2 %) containing medium until early log phase (0.5 x 10<sup>7</sup> cells/ml), washed once with 1 ml ddH<sub>2</sub>O, transferred into galactose (2 %) containing medium and grown

for 6 h. Fixation with 4 % formaldehyde was done for 1 min at room temperature, followed by washing twice with 1 ml P-Solution before a small aliquot of 20  $\mu$ l was incubated on a polylysine-coated slide for 15 min at room temperature. Permeabilization, DNA staining, microscopy and quantification were carried out as described in the FISH experiment.

### 3.8 Bioinformatics

#### 3.8.1 RNA-sequencing

The sequencing of RNA samples was conducted at the Microarray and Deep-Sequencing Facility Göttingen (Transcriptome and Genome Analysis Laboratory, TAL). Samples were prepared with the "TruSeq RNA Sample Prep Kit v2" according to the manufacturer's protocol (Illumina). Single read (50 bp) sequencing was conducted using a HiSeq 4000 (Illumina). Fluorescence images were transformed to BCL files with the Illumina BaseCaller software and samples were demultiplexed to FASTQ files with *bcl2fastq* (version 2.17). Sequences were aligned to the genome reference sequence of *Saccharomyces cerevisiae* (sacCer3, obtained from UCSC, <https://hgdownload.cse.ucsc.edu/goldenPath/sacCer3/bigZips/>) using the *STAR* software ((Dobin et al., 2013); version 2.5) allowing for 2 mismatches. Subsequently, abundance measurement of reads overlapping with exons or introns was conducted with *featureCounts* (Liao et al., 2014), *subread* version 1.5.0-p1, Ensembl (EF4.68) supplemented with the coordinates of UTRs, CUTs and SUTs (Xu et al., 2009), antisense and intergenic lncRNAs (Granovskaia et al., 2010; Yassour et al., 2010) and Xrn1-sensitive unstable transcripts (van Dijk et al., 2011). (Tuck & Tollervey, 2013) Data was processed in the R/Bioconductor environment ([www.bioconductor.org](http://www.bioconductor.org), R version 3.6.1) using the *DESeq2* package ((Love et al., 2014); version 1.24.0). Overlapping features were identified with BEDTools intersect (Quinlan & Hall, 2010) requiring overlaps to occur on the opposite strand with a minimum overlap of 0.5.

The sequencing data and abundance measurement files have been submitted to the NCBI Gene Expression Omnibus (GEO) database.

#### 3.8.2 Accession number

Cytoplasmic fractionation-Seq data have been deposited at the NCBI gene expression omnibus (GEO; [www.ncbi.nlm.nih.gov/geo/](http://www.ncbi.nlm.nih.gov/geo/)) with the GEO accession number GSE93307.

### 3.8.3 Gene ontology analysis

Gene ontology was analyzed with the Gene Ontology Term Finder from the *Saccharomyces* GENOME DATABASE (SGD). Genes were filtered to show a log<sub>2</sub> fold change above or less than 0 in the respective RNA-seq. As ontology aspect, “component” was selected and the minimum p-value set to 0.05.

### 3.8.4 Quantification

All experiments shown in this work were carried out at least three times independently. Error bars represent the standard deviation. P values were calculated using a one-tailed, two-sample unequal variance t-test. P values are indicated as follows: \*\*\*p < 0.001, \*\*p < 0.01, \*p < 0.05. For quantification of cells with the displayed phenotypes (Fig. 3b), 30 cells were counted for each experiment.

## 4. Results

### 4.1 The loss of *NPL3* leads to alterations in the cellular RNA composition of all classes of RNAs based on their type, abundance, and half-life

Npl3 is a major factor in gene expression, which stays associated with RNA transcripts from transcription to translation (Baierlein et al., 2013). Therefore, it is of great interest to find out how cells keep their RNA biogenesis up running after loss of *NPL3*. Previous publications have shown that pervasive transcription increases in *np13Δ* due to defects in transcription termination (Holmes et al., 2015). To further investigate, how the loss of *NPL3* influences the transcriptome of lncRNA and mRNA, RNA-sequencing was carried out in *np13Δ* and compared to wild type (Figure 5). Both strains were grown to log phase and shifted to 37°C for 1h before RNA-isolation and sequencing. The loss of Npl3 reduced the overall RNA amount by half, showing its great importance as an RNA binding factor in cells. Figure 5a shows the log<sub>2</sub> fold change of several RNA classes in *np13Δ*. mRNAs decreased on average, while only less than 25% showed a slight increase, indicating that Npl3, has on one hand, a strong stabilization effect on mRNA in wild type cells, but, on the other hand, can function as a repressor for different targets. In contrast, asRNAs were mostly upregulated but still comprised a similar range in their change upon loss of Npl3 as mRNAs. Because they are mostly generated through pervasive transcription or bidirectional promoters, their average enrichment in *np13Δ* indicates the previously described readthrough phenotype (Holmes et al., 2015). Like asRNAs, SUTs, XUTs and CUTs overall increased in *np13Δ*, displaying their similar regulation. Looking further at small ncRNA, the amounts of snoRNAs and rRNAs were both strongly reduced. In both cases, a regulatory role of Npl3 or its involvement in the processing of snoRNAs and rRNAs can be suggested. Overall, the loss of Npl3 clearly showed a huge impact on all transcripts, including a tight regulation of asRNA and thereby pervasive transcription.

## RESULTS

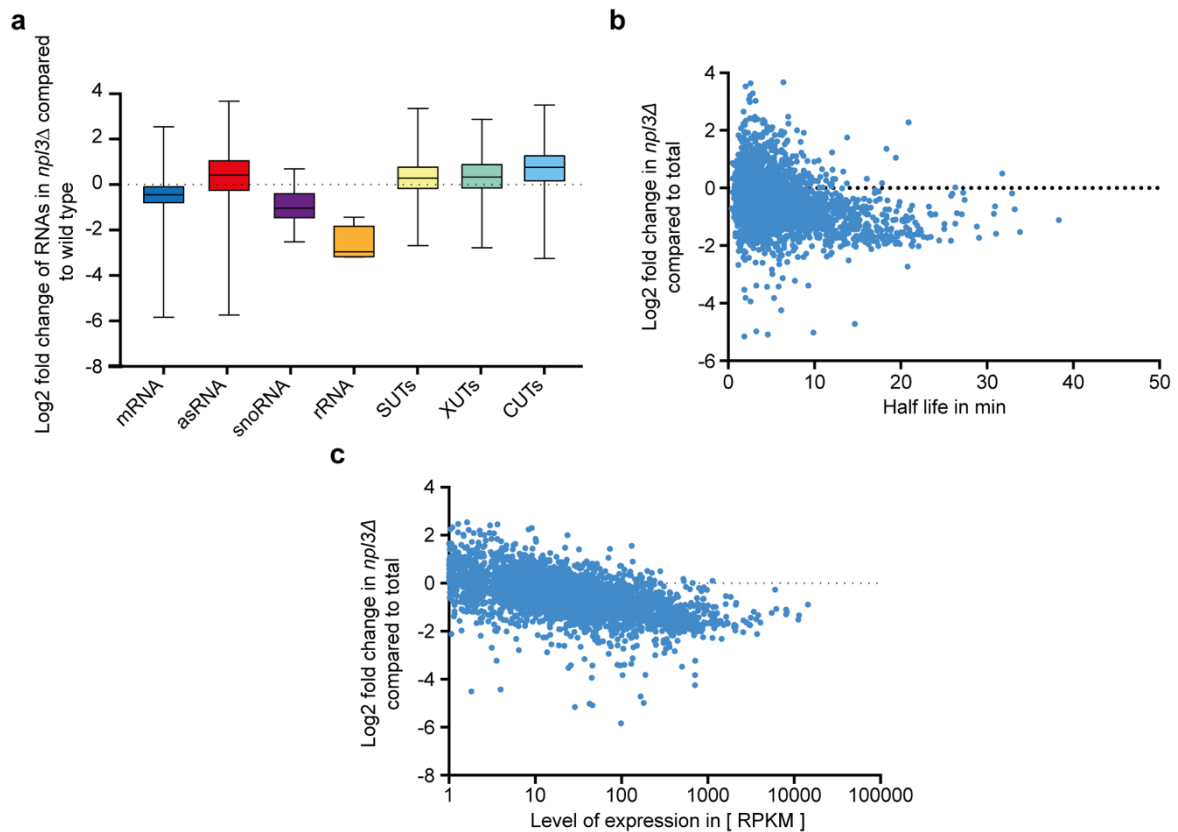


**Figure 5** *np13Δ* RNA-seq shows different alterations in the RNA level. **a)** *np13Δ* RNA-seq was grouped by RNA species and the log<sub>2</sub> fold change in *np13Δ* compared to wild type is represented as boxplots. The dotted line indicates the point zero (no change). **b)** Log<sub>2</sub> fold change of *np13Δ* compared to wild type was applied together with the measured RNA half-life from Chan et al. 2018. **c)** Log<sub>2</sub> fold change of *np13Δ* compared to wild type was applied together with the RNA expression level in RPKM (reads per kilobase million).

Since mRNAs overall showed great differences upon *NPL3* deletion, we further identified attributes that make mRNAs more likely to be affected. Application of the log<sub>2</sub> fold change in *np13Δ* with the abundance of mRNAs represented by their RPKM (reads per kilobase million) showed a strong negative correlation with a Spearman value of  $r = -0.59$  (Figure 5c). Highly expressed RNAs were therefore more affected in *np13Δ*, indicating a higher sensitivity to the loss of Npl3 as a potential stabilization factor. Highly expressed genes have also been suggested to be more stable as they have a higher half-life (Chan et al., 2018). By comparing the half-life of mRNAs as the degree of stability with the change in *np13Δ*, again, a negative correlation became evident (Spearman  $r = -0.4$ ; Figure 5b). Moreover, enriched targets in *np13Δ* were rather low abundant or even not expressed at all in wild type cells (Figure 5b). This suggests that Npl3 represses genes that are currently not needed.



## 4.2 Cytoplasmic fractionation RNA-seq analysis identifies properties of RNAs influencing their nucleo-cytoplasmic distribution

### 4.2.1 Cytoplasmic fractionation experiment and subsequent RNA-seq analysis unravels the nucleo-cytoplasmic distribution of RNAs

mRNAs are transcribed and processed in the nucleus and only after quality control exported from the nucleus into the cytoplasm, separating the place of transcription and processing from the place of translation. Intermediary quality control steps prevent the translation of faulty RNAs. This separation is similar for rRNAs, which are processed in the nucleolus, a subnuclear compartment of the nucleus, and afterwards are assembled in ribosomal subunits and exported into the cytoplasm (reviewed in Fernández-Pevida et al., 2015). For the nuclear splicesosomal snRNAs and telomerase *TLC1* lncRNA, a cytoplasmic phase for the RNP maturation has been observed (Becker et al., 2019; Hirsch et al., 2021). For these types of RNA, the cellular localization and nucleo-cytoplasmic distribution is known, while the knowledge of the cellular localization of lncRNAs in *S. cerevisiae* is still inadequate.

We carried out cytoplasmic fractionation followed by RNA-sequencing analysis to identify the nucleo-cytoplasmic distribution of RNAs in *S. cerevisiae*. Cells were subsequently grown to log phase, digested with zymolyase to remove the cell wall, and shifted to 37°C for 1 hour. Next, the cytoplasm content was isolated from the yeast cells, followed by RNA-isolation and RNA-seq (Figure 6a). The cytoplasmic RNA amount was then compared to the RNA isolated from whole cell lysates. The log<sub>2</sub> fold change of the cytoplasmic fraction compared to the total gave rise to the nucleo-cytoplasmic distribution of each RNA (Figure 6b). For following analysis of the export of RNAs, this experiment was additionally done in the double mutant *mex67-5 xpo1-1* (Figure 6a, Figure 11).

As expected, the rRNAs as part of the ribosome had a mostly cytoplasmic localization and were therefore enriched in the cytoplasmic fraction (Fernández-Pevida et al., 2015). Further, snoRNAs, which are known to be localized in the nucleolus to process rRNAs (Dupuis-Sandoval et al., 2015) were decreased in the cytoplasmic fraction. Both results verified the reliability of the method. In comparison, mRNAs showed a wide range between cytoplasmic and nuclear localization, indicating that they are no homogenic mass and that their nucleo-cytoplasmic distribution relies on different conditions or properties. Interestingly, the vast majority (~70

## RESULTS

%) of mRNAs were rather nuclear distributed, while approximately 25% showed a cytoplasmic enrichment.

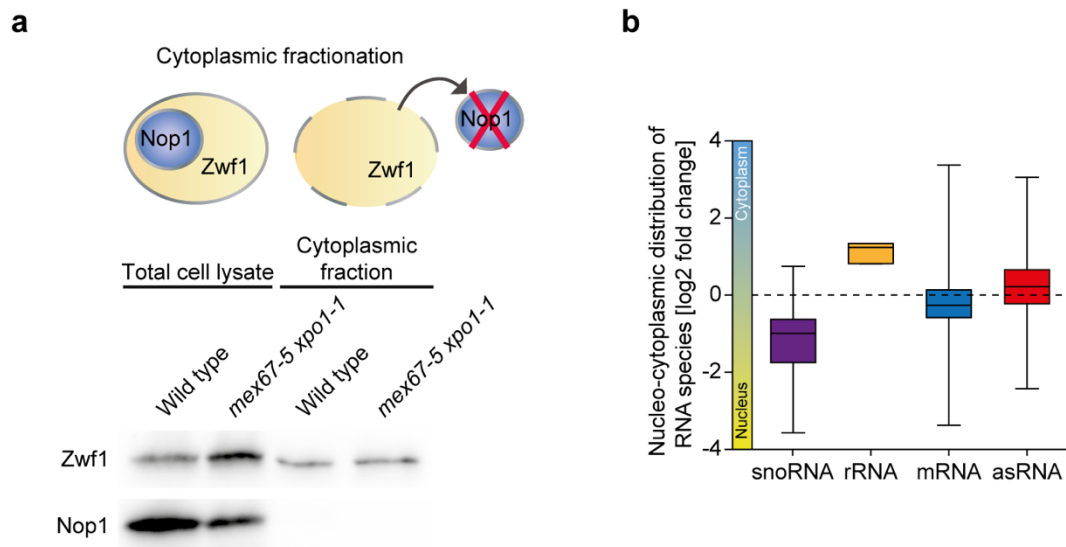


**Figure 6 Cytoplasmic fractionation followed by RNA-seq shows the nucleo-cytoplasmic distribution of RNAs (together with Anna Greta Hirsch and Orr Shomroni).** **a)** Cytoplasmic fractionation was conducted to isolate cytoplasmic RNAs. For comparison, total cell lysate was used. To validate the successful lysis and fractionation, Zwf1 (cytoplasmic protein) and Nop1 (nuclear protein) were detected in western blot analysis. **b)** RNA-seq data was grouped by RNA species and the log<sub>2</sub> fold change of the cytoplasmic fraction compared to total lysate gave rise to the nucleo-cytoplasmic distribution and is represented as boxplots. The dotted line indicates no change.

To identify possible properties, that influence the distribution of mRNAs, we first conducted gene ontology (GO)-term analysis. We grouped RNAs into being enriched or decreased in the cytoplasmic fraction of the wild type and got highly significant groups for both (Figure 7). More likely to be cytoplasmic distributed were mRNAs of membrane associated proteins (Figure 7a). After nuclear export, these RNAs are known to be transported further to the membrane by the She-machinery before translation (reviewed in Chartrand et al., 2001). Upon arrival, the proteins are translated and immediately incorporated into the membrane. This additional step of localizing the mRNA within the cytosol increases their time in the cytoplasm and could therefore explain their rather cytoplasmic distribution. Nuclear distributed mRNAs mostly encode cellular proteins and ribosomal proteins that are immediately translated after export (Figure 7b). Thus, GO-term analysis already revealed properties, that influence the nucleo-cytoplasmic distribution of mRNAs.

## RESULTS

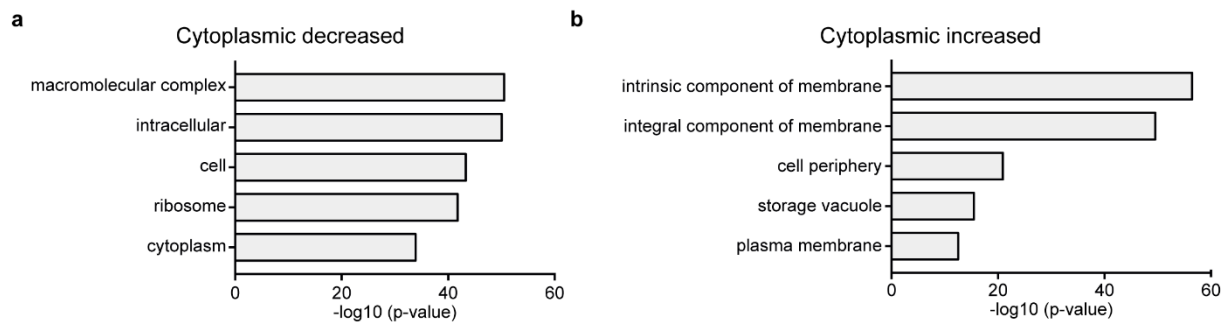


**Figure 7 Gene ontology (GO)-analysis of cytoplasmic fractionation RNA-seq shows terms of RNAs enriched or decreased in the cytoplasmic fraction. a)** GO-terms regarding the cellular components of cytoplasmic decreased RNAs from the cytoplasmic fractionation RNA-seq and their p-value as  $-\log_{10}$  are depicted. The higher the achieved value the higher the significance. **b)** Terms of cytoplasmic enriched RNAs from cytoplasmic fractionation RNA-seq and their p-value as  $-\log_{10}$  are depicted.

To further understand, how different RNAs are distributed, we additionally analyzed the distribution of lncRNAs, especially asRNAs, as they have been shown to be able to influence expression of protein coding genes. asRNAs were present in the cytoplasm and showed an enrichment on average (Figure 6b), which fits to the aspect, that they are mostly XUTs and thus degraded by the cytoplasmic exonuclease Xrn1 (van Dijk et al., 2011). Although cytoplasmic, their function has so far mostly been assigned to the modulation of transcription in the nucleus (Huber et al., 2016; van Dijk et al., 2011; Xu et al., 2011). In this regard, the localization of asRNAs does not match the place of their attributed function, thus indicating an incomplete view on asRNAs in the current literature.

### 4.2.2 dsRNAs are enriched in the cytoplasmic fraction

The cytoplasmic fractionation followed by RNA-seq revealed the cytoplasmic distribution of the average asRNA. It is currently unclear why asRNAs are exported into the cytoplasm, since only a widespread nuclear function has so far been assigned in yeast (Huber et al., 2016; van Dijk et al., 2011; Xu et al., 2011). Wery and colleagues, suggested that senseRNA and asRNA might form dsRNA, which would explain their nuclear export (Wery et al., 2016). In the model of Wery et al., dsRNA affiliated asRNAs are degraded via NMD, a translation associated degradation pathway, upon unwinding by the helicases Dbp2 and Mtr4. This raised the question whether the enrichment of asRNAs in the cytoplasm is mirrored by their sense counterparts. Assuming, that they would be exported as dsRNA, we first analyzed mRNAs whose asRNAs are expressed in at least similar levels. In that case, every mRNA had a potential asRNA. Indeed, mRNAs that had an equally expressed asRNA showed a cytoplasmic

## RESULTS

distribution on average, whereas mRNAs with no or less expressed asRNAs were on average nuclear distributed (Figure 8a). Further, Wery and colleagues have identified possible dsRNAs with an RNAi based RNA-seq approach. For that purpose, they used a *S. cerevisiae* strain that expressed *ARGO* and *DICER* of the RNAi-system, which *S. cerevisiae* has lost during evolution. (Drinnenberg et al., 2009) Dicer cuts dsRNAs in 23nt long RNA degradation products, which have subsequently been isolated and sequenced (Wery et al., 2016). We set up a probability to form dsRNA based on the log<sub>2</sub> fold change of degradation products in the RNAi strain compared to wild type. Thus, the higher the log<sub>2</sub> fold change, the higher the possibility to form dsRNA. We applied the resulting groups together with the nucleo-cytoplasmic distribution. Astonishingly, with higher probability to form dsRNA, the average nucleo-cytoplasmic distribution shifted to the cytoplasm (Figure 8b). This indicates that dsRNAs have a higher cytoplasmic distribution compared to single stranded mRNAs.

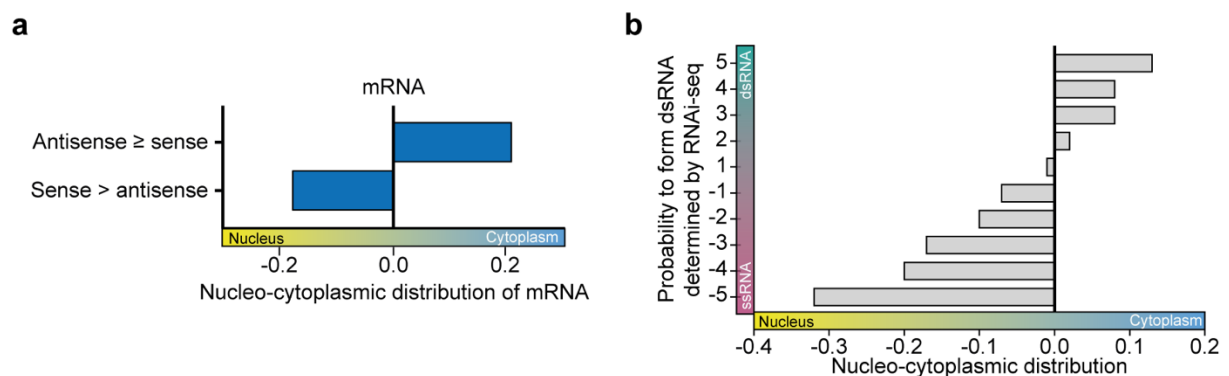


**Figure 8 dsRNAs are enriched in the cytoplasmic fraction. a)** The log<sub>2</sub> fold change of mRNAs in the cytoplasmic fractionation RNA-seq (nucleo-cytoplasmic distribution) is presented and grouped by their relative asRNAs levels. **b)** RNAs were grouped based on their probability to form dsRNA (log<sub>2</sub> fold change in RNAi-seq; Wery et al., 2016) and applied with their average nucleo-cytoplasmic distribution.

### 4.2.3 The cytoplasmic distribution of dsRNA is asRNA mediated

If asRNAs have the potential to influence the nucleo-cytoplasmic distribution of their mRNAs mediated by dsRNA formation, expressing an asRNA to a mRNA should change the mRNA's distribution. We conducted cytoplasmic fractionation experiments after overexpressing an asRNA to the intron containing *PHO85* mRNA (Figure 9a). For this purpose, we set the *asPHO85* (*SUT412*) under the control of the *GAL1* promoter and grew cells overnight in galactose containing media. Subsequential qPCR showed that the level of *asPHO85* reached the level of *PHO85* mRNA (Figure 9b). Astonishingly, the amount of the *PHO85* mRNA in the

## RESULTS

cytoplasm indeed increased about 2.5-fold after overexpression of the asRNA compared to no overexpression, whereas the total amount stayed the same (Figure 9c). This indicates a cytoplasmic shift of *PHO85* mRNA. Thus, the asRNA changed the nucleo-cytoplasmic distribution of its mRNA most likely through dsRNA formation. Interestingly, splicing was not negatively affected, but was rather improved since the amount of intron containing mRNA decreased with the asRNA overexpression (Figure 9c). Moreover, the mRNAs that reached the cytoplasm were spliced, indicating a functional quality control.

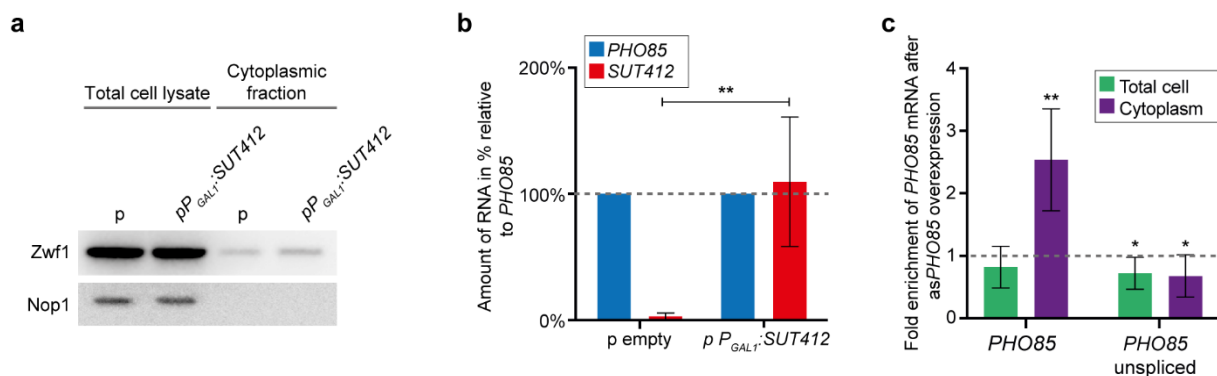


**Figure 9 Overexpression of *asPHO85* (*SUT412*) leads to a cytoplasmic shift of the corresponding mRNA *PHO85*.** **a)** Western blot analysis of the successful cytoplasmic fractionation was shown by using antibodies for Zwf1 as a cytoplasmic and Nop1 as a nuclear protein control. **b)** *asPHO85* (*SUT412*) was overexpressed under the control of the *GAL1* promoter. RNA levels were determined by qPCR and related to *PHO85* mRNA levels in the respective strain. **c)** After overexpressing *asPHO85*, cytoplasmic fractionation was carried out and RNA levels were analyzed by qPCR and compared to no overexpression. The dashed line indicates the wild type level.

### 4.2.4 A rather nuclear distribution of mRNAs is caused by a reduced export rate and affects highly expressed genes

After verifying the asRNA mediated cytoplasmic enrichment of mRNAs, we wanted to address the cause. A cytoplasmic enrichment does not necessarily imply an increased cytoplasmic lifespan like we suggested for mRNAs of membrane proteins (Figure 7b). Other variables can also influence the nucleo-cytoplasmic distribution of an RNA. Transcription, degradation, translation, storage, and the export rate can alter the visible distribution of an RNA in the cell (Bahar Halpern et al., 2015). A slow cytoplasmic degradation or high translation rate would stabilize an RNA in the cytoplasm, leading to a cytoplasmic localization but also to a longer half-life. There are several publications that have identified the half-life of RNAs transcriptome wide (Miller et al., 2011; Peccarelli & Kebaara, 2014; Presnyak et al., 2015). The results of these studies differ highly as they have used different methods. To compare the half-life with the

## RESULTS

probability to form dsRNA, we used the data of the latest publication, which have utilized a refined pseudo uridylation method (Chan et al., 2018b) and applied it together with the RNAi-seq data (Wery et al., 2016). The half-life of an RNA did not correlate with the probability to form dsRNA, ruling out a stabilizing effect for the cytoplasmic enrichment of dsRNA (Figure 10a). Analyzing the half-life regarding the nucleo-cytoplasmic distribution of RNAs, however, showed a significant correlation (Figure 10b).

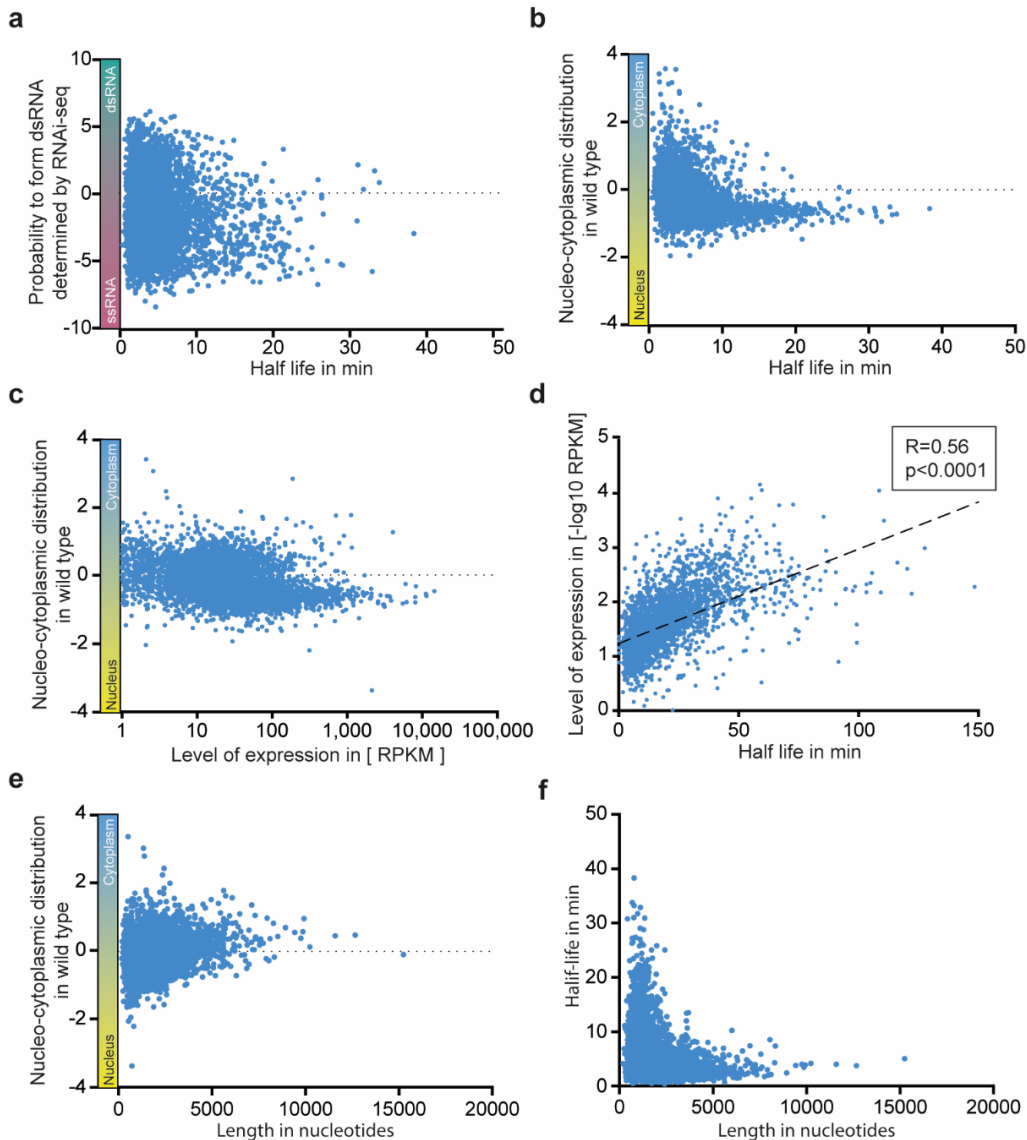


**Figure 10 The nucleo-cytoplasmic distribution correlates with the half-life, the level of expression and the length of transcripts.** **a)** The probability to form dsRNA (based on Wery et al., 2016) was applied with their measured half-life (Chan et al., 2018) **b)** The nucleo-cytoplasmic distribution determined by cytoplasmic fractionation RNA-seq was applied with the half-life of RNAs. **c)** The comparison of the nucleo-cytoplasmic distribution with the level of expression in RPKM of RNAs is displayed. **d)** The correlation of the level of expression in RPKM and the half-life of RNAs is displayed. **e)** The nucleo-cytoplasmic distribution of RNAs was applied with their length in nucleotides. **f)** The half-life measured by Chan et al. is displayed with the length of transcripts in nucleotides.

Interestingly, RNAs with a rather long half-life tend to show a nuclear distribution and thus spend more time in the nucleus. RNAs with a long half-life are almost exclusively nuclear. This shows that RNAs are differently fast processed in the nucleus and exported. Therefore, the time of export represents a new key factor influencing the half-life of RNAs. Previously, a correlation between the half-life and the expression level of RNAs was found (Chan et al., 2018). We verified that and wondered, whether a nuclear distribution is based on the expression level (Figure 10d). Therefore, we applied the RPKM value of each RNA with its nucleo-cytoplasmic distribution (Figure 10c). mRNAs that have a read count higher than 100 RPKM indeed showed a more nuclear localization. Further, we analyzed the nucleo-cytoplasmic distribution of RNAs based on their length and found that the length of a transcript did correlate with a cytoplasmic localization. In that case, the longer a transcript the less likely it is nuclear localized (Figure 10e). Interestingly, long transcripts had a rather short half-life (Figure 10f). Therefore, transcripts with a short half-life are rather long and cytoplasmic and transcripts with a long half-life are rather highly expressed and nuclear. Taken together, nuclear mRNA distribution can be explained by a longer nuclear timespan, but at least in the case of dsRNA, their cytoplasmic distribution is not due to a longer cytoplasmic lifetime.

### **4.3 dsRNAs are preferentially exported mediated by Mex67**

#### **4.3.1 The nuclear export block in *mex67-5 xpo1-1* retains ssRNAs and dsRNA**

The longer lifetime of nuclear RNAs can be explained by a slower nuclear export rate. In this case, export would be the determinant for a nuclear distribution of transcripts. The cytoplasmic localization of dsRNAs could be mediated by the nuclear export process, too.

To investigate our hypothesis, we first wanted to prove, that dsRNAs are exported like ssRNAs. Thus, we analyzed the cytoplasmic fractionation experiment in the nuclear export mutant *mex67-5 xpo1-1* (Figure 6a). We found a similar retention of RNAs in the nucleus based on their probability to form dsRNA. All groups of transcripts based on the RNAi-seq showed a decrease in the cytoplasm compared to the whole cell lysate (Figure 11a). Again, validating the reliability of our cytoplasmic fractionation seq and determining Mex67 and Xpo1 to be responsible for dsRNA export.

## RESULTS

Interestingly, GO analysis in the *mex67-5 xpo1-1* double mutant showed an enrichment of specific RNA classes in the cytoplasm, including mRNAs associated with cell division, meiosis, and developmental processes (Figure 11b). These mRNAs code for proteins that help newly derived daughter cells to establish their integrity. Therefore, they are stored in the cytoplasm to be immediately translated after cell division. Blocking export did not affect their cytoplasmic distribution.

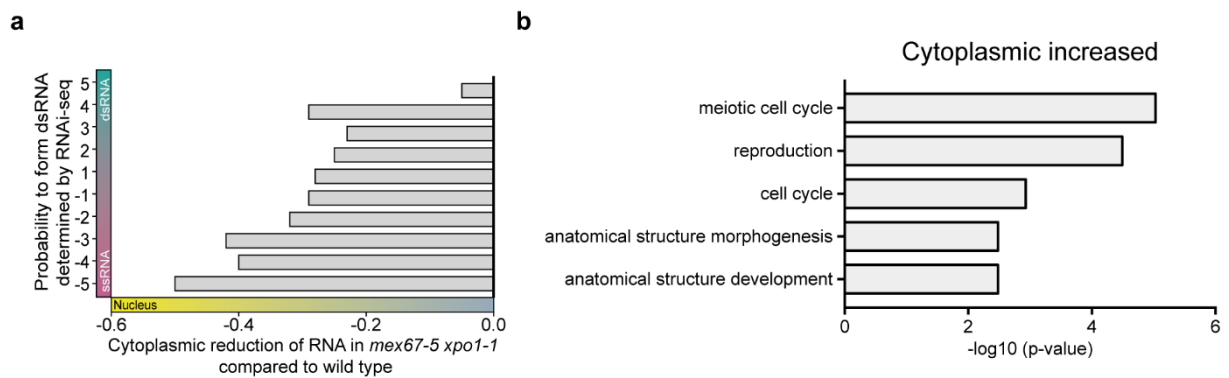


**Figure 11** In the double mutant *mex67-5 xpo1-1*, most RNAs are retained in the nucleus. **a**) RNAs were grouped by their probability to form dsRNA determined by RNAi-seq and applied with the nucleo-cytoplasmic distribution in *mex67-5 xpo1-1*. **b**) Terms of cytoplasmic enriched RNAs from the cytoplasmic fractionation seq and their p-value as  $-\log_{10}$  are depicted.

### 4.3.2 dsRNAs are exported through Mex67 and Xpo1 and are detached during translation

Next, we wanted to verify our findings of Mex67 and Xpo1 being responsible for dsRNA export. dsRNA associated asRNAs are post-transcriptionally processed like mRNAs and degraded by NMD (de Andres-Pablo et al., 2017; Quinn et al., 2016; Wery et al., 2016).

Because dsRNA targets are retained in the nucleus of *mex67-5 xpo1-1* cells (Figure 11a), they should be exported and processed by the same factors and mechanisms as single stranded mRNAs. To figure out the crucial steps of dsRNA transport, we utilized the dsRNA specific antibody J2 (Schonborn et al., 1991; Xie et al., 2019). To show its specificity for dsRNA in yeast, we first conducted immunoprecipitation analysis. Because of the potential vulnerability of dsRNA to helicases, we UV crosslinked cells before lysis. For qPCR, we chose four dsRNA targets based on their enrichment in the RNAi-seq and a higher expressed asRNA. All four identified dsRNA targets were enriched after J2 pulldown compared to a single stranded mRNA (Figure 12a). If export is blocked in the *mex67-5 xpo1-1* mutant, the amount of co-precipitated dsRNA enriched further indicating their nuclear formation (Figure 12b).



## RESULTS

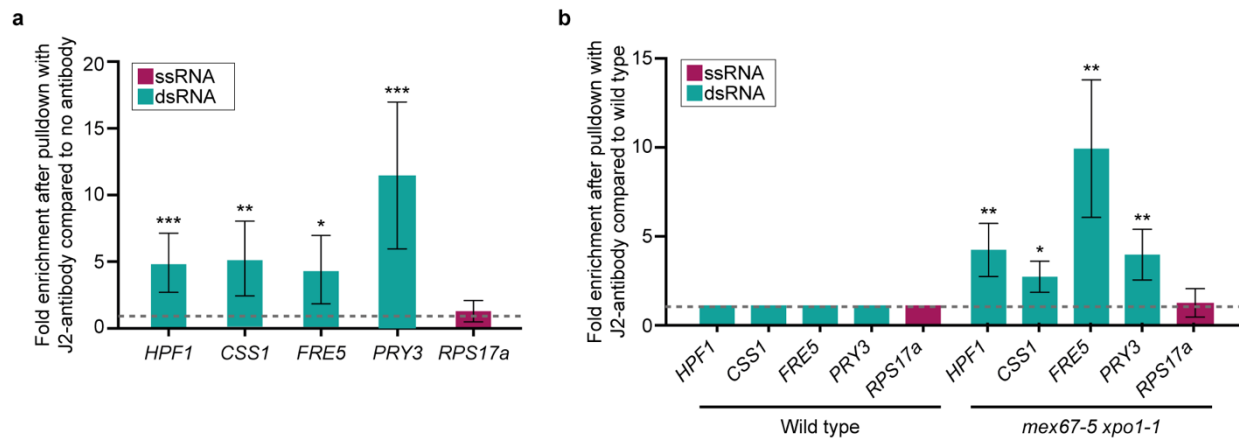


**Figure 12 J2-immunoprecipitation validates dsRNA targets and shows their accumulation upon nuclear export block. a)** Immunoprecipitation with the J2 antibody in wild type cells was carried out followed by RNA isolation and qPCR. The pull-down was related to a no antibody control. **b)** J2-IPs in *mex67-5 xpo1-1* were compared to J2-IPs in wild type cells after 2h shift to 37°C.

Further, we developed an immunofluorescence protocol with the dsRNA specific antibody J2. With that, the nuclear accumulation of dsRNA in *mex67-5 xpo1-1* was further noticeable (Figure 13a), as the Cy3 signal colocalized with the DAPI signal. Interestingly, in wild type, the J2 antibody showed a dot-like staining, primarily in the cytoplasm. This could indicate an arrangement of dsRNA in certain bodies or multiple binding of antibodies to one dsRNA. NMD, the main degradation pathway of cytoplasmic asRNAs, takes place during translation. Thus, we additionally carried out J2 immunofluorescence in the *nmd3Δ* or *rpl10(G161D)* translation inhibiting mutants. Nmd3 is involved in the nuclear export of the large ribosomal subunit and in the *rpl10(G161D)* mutant the subunit joining of the ribosomes is inhibited (Hedges et al., 2005; Ho et al., 2000). In both mutants, dsRNA amounts increased in the cytoplasm, indicating that the dsRNA separation requires functional translation.

These experiments suggest that mRNA and asRNA form a double strand in the nucleus and are exported as such. In the cytoplasm, they engage the ribosome as dsRNA, which probably separates the dsRNA, followed by degradation of the asRNA through NMD and translation of the mRNA. Therefore, double stranded mRNAs showed a similar behavior as single stranded mRNAs (Figure 13b).

## RESULTS

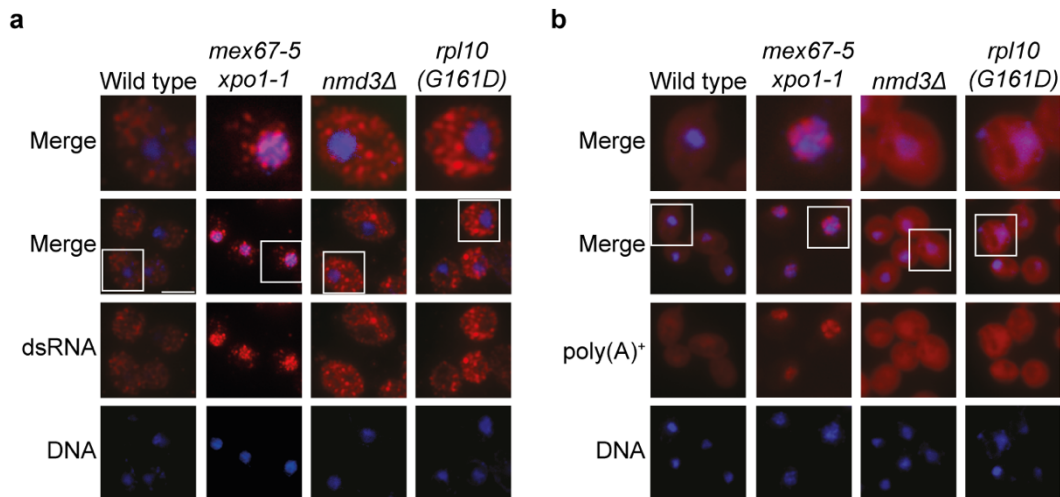


**Figure 13 dsRNAs are formed in the nucleus and detached at the ribosomes.** a) Immunofluorescence using the J2 antibody and a Cy3-labeled secondary antibody was conducted in indicated strains after 3h at 37°C. DNA was stained with DAPI. b) FISH was carried out using a Cy3-labeled oligo d(T) probe to visualize poly(A)<sup>+</sup> RNA in indicated strains.

### 4.3.3 dsRNAs are preferentially exported compared to ssRNA

Knowing the export receptors and the destination of dsRNA, we wanted to compare the export of dsRNA and ssRNA by investigating which RNA reaches the ribosomes first after an export block and the subsequent release. First, the export of all RNAs was inhibited by shifting the export mutant *mex67-5* to its non-permissive temperature of 37°C for 2h. It has been shown that the export defect is reversible within minutes by shifting the strain back to 25°C (Segref et al., 1997). We took samples of cells at 0, 5, 10, 15, 30 and 60 minutes after shifting back to 25 °C and, in addition, cells that were not shifted at all. Subsequently, we conducted RNA-CoIP experiments with Rps2-GFP (Figure 14a), a protein of the small ribosomal subunit. In the RNA-CoIP, Rps2-GFP and bound RNAs were isolated from the cell lysate with the help of αGFP-agarose beads. Further isolation of bound RNA followed by qPCR allowed us to quantify the amount of specific RNA targets bound to Rps2 and thus the ribosome at the different time points. We picked three dsRNA and three ssRNA targets for qPCR. Comparing the pulldown of cells shifted to 37 °C to non-shifted cells, all RNAs bound to Rps2 decreased significantly (Figure 14b). After releasing the export for 5 min, the binding of ssRNA and dsRNA increased significantly compared to no release. While the dsRNA median was already at ~80% of the binding under normal conditions, ssRNA just reached ~25%. At 10 min after release, the difference was even more pronounced: The binding of dsRNAs even exceeded the starting point with a median of ~143%, whereas ssRNAs did not exceed ~40%. At timepoints 15 min

## RESULTS

and 30 min, the binding of dsRNAs and ssRNAs to Rps2 was still higher than before the backshift, but lower as compared to the previous timepoints. This could point out the necessary cytoplasmic recycling of the RBPs and export factors involved in nuclear export. With elapsing time (60 min), the binding of ssRNA and dsRNA to Rps2 approached the initial situation. Here, the median of dsRNAs reached ~93% and of ssRNAs ~84%.

This impressively shows that dsRNAs indeed leave the nucleus faster or preferentially compared to ssRNAs, explaining their high cytoplasmic representation and confirms the idea that the time of nuclear export is the key determinant for the nucleo-cytoplasmic distribution of RNAs.

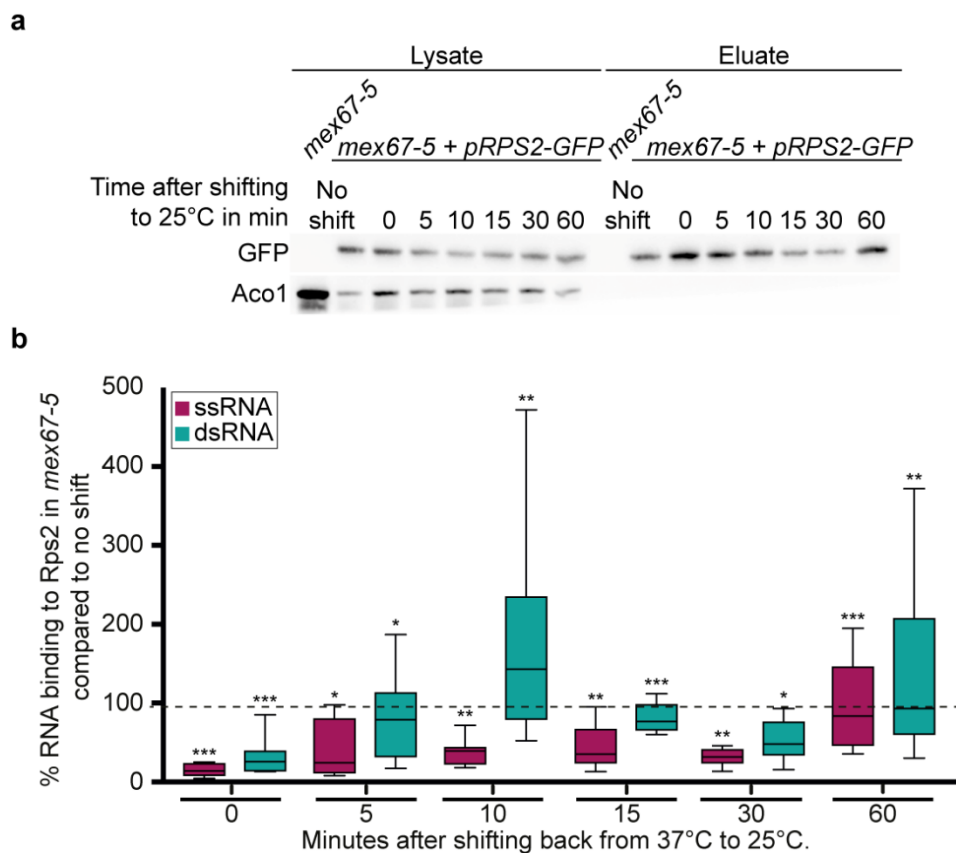


**Figure 14 dsRNAs reach ribosomes first after export release compared to ssRNA targets. a)** Rps2-RIP was conducted at several time points before and after export release in *mex67-5* by shifting cells back from 37°C to 25°C. Western blot is shown confirming the successful pulldown of the ribosomal protein by using a primary GFP antibody. Aco1 was used as negative control. **b)** After pulling down Rps2-GFP, bound RNA was isolated and qPCR of three dsRNA targets (*FRE5*, *HPF1* and *PRY3*) and three ssRNA targets (*RPS6a*, *RPS17a* and *HEM15*) was conducted. The fold enrichment of each group is displayed in one box plot for every time point compared to no shift. The significance of the time point 0 is given compared to no shift, the significances of time points 5 to 60 is given compared to time point 0.

#### **4.3.4 Mex67 preferentially binds to dsRNAs which possess a higher capacity for Mex67 attachment compared to ssRNAs**

With the release assay, we were able to highlight the preferential nuclear export of dsRNAs. Previous studies have shown that increasing transport receptor coverage along an mRNA and the affinity of the export receptor to the RNA improves initiation and the successful export (Azimi et al., 2014; Soheilypour & Mofrad, 2018). Hence, we wanted to know whether there is a difference between ssRNA and dsRNA in binding the export heterodimer Mex67-Mtr2, which could be the mediator of preferential export.

First, we conducted J2-immunoprecipitation experiments followed by SDS-PAGE and western blot analysis to prove Mex67 binding to dsRNA *in vivo* (Figure 15a). Next, *in vitro* electro mobility shift assays (EMSA) were conducted using the heterodimer Mex67-Mtr2 expressed and isolated from *E. coli* and synthesized RNAs (Sigma Aldrich). Mex67-Mtr2 was added in increasing amounts to the ssRNA or dsRNA. Comparing both gels, the dsRNA alone and in complex with Mex67-Mtr2 did run faster and appeared at a lower height than the respective ssRNA, most likely because of its higher negative charge (Figure 15b). The addition of Mex67-Mtr2 to ssRNA lead to a complete shift of the RNA at a 2-molar excess of the protein and a saturation at a 5-molar excess. For dsRNA, the complete shift was accomplished with only a 3-molar excess and the saturation was reached at a 10-molar excess of Mex67-Mtr2. This shows a higher capacity of dsRNA to bind Mex67 compared to ssRNA.

Next, we conducted a competition assay based on the previous EMSA. For a better differentiation of ssRNA and dsRNA and to prevent interaction between them, RNA oligos with different sequences and tags were used. Both RNAs had the same amount of C, G, T and A and the ssRNA was labeled with Cy3, whereas the dsRNA was FAM labeled. First, ssRNA or dsRNA was incubated with a 4-molar excess of Mex67-Mtr2 for 15 min at 30 °C, to ensure a strong upshift but not too much excess of Mex67. Subsequently, either ssRNA or dsRNA was added as a competitor, incubated for an additional 15 min at 30 °C, and applied on the agarose gel. Adding dsRNA as the competitor to the Mex67-Mtr2 prebound ssRNA, it was displaced already at a ratio of 3:1 (substrate:competitor). The Cy3 labeled ssRNA showed up at the non-bound RNA height, which increased with increasing amounts of dsRNA competitor. Additionally, the RNP complex shifted to the dsRNA complex, which is visible by the height of the band and the dominant fluorescent color of the FAM label. This indicates a higher affinity of Mex67-Mtr2 to dsRNA compared to ssRNA (Figure 15c). When using dsRNA as the substrate and ssRNA as the

## RESULTS

competitor, only the addition of 4  $\mu\text{M}$  ssRNA to 3  $\mu\text{M}$  dsRNA led to a slight displacement of dsRNA. Apart from that, a noticeable proportion of the added ssRNA was present as unbound. Thus, ssRNA seems to be a weak competitor against dsRNA. We concluded that the higher affinity and the higher capacity of dsRNA for Mex67-Mtr2 could be the reason for the preferential export of dsRNA.

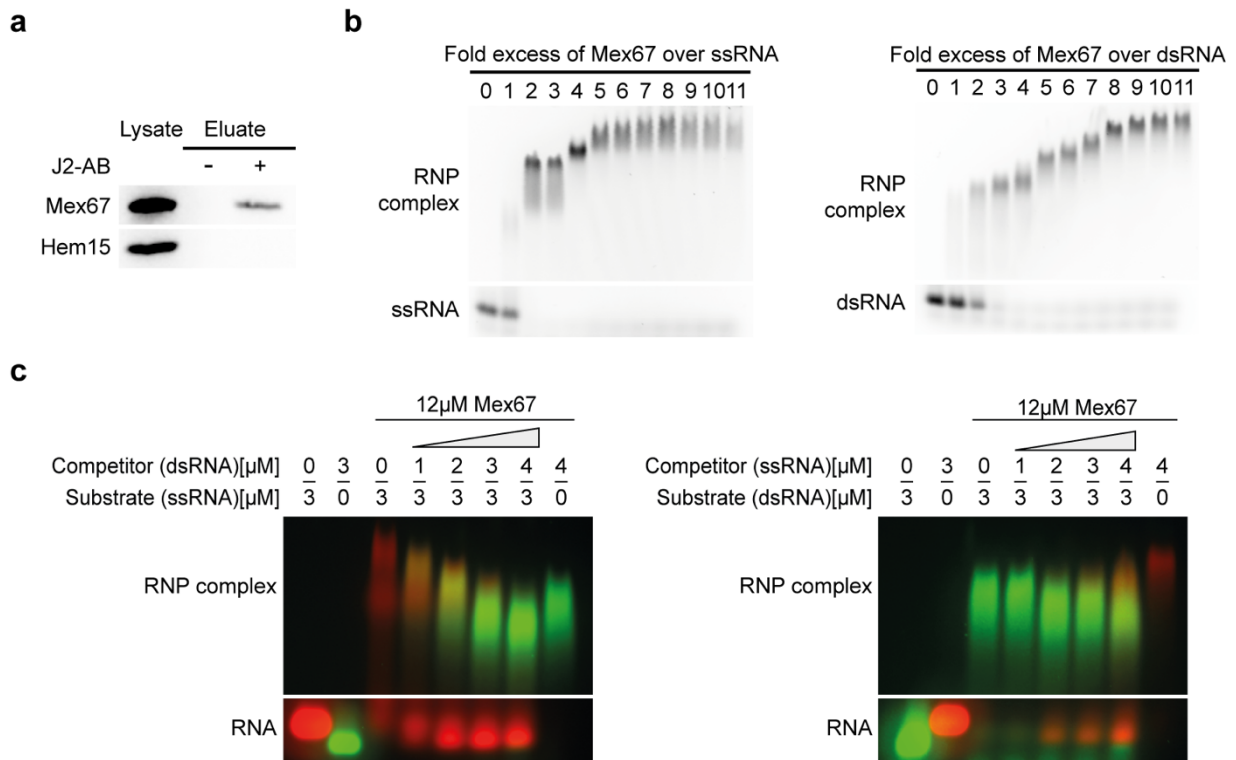


**Figure 15 Mex67 preferentially binds to dsRNA and dsRNA shows a higher capacity for Mex67 compared to ssRNA. a)** J2-immunoprecipitation in wild type cells followed by SDS-PAGE and western blot was conducted. To detect Mex67, the membrane was incubated with primary Mex67 and secondary HRP-coupled antibody. Hem15 served as negative control. **b)** FAM labeled ssRNA or dsRNA was incubated with increasing amounts of Mex67-Mtr2 and loaded on a native agarose gel. The in-gel detection of the FAM label was carried out with the Fusion FX7 Edge 18.06c. **c)** For the competition assay, the substrate was first incubated with a 4-molar excess of Mex67 before the competitor RNA was added in increasing amounts and incubated again for 15 min at 30 °C. For comparing the unbound fraction, the substrate and the competitor were loaded without protein. The samples were loaded on a native agarose gel and the signal was detected with Fusion FX7 Edge 18.06c. For better differentiation, the ssRNA was labeled with Cy3 and the dsRNA with FAM.

#### 4.4 dsRNA formation is essential for cells particularly during adaptation to environmental change like stress conditions

##### 4.4.1 dsRNAs are essential for cells

Identifying a new mechanism of gene regulation at the level of export, we wondered about its importance for cells. If dsRNAs are crucial for cell fitness, their degradation should be harmful for cells. Previously, the overexpression of the dsRNase RNaseIII from *E. coli* in *S. cerevisiae* and its nuclear localization has been shown to cause a growth defect (Pines et al., 1988). At that time, the authors could not find a reason, since known possible target-like rRNAs were unchanged.

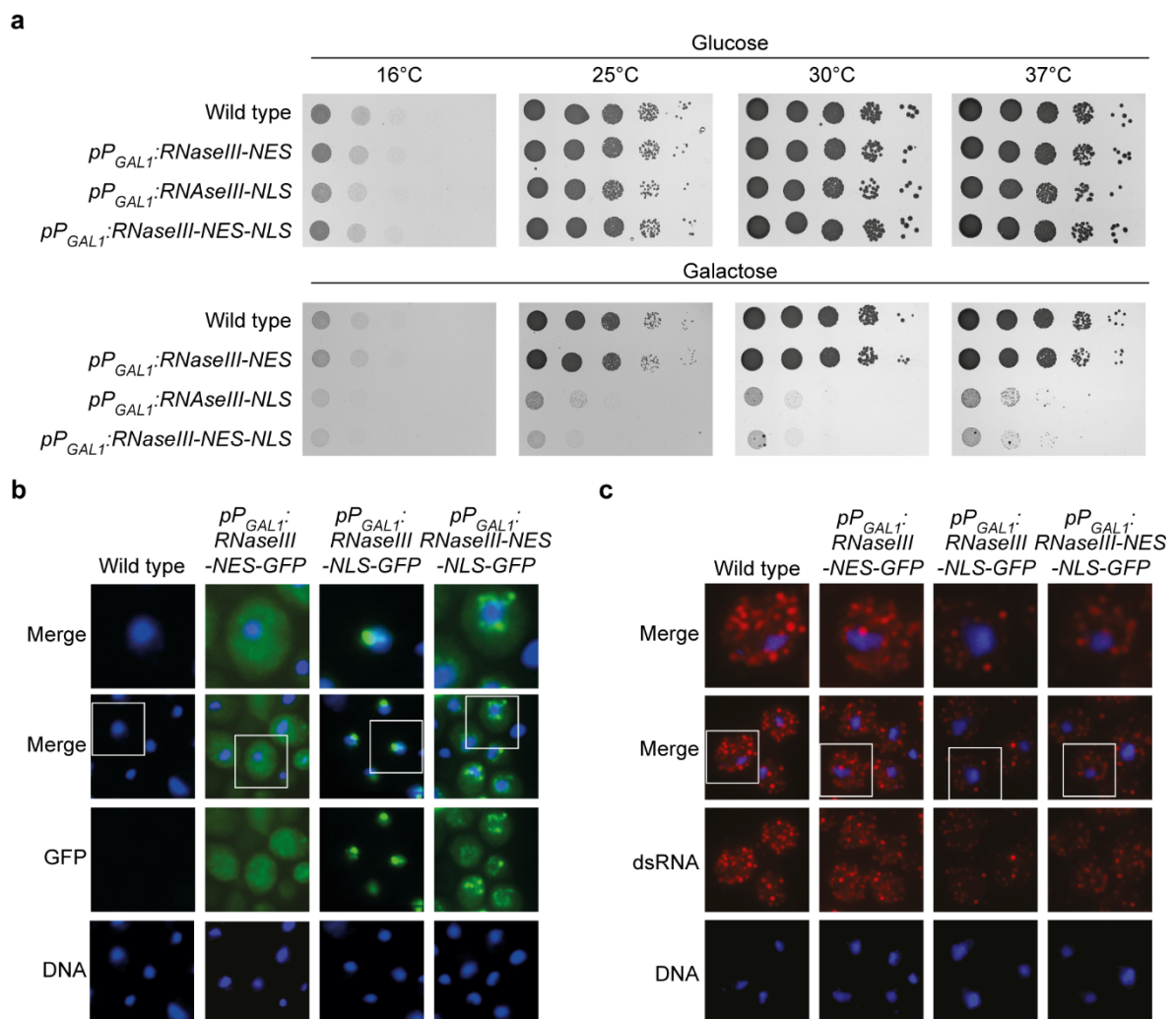


**Figure 16 Nuclear RNaseIII expression is toxic to cells. a)** Serial dilution of strains that either contained the  $P_{GAL1}:RNaseIII-NES$ ,  $P_{GAL1}:RNaseIII-NLS$  or the  $P_{GAL1}:RNaseIII-NES-NLS$  were spotted onto glucose and galactose containing plates. A wild type strain containing an empty vector served as a control. **b, c)** GFP microscopy (b) and J2-immunofluorescence (c) of strains used in a) after 6h of galactose induction are shown.

## RESULTS

We repeated the experiment and expressed *RNaseIII* under the *GAL1* promoter in *S. cerevisiae* cells and located the enzyme to the cytoplasm or nucleus with a nuclear export (NES) or nuclear localization signal (NLS). All *RNaseIII* constructs were *GFP* tagged and therefore their localization could be analyzed with fluorescence microscopy (Figure 16b). The expression of the *RNaseIII* construct was induced for 6h by the addition of galactose (Figure 16b, Figure 16c). A longer incubation led to overexposed signals (not shown). As expected for the respective localization signal, the *RNaseIII*-NES was present in the cytoplasm, *RNaseIII*-NLS in the nucleus and *RNaseIII*-NES-NLS at the nuclear rim. Analyzing the cell viability via growth test showed, that if the *RNaseIII* was localized to the nucleus as in the case for the *RNaseIII*-NLS or *RNaseIII*-NES-NLS, cells did not survive (Figure 16a). dsRNAs are hence essential for cell survival. As soon as the *RNaseIII* was only located to the cytoplasm, cells showed no growth defect under normal conditions. The growth test is supported by a J2-immunofluorescence, that showed a great reduction of dsRNAs after 6h of *RNaseIII*-NLS or *RNaseIII*-NES-NLS induction, but almost no change in cells expressing the cytoplasmic *RNaseIII*-NES (Figure 16c). This leads to the assumption, that the degradation of dsRNA is the cause for the cell death. The difference between the nuclear and cytoplasmic *RNaseIII* might be a higher vulnerability of dsRNAs in the nucleus. It is also possible, that the *RNaseIII* reaches a higher concentration in the nucleus and thereby increased chances to catch and degrade a dsRNA. Still, the expression of nuclear *RNaseIII* demonstrated the essentiality of dsRNA and again supports their nuclear formation.

### **4.4.2 Stress associated SRATs can form dsRNA structures leading to the cytoplasmic enrichment of their mRNA**

dsRNAs are essential for *S. cerevisiae* cells. However, the question remained, when an asRNA mediated preferential export of mRNAs is needed. Previous studies have linked lncRNAs and especially asRNA transcription to inducible genes, that are involved in environmental changes or stress response (Wery et al., 2016; Xu et al., 2011).

## RESULTS

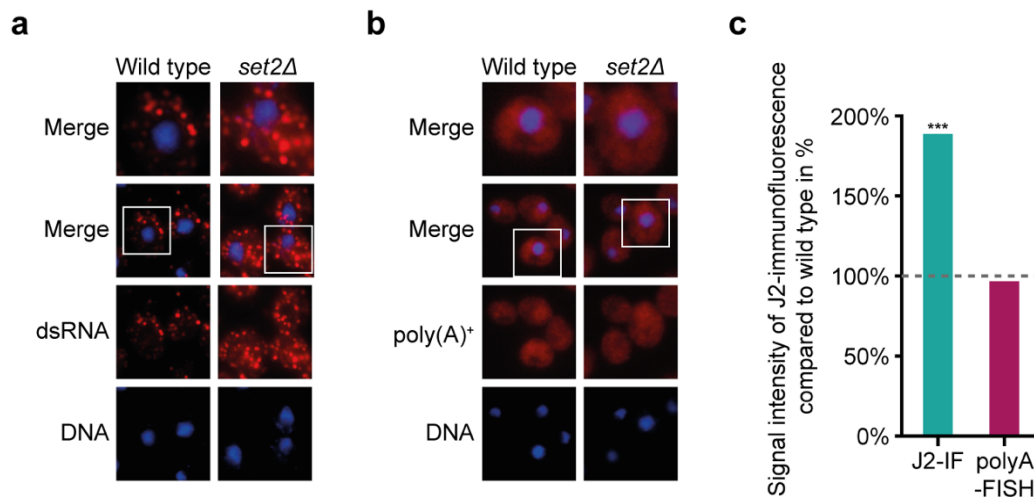


**Figure 17 Higher concentration of SRATs in *set2Δ* form dsRNAs with their mRNA counterpart and are exported. a) J2-immunofluorescence and b) poly(A)<sup>+</sup> FISH in *set2Δ* and wild type cells are shown. c) Quantification of the signal in the Immunofluorescence or FISH in *set2Δ* compared to wild type.**

It has been shown earlier, that after depletion of the histone methylase *SET2*, a set of asRNAs called Set2-repressed antisense transcripts (SRATs) increases (Venkatesh et al., 2016). Most of them are antisense to stress response genes or genes involved in aging, which suggests that these asRNAs are regulated through Set2 and could therefore play a regulatory role. We carried out J2-immunofluorescence analysis in the *set2Δ* strain and showed an increased amount of dsRNAs, while general poly(A)<sup>+</sup> RNA levels remained similar (Figure 17). Thus, the upregulation of new asRNAs led to more exported dsRNAs. Further, we conducted cytoplasmic fractionation experiments in the *set2Δ* strain in order to investigate, whether newly formed dsRNAs are enriched in the cytoplasm (Figure 18a). We chose the SRAT *asSEG2* that reached a similar amount to its *SEG2 mRNA* in *set2Δ* (Figure 18b). While the previous study did not find a change in the amounts of mRNAs opposite to SRATs, in our experiment total *SEG2 mRNA* increased slightly about 1.5-fold (Figure 18c). However, the enrichment in the cytoplasmic fraction exceeded the total one twice, showing a clear cytoplasmic shift of the *SEG2 mRNA*. It is the same effect we saw for the *PHO85 mRNA* after galactose induction of the *asPHO85* overexpression. This finding supports our idea of an asRNA mediated preferential export.



## RESULTS

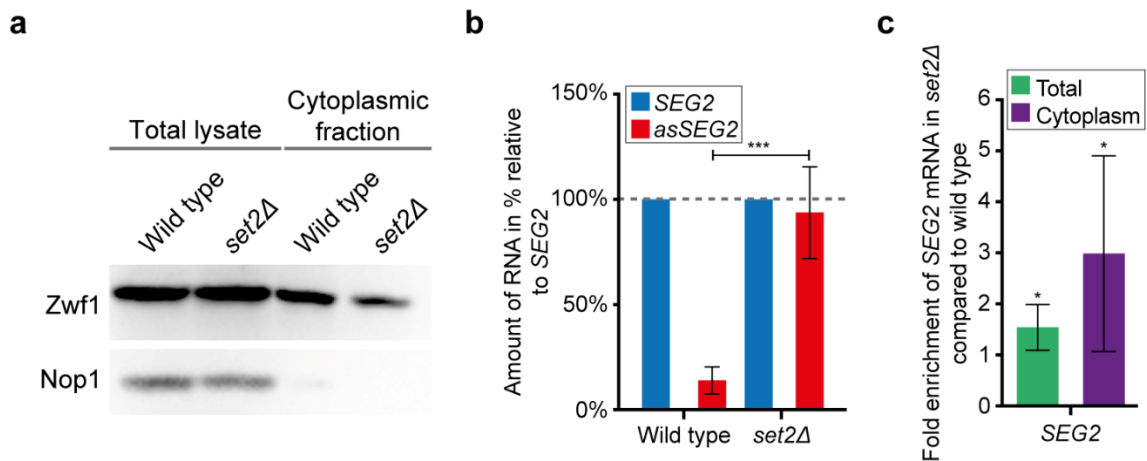


**Figure 18 Increased levels of *asSEG2* in *set2Δ* leads to a cytoplasmic shift of its mRNA *SEG2*.** **a)** Western blot analysis of cytoplasmic fractionation experiments in *set2Δ* and wild type. The cytoplasmic Zwf1 resembles the cytoplasmic part and the nucleolar Nop1 the nuclear part of a cell. **b)** qPCR of *SEG2* and *asSEG2* was conducted in wild type and *set2Δ*. Their level was related to *SEG2* mRNA in the respective strain. **c)** qPCR after RNA isolation from the cytoplasmic fractionation experiment shows *SEG2* mRNA level in *set2Δ* compared to wild type in the cytoplasmic fraction and the total lysate.

### 4.4.3 The general asRNA level is increased under stress conditions, leading to more dsRNA formation

Stress response is widely studied and of great interest, being crucial for cell fitness and survival. In *S. cerevisiae*, stress response can be triggered, for example, by heat, changes in osmolarity or ethanol (de Nadal et al., 2011). Here, cells must react fast to sudden changes in the environment. We analyzed the RNA-seq data of Lahtvee et al. to investigate possible changes in asRNA expression during osmotic stress. In their experiment, Lahtvee and colleagues shifted cells for 30 min to 0.6 M NaCl before RNA isolation and sequencing. (Lahtvee et al., 2016) In our analysis, we aligned their data to the annotation used in our cytoplasmic fractionation and *np13Δ* RNA-seq that comprises lncRNAs. Figure 19a shows the log<sub>2</sub> fold change of mRNAs and asRNAs in cells shifted to 0.6M NaCl compared to no shift. As expected, mRNAs showed a wide range of changes after stress induction, reaching from a ~10 log<sub>2</sub>-fold increase to a -5 log<sub>2</sub>-fold decrease. To prevent cell damage, stress response genes are upregulated and wild typic expressed genes are rather downregulated (Nadal-Ribelles et al., 2012). Not only mRNAs were regulated during osmotic stress but also asRNAs, showing their inclusion in response to osmotic stress (Figure 19a). asRNAs even showed an increase on average, but a slightly lower range than mRNAs. To see, whether the upregulation of stress response genes and asRNAs leads to increased dsRNA amounts, we stressed cells either with

## RESULTS

10% EtOH or 0.7 M NaCl for 5 min and 10 min and conducted J2-immunofluorescence (Figure 19b). In both cases, dsRNAs increased strongly in the cytoplasm compared to wild typical conditions. This confirms the involvement of asRNAs and dsRNAs in the rapid stress response.

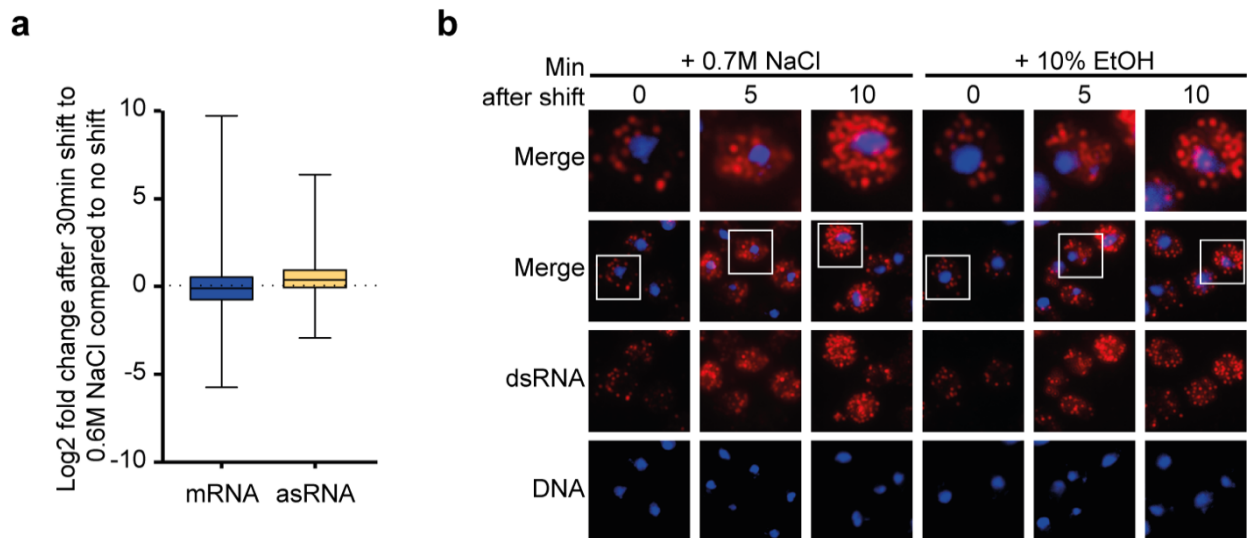


**Figure 19 asRNA and dsRNA take part in stress response. a)** The data of Lahtvee et al. was analyzed for mRNA and asRNA change after 30min exposure to 0.6 M NaCl compared to standard media (Lahtvee et al., 2016). The log2 fold change of both RNA classes is shown as a box plot. **b)** J2-Immunofluorescence was conducted after exposing cells to 0.7 M NaCl and 10 % EtOH. Cells were fixated at 5 min and 10 min after addition and with no addition of NaCl or EtOH.

### 4.4.4 dsRNA formation is advantageous for stress response

The immediate dsRNA formation after stress induction and the nuclear export of these new dsRNAs highlight their role in stress response. Already under normal conditions, dsRNA is necessary for cell survival, but only significantly decreased if degraded by RNaseIII in the nucleus (Figure 16). Here, we used the *RNaseIII-NES* construct under the *ADH1* promoter, that was directed into the cytoplasm and not toxic to cells (Figure 16). The cells were stressed by either exposing them to 10% EtOH or 0.7 M NaCl. The previously described increase of cytoplasmic dsRNA was again neglected after expressing the cytoplasmic RNaseIII (Figure 20a), showing its functionality and potency under these conditions. Consequentially, under both stress conditions, the growth of cells expressing *RNaseIII-NES* was reduced compared to wild typical cells (Figure 20b). This shows that dsRNA is specifically needed during stress conditions. In that case, cells must react fast and quickly induce stress responsive genes for survival. A preferential export mechanism is advantageous in these situations and explains its need.

## RESULTS

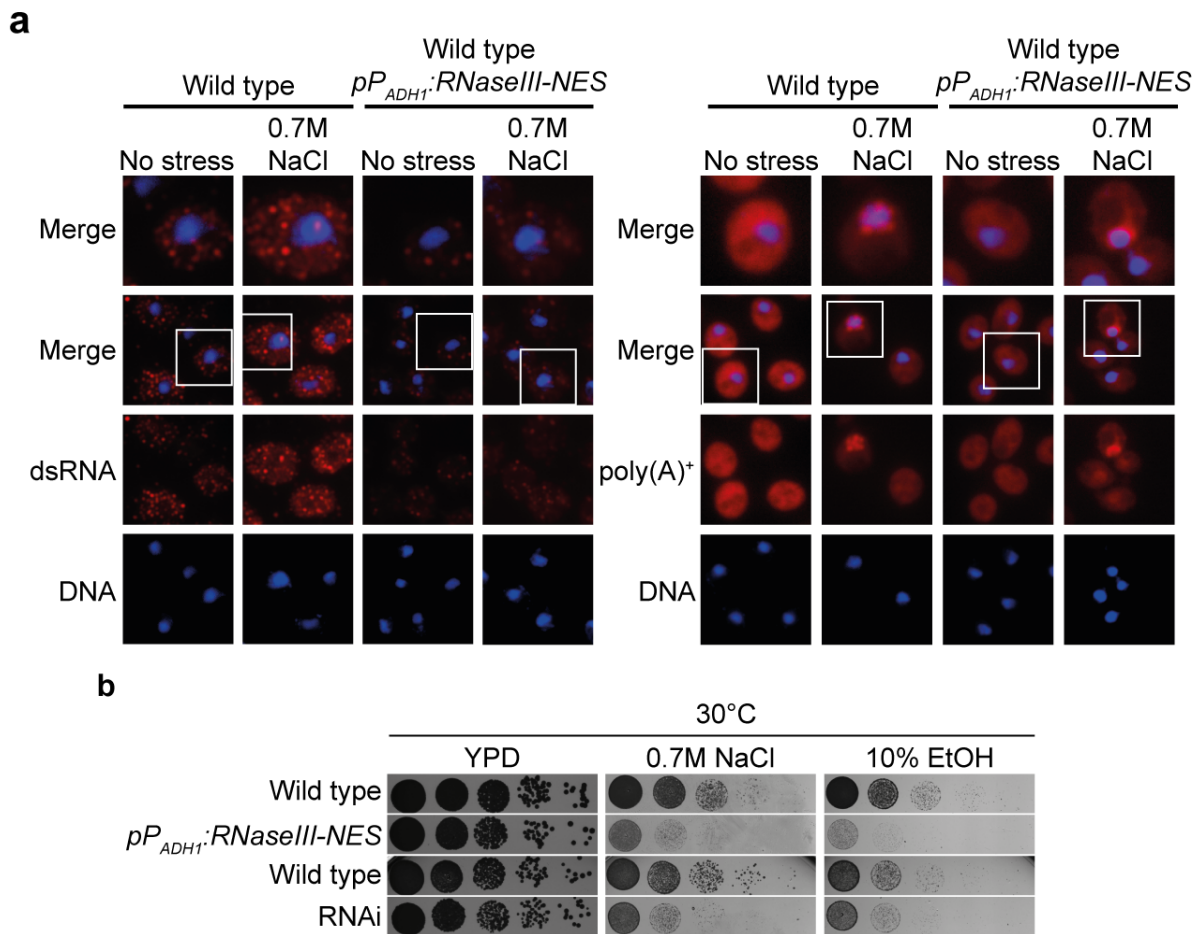


**Figure 20 Restriction of dsRNAs during stress leads to a growth defect of cells. a, b)** J2-Immunofluorescence and poly(A)<sup>+</sup>-FISH were carried out with cells expressing *RNaseIII-NES* under the *ADH1* promoter and exposed to 0.7 M NaCl for 30 min. For comparison, cells were either not stressed or did not express the *RNaseIII*. **b)** Growth test was conducted on plates containing either 0.7 M NaCl or 10% EtOH compared to regular YPD plates of strains either expressing *RNaseIII-NES* or the RNAi-system compared to their respective wild types.

## 4.5 The helicase Dbp2 plays a key role in dsRNA formation

### 4.5.1 Dbp2 interacts with dsRNA and its loss leads to reduced dsRNA amounts

From our data we suggest a new mechanism of preferential gene expression. It is mediated by asRNAs through dsRNA formation with its mRNA, leading to a preferential Mex67 binding and nuclear export. We further wondered whether factors are directly involved in dsRNA formation and thereby are crucial for this mechanism. There is one nuclear and one cytoplasmic helicase in *S. cerevisiae*, that can not only unwind dsRNA structures. Under certain circumstances, these helicases are also able to hybridize two RNA strands (Putnam &

## RESULTS

Jankowsky, 2013). The nuclear one is Dbp2, which has a strong preferred binding to dsRNA. In complex with Yra1, its helicase function is inhibited, and the dsRNA binding dominates, leading to the hybridization of bound complementary strands *in vitro* (Ma et al., 2013, 2016). Because dsRNA formation takes place in the nucleus, Dbp2 could be a reasonable candidate for sense-antisense dsRNA hybridization *in vivo*. To test that, we used the J2 antibody for co-immunoprecipitation experiments, in which we were able to show a binding of Dbp2 to dsRNA in wild type cells (Figure 21a).

Furthermore, we carried out J2-immunofluorescence experiments in *dbp2Δ*. First, we created the haploid *dbp2Δ* strain and verified its cold sensitivity (Cloutier et al., 2012). Interestingly, *dbp2Δ* does not grow at 25 °C and 30 °C, but at 37 °C (Figure 21b). Therefore, the strain was grown at 37 °C and shifted to its non-permissive temperature of 25 °C for 2 hours prior to the immunofluorescence experiment. Indeed, *dbp2Δ* showed a nearly complete loss of dsRNA at its non-permissive temperature, whereas poly(A)<sup>+</sup> RNA accumulated in the nucleus (Figure 21b, c). These findings indicate a direct involvement of Dbp2 in dsRNA formation and show its necessity for proper mRNA export.

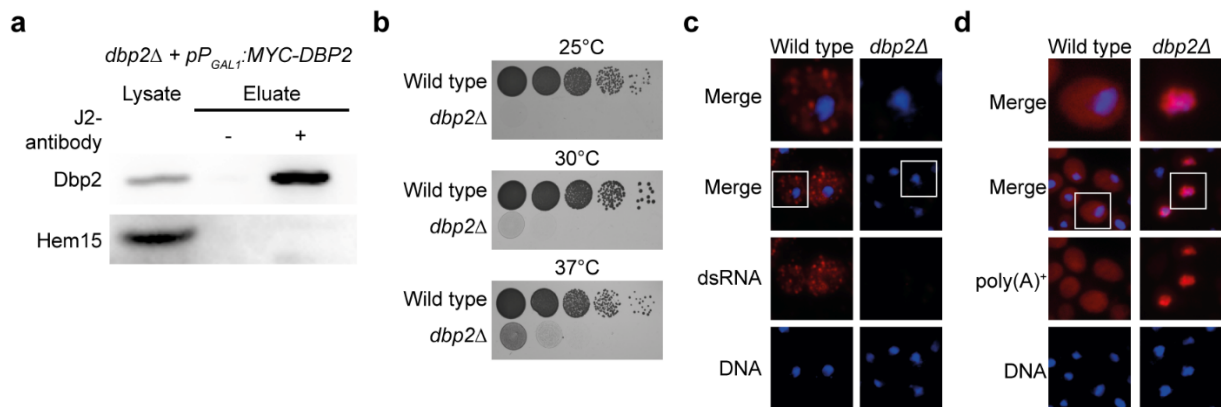


**Figure 21 Dbp2 is involved in dsRNA hybridization.** **a)** The J2 antibody was used for co-immunoprecipitation experiment with myc-tagged Dbp2 followed by SDS-PAGE and western blot analysis. **b)** Serial dilution test of *dbp2Δ* at the indicated temperatures is displayed. A wild type strain acts as the control. **c)** J2-Immunofluorescence and **d)** poly(A)<sup>+</sup> was conducted in *dbp2Δ* and wild type cells after shifting cells from 37 °C to 25 °C for 2 h, the non-permissive temperature of *dbp2Δ*.

### 4.5.2 The asRNA mediated preferential export is lost in the *dbp2Δ* mutant

If Dbp2 is required for dsRNA formation, asRNA mediated preferential export should be lost in *dbp2Δ*. Previously, we showed that overexpressing *asPHO85* lead to the cytoplasmic

## RESULTS

enrichment of the *PHO85* mRNA (Figure 9). We repeated this experiment in *dbp2Δ* cells (Figure 22a). Overexpression of the *asPHO85* in *dbp2Δ* and subsequent cytoplasmic fractionation showed no effect on the nucleo-cytoplasmic distribution of its *PHO85* mRNA anymore (Figure 22c). While the asRNA reached even higher amounts in *dbp2Δ* compared to wild type after galactose induction (Figure 22b), the cytoplasmic mRNA level stayed the same. This indicates that Dbp2 is a key player in dsRNA formation and in the asRNA mediated preferential export of mRNAs.

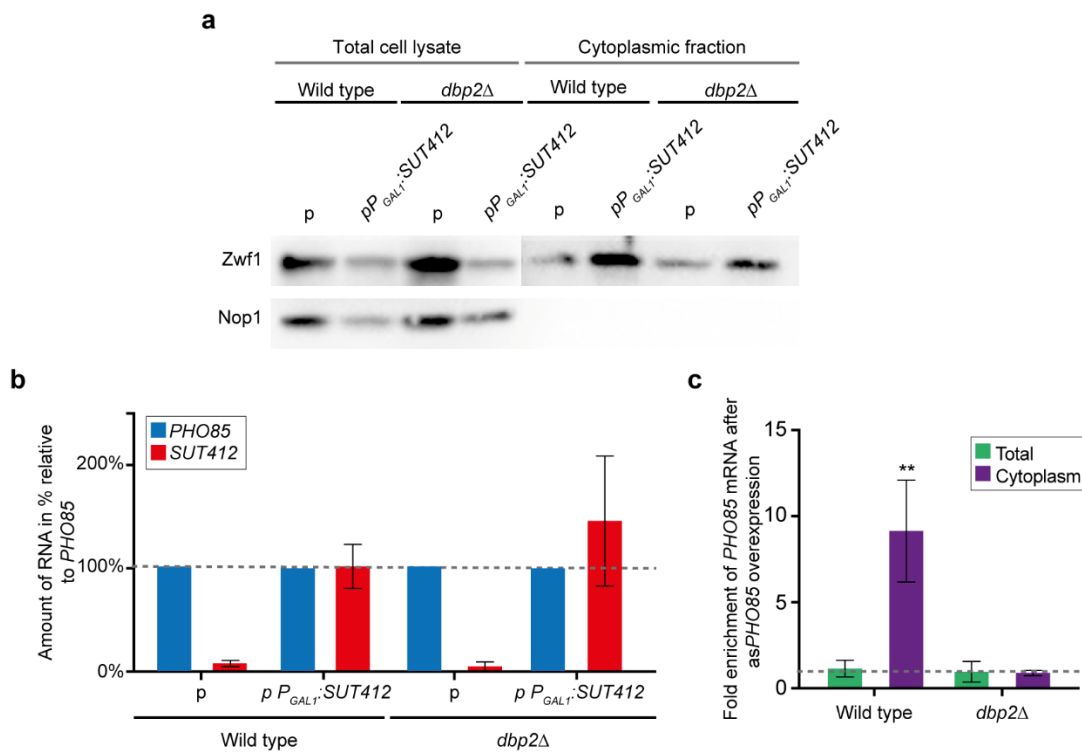


**Figure 22 Loss of *DBP2* negates the preferential export effect of *PHO85* mRNA after *asPHO85* (*SUT412*) overexpression.** **a)** Western blot analysis of successful cytoplasmic fractionation is shown. **b)** Overexpression of *asPHO85* under the control of the *GAL1* promoter and subsequent cytoplasmic fractionation, qPCR of *PHO85* and *asPHO85* was conducted in wild type and *dbp2Δ*. The total RNA level is related to *PHO85* mRNA level in the respective strain. **c)** The experiment was conducted as described in b), but the cytoplasmic and total *PHO85* level in *dbp2Δ* and wild type were compared after overexpression of *asPHO85* relative to no overexpression.

## 4.6 asRNAs can have multiple conditional functions on different levels of gene expression

### 4.6.1 The stability of the *FRE5* mRNA relies on asRNA *SUT802*

In the previous chapters, this work unraveled a so far unknown mechanism in gene regulation that utilizes asRNA to mark mRNAs for preferential export. It is a complementation to already discovered functions of distinct asRNA groups. In many cases, described cytoplasmic functions of asRNAs are related to translation, either in accelerating or in inhibiting the translation of their mRNA (Schein et al., 2016; Simone et al., 2021). The question arises, whether these functions complement each other and thus, whether one asRNA could fulfill several functions at different levels of gene expression.

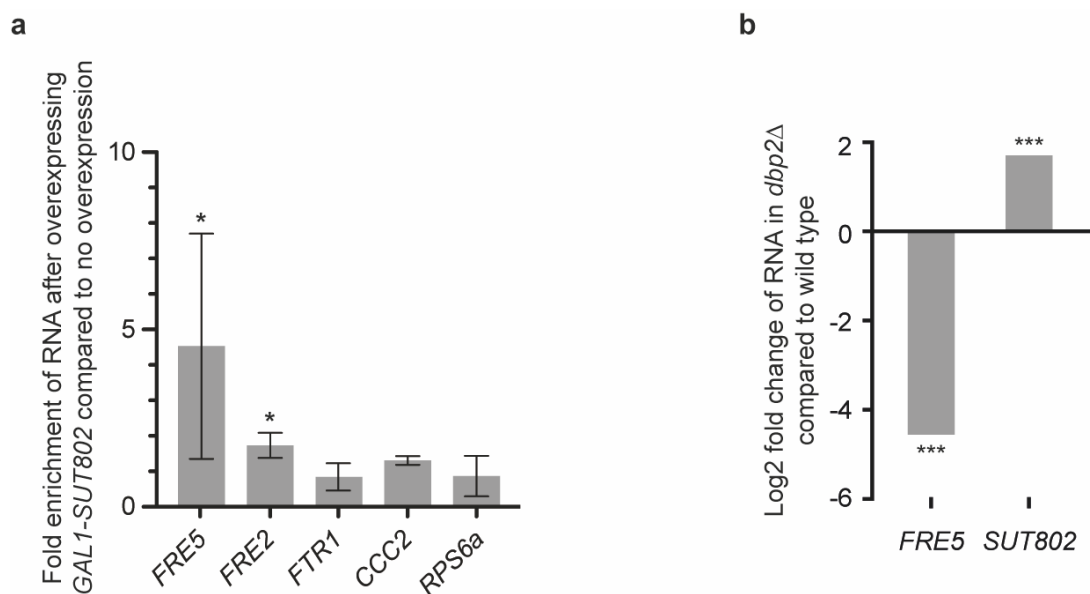


**Figure 23** *FRE5* mRNA stability depends on its asRNA *SUT802* (together with Judith Aylin Weyergraf). **a)** *SUT802* was overexpressed under the *GAL1* promoter with addition of 2 % galactose. After incubation overnight, cells were harvested, and RNA amounts were measured by qPCR. RNA levels after overexpressing *SUT802* are related to no overexpression. **b)** *dbp2Δ* RNA-seq was analysed and the log<sub>2</sub> fold change compared to wild type is shown (Beck et al., 2014).

To investigate the possible multifunctional properties of asRNAs in yeast, we studied the *FRE5-SUT802* sense-antisense pair. First, we overexpressed *SUT802* from the *GAL1* promoter, which led to an ~4.5-fold increase of the *FRE5* mRNA amount (Figure 23a). Interestingly, the *FRE2* mRNA also raised significantly, about 1.5-fold. Next, we analyzed *dbp2Δ* RNA-seq data (Beck et al., 2014) to identify changes in the *FRE5-SUT802* pair, when dsRNA formation is lost. With the inhibition of dsRNA formation, a strong drop in *FRE5* mRNA levels became visible, while

## RESULTS

*SUT802* was rather increased (Figure 23b). Both experiments indicate the dependency of *FRE5* mRNA stability on *SUT802* asRNA.

### 4.6.2 *SUT802* and *FRE5* levels depend on iron

*FRE5* is one of several iron reductases and thereby involved in iron homeostasis (Ramos-Alonso et al., 2020). It is the only known iron reductase localized to mitochondria, where it is probably reducing cellular  $\text{Fe}^{3+}$  to  $\text{Fe}^{2+}$  for mitochondrial iron uptake (Sickmann et al., 2003). The right cellular iron level is crucial for cells, since too high or low amounts are toxic. Only the reduced  $\text{Fe}^{2+}$  is physiologically active, for which reason the Fre reductases play a crucial role to maintain stable nontoxic  $\text{Fe}^{2+}$  levels. To accomplish that, the transcription factor Aft1 senses  $\text{Fe}^{2+}$  levels and regulates the transcription of genes involved in iron homeostasis like *FRE5* (Rutherford et al., 2003).

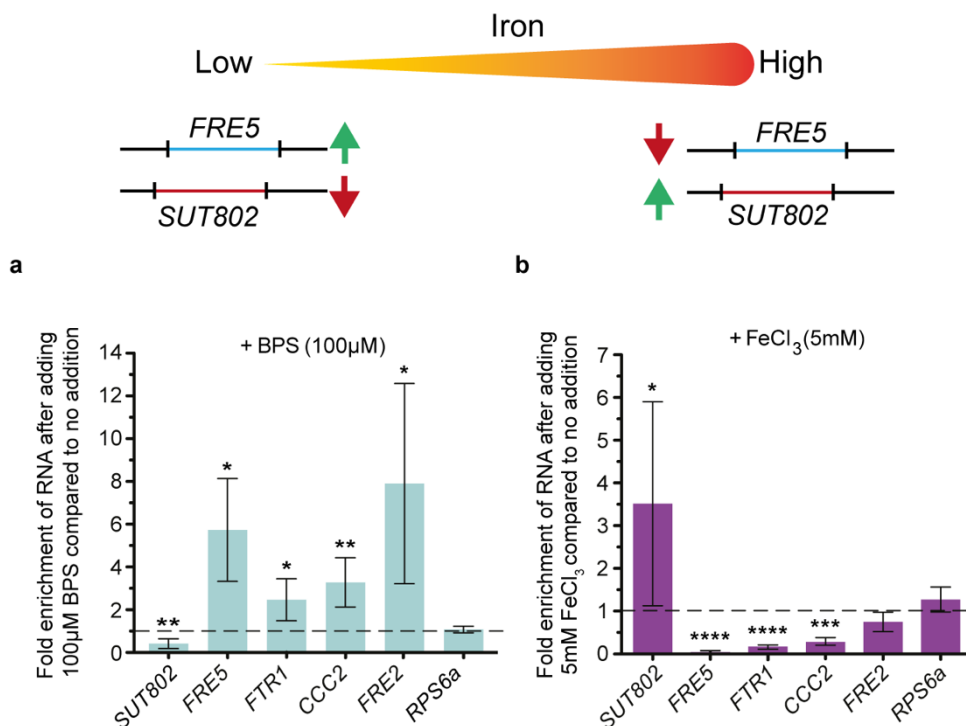


**Figure 24** *FRE5* and *SUT802* levels anticorrelate at different iron concentrations (together with Judith Aylin Weyergraf). **Top:** Illustration of the changing *FRE5* and *SUT802* transcript levels in response to the iron level. **a)** RNA isolation followed by qPCR of wild type cells grown in YPD medium supplemented with 100  $\mu\text{M}$  BPS was conducted. The RNA values were compared to no supplementation. **b)** The experiment was done as described in a), except with the addition of 5 mM  $\text{FeCl}_3$  instead of BPS.

## RESULTS

To identify the possible additional role of *SUT802*, we first exposed cells either to low iron conditions with the addition of 100  $\mu$ M BPS, an iron chelator, or to high iron amounts by adding 5 mM  $\text{FeCl}_3$  to the media (Figure 24). At low iron concentrations, *SUT802* decreased and *FRE5* increased (Figure 24a), whereas at high iron level, *SUT802* increased while *FRE5* decreased (Figure 24b). Because the other iron responsive genes *FTR1*, *CCC2* and *FRE2* were also affected by the different iron levels, like *FRE5*, it is conclusive, that their response is due to transcription regulation by Aft1. *SUT802*, on the other hand, is not regulated by Aft1. Thus, it responded most likely to the change of *FRE5*. At high iron concentrations it probably accumulated because of the missing sense counterpart (Figure 24b). However, the decrease at low iron concentrations (Figure 24a) could be due to translation of *FRE5* mRNA and thus degradation of *SUT802* via NMD.

### 4.6.3 *SUT802* prevents *FRE5* expression in the presence of high iron levels

The stabilization of *FRE5* by *SUT802* and their anticorrelation at different iron concentrations suggest a repressive role of *SUT802* on *FRE5* mRNA at high iron concentrations. To address this aspect, we used the *fre5-sut802 $\Delta$*  strain and overexpressed *FRE5* without *SUT802* and in the presence of *SUT802*. Both RNAs were under the control of the *GAL1* promoter.

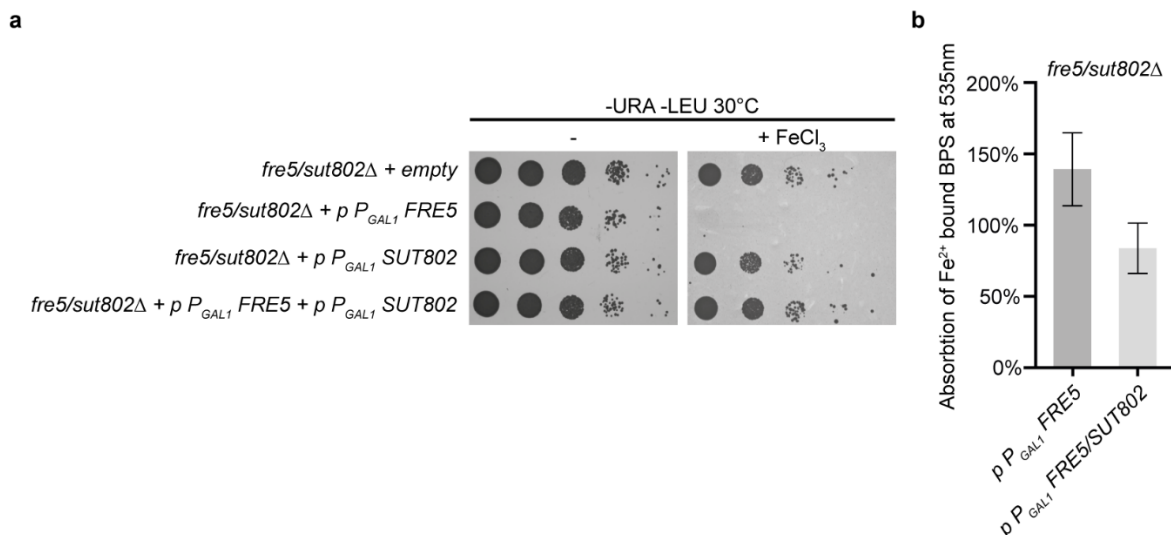


**Figure 25 *FRE5* overexpression is toxic under high  $\text{Fe}^{3+}$  due to cellular accumulation of  $\text{Fe}^{2+}$ .** **a)** Growth test of the strain *fre5/sut802 $\Delta$*  with respective plasmids was conducted on synthetic -URA, -LEU plates supplemented with 5 mM  $\text{FeCl}_3$  and compared to plates with no addition. **b)** Cellular  $\text{Fe}^{2+}$  of *fre5-sut802 $\Delta$*  with respective plasmids was measured by the absorption of BPS bound  $\text{Fe}^{2+}$  at 535 nm and compared to *fre5-sut802 $\Delta$*  with an empty plasmid.



## RESULTS

Astonishingly, if *FRE5* was overexpressed at high iron (5 mM FeCl<sub>3</sub>), cells did not survive in growth test analysis (Figure 25a). Addition *SUT802* rescued the effect and cells grew like the control *fre5-sut802Δ* strain and cells overexpressing *SUT802* alone. This shows, that *SUT802* can prevent *FRE5* expression at high iron levels. At regular iron levels, all strains showed the same growth, indicating that this prevention does not occur at normal conditions.

The effect of *FRE5* overexpression is most likely due to more cellular Fe<sup>2+</sup> reduced by Fre5. To verify our assumption, we developed a protocol to measure cellular Fe<sup>2+</sup> levels by using BPS. BPS is used as an iron chelator. After binding Fe<sup>2+</sup>, it appears red and absorbs light at 535 nm, which can be measured by the Nano-drop 2000 (Pqlab). We created cell lysates of the *fre5-sut802Δ* strain, which was grown in medium supplemented with 5 mM FeCl<sub>3</sub>, either overexpressing *FRE5* alone or together with *SUT802*. Next, 200 μM/μl BPS was added to the lysates, followed by measuring the light absorbance at 535 nm. Indeed, in comparison to no overexpression of any construct, we were able to identify an increase of cellular Fe<sup>2+</sup> of about 145%, if *FRE5* is expressed under the *GAL1* promoter (Figure 25b). Taking the high toxicity of excess Fe<sup>2+</sup> into account, this would explain the death of cells overexpressing *FRE5*. The addition of *SUT802* again lowered the cellular Fe<sup>2+</sup> amounts to the wild type level. Taken together, this shows a repressive role of *SUT802* on *FRE5* expression. The repression only takes place under repressive conditions with high iron concentrations, when *FRE5* expression would lead to a toxic amount of cellular Fe<sup>2+</sup>. However, under inducing conditions, the described preferential expression still takes place.

#### 4.6.4 *SUT802* recruits Hek2 to prevent *FRE5* translation

Next, we wondered how *SUT802* mediates the repression of the *FRE5* expression. Tuck and Tollervey created an atlas of RBP binding sites via CLIP RNA-seq. Using their data, we identified Hek2 binding to *SUT802* (Tuck & Tollervey, 2013; Figure 26). Hek2 is a cytoplasmic protein, known to be part of the cytoplasmic transport machinery of RNAs. By preventing the small ribosomal subunit from binding to the mRNA, it secures translation only at the mRNA destination. In our case, we suggest that *SUT802* can prevent translation of *FRE5* mRNA under high iron conditions by recruiting Hek2. Thereby, Hek2 may prevent accumulation of excess Fe<sup>2+</sup>, which is toxic for cells. This indicates two possible roles of asRNA *SUT802* on *FRE5* expression. First, it can accelerate *FRE5* expression through preferential export and expression

## RESULTS

if cells grow in low iron concentrations. Secondly, at high iron conditions, it prevents translation by recruiting Hek2.

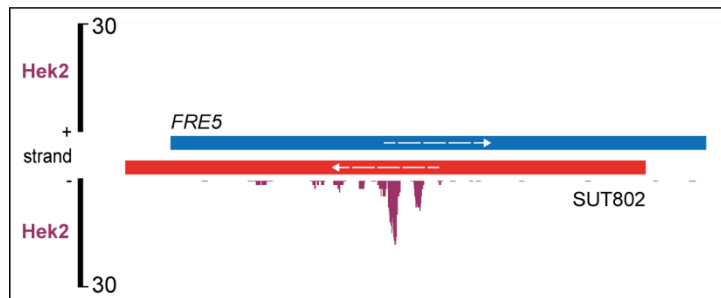


**Figure 26 Hek2 binds to *SUT802*.** The CLIP seq data for Hek2 from Tuck and Tollervy 2013 was analyzed and displayed with the Integrated Genome Browser (IGB).

## 5. Discussion

### 5.1 Model of the preferential mRNA export

Since the discovery of lncRNA and their wide existence throughout the genome of all kinds of eukaryotes, unraveling their function has become a great interest in science (Carninci et al., 2005; David et al., 2006; L. Li et al., 2006; Stolc et al., 2004). Their importance was questioned at first (Hüttenhofer et al., 2005). However, with the scientific progress in molecular biology, the scope of lncRNAs has become clearer, as they have been shown to play key roles in diverse mechanisms (Statello et al., 2020). asRNAs can be major regulators of their senseRNA. Still, a complete and complex view is lacking. In this study, we present a new global function of asRNAs, closing a decisive gap in their functionality (Figure 27).

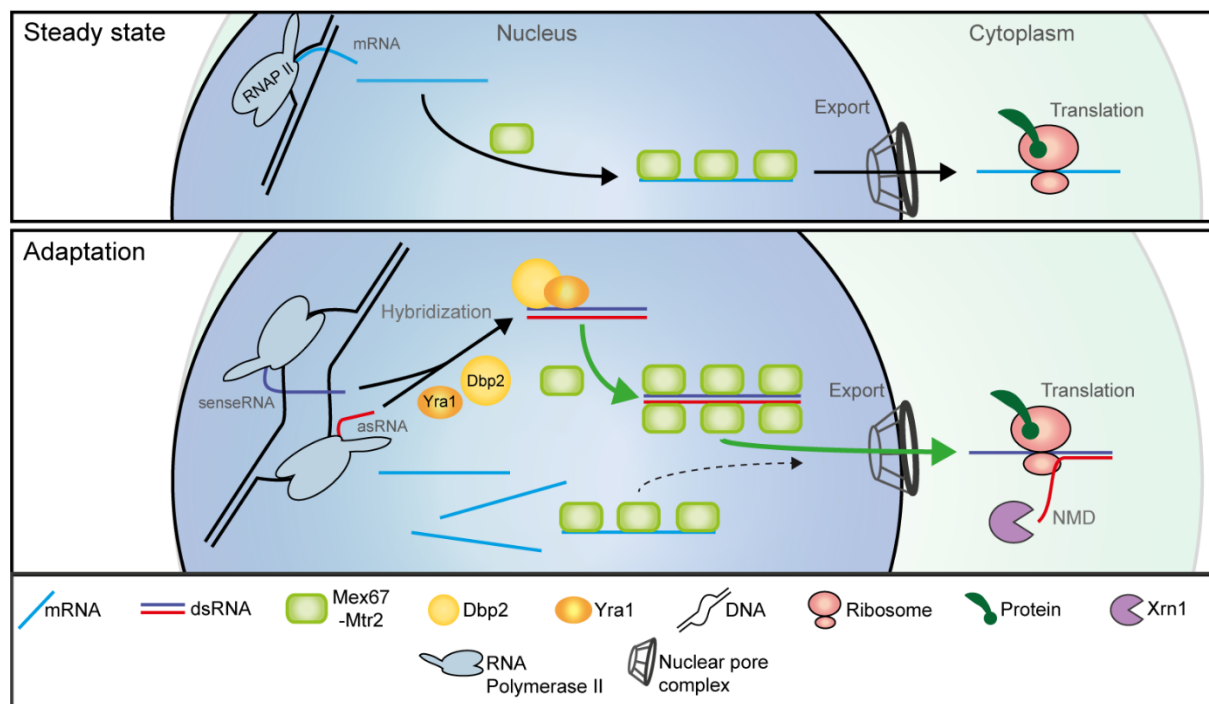


**Figure 27 Model for the preferential gene expression of dsRNAs.** Top: mRNAs are transcribed by RNA polymerase II and eventually bound by Mex67, leading to export and translation in the cytoplasm. Bottom: Preferential expression during cellular adaptation. Dbp2 and Yra1 mediate dsRNA formation of mRNAs and their asRNAs. Preferential binding of Mex67 to dsRNAs leads to the favoured nuclear export and thus translation of the corresponding mRNA. As translation leads to the separation of the dsRNA, also the corresponding asRNA is scanned by ribosomes, however, it is then subsequently degraded by NMD. In this way, preferential gene expression is established.

We propose that the dsRNA formation of a mRNA and asRNA leads to their preferential nuclear export, which supports the adaptation of gene expression. asRNAs are transcribed

genome wide, mostly by pervasive transcription and bidirectional promoters. As soon as a cell must adapt to new conditions and thus, has to change its expression program, the transcription of the responsive sense gene is activated. The available asRNA is hybridized with the newly made mRNA in a process which is mediated by Dbp2 and Yra1, leading to a dsRNA. Mex67 preferentially binds to dsRNA in higher amounts, thereby accelerating its nuclear export. The accelerated export is the key point for preferential gene expression, leading to a faster establishment of the urgently required proteins in the cell. Upon translation of the mRNA, the ribosome separates the dsRNA followed by the NMD mediated degradation of the asRNA. This mechanism represents an advantage for cells, which are continuously confronted with new requirements.

## **5.2 The limiting amounts of RBPs represent an evolutionary concept on the molecular level**

One major theme in a eukaryotic cell is the transfer of information from DNA to RNA to proteins. On their way, RNA transcripts are protected and guided by RBPs (Hackmann et al., 2014). Their binding stabilizes the RNA and only properly formed mRNPs are exported, while faulty RNAs are degraded. One major factor already loaded during transcription is Npl3. It regulates transcription termination, splicing and export of RNAs and additionally translation of mRNAs (Baierlein et al., 2013; Holmes et al., 2015; Huang & Steitz, 2005). Our RNA-seq data in *np13Δ* showed great alterations in the transcriptome of *S. cerevisiae* cells, underlining the importance of this protein. Here, especially RNAs with long half-lives and RNAs of highly expressed genes are destabilized and reduced, while asRNAs are on average increased (Figure 5). The increased asRNA amount has earlier been described to be a cause of defective transcription termination (Holmes et al., 2015). Thus, Npl3 has been suggested to be a stimulator of mRNA production and a repressor of pervasive transcription.

It is noticeable that especially RNAs with a long half-life are affected by the loss of *NPL3* (Figure 5b). We further showed that RNAs with a long half-life are also prone to stay in the nucleus for longer (Figure 10b). Taken together, it displays that especially nuclear retained mRNA transcripts are vulnerable for the loss of *NPL3*. Since the nucleus represents an environment for active decay of RNAs, transcripts that reside in the nucleus for longer are more prone to degradation in the absence of Npl3. mRNAs that are exported rapidly, on the other hand, are more likely to escape nuclear degradation, although not protected by Npl3. We identified another correlation between the loss of *NPL3* and the expression level of RNAs. With

increasing mRNA levels, genes were more vulnerable when Npl3 was missing. It is reasonable, that highly expressed genes consume more RBPs, therefore they decrease stronger if Npl3 is missing.

Overall, the RNA-seq in *npl3Δ* shows that the limitation of RBPs, for instance upon deletion, has an impact on the RNA amounts. However, even in wild type, the amount of RBPs exists in a defined equilibrium with RNAs. An export block by anchoring Mex67 to the cell membrane showed the immediate decay of nuclear poly(A)<sup>+</sup> RNA without affecting their transcription. Since the nuclear RBPs were already in complex with nuclear retained mRNPs, newly transcribed RNAs had no protection against degradation, which was partially reversed when overexpressing the RBP Nab2 (Tudek et al., 2018). This indicates the tight equilibrium between RNAs and nuclear RBPs and the limitation set by RBPs on cellular RNA amounts. On the one hand, it shows that upregulating genes through transcription is limited by the access of RBPs and, on the other hand, it indicates the competition of RNAs for RBPs. The competition for limited resources such as food is a well-known evolutionary concept at the level of populations. It could be transferred to the level of RNAs, which compete for RBPs as the limited resource. This evolutionary concept would provide a system, where RNAs that present a better platform for RBPs should have an advantage. In our model, the preferential binding of Mex67 to dsRNAs represents such an advantage and leads to the preferential export of mRNAs mediated by asRNA. This could be applicable for other RBPs, too.

### **5.3 The function of asRNA depends on the transcription state of the sense gene**

With our results in this study, we expanded the knowledge of asRNA function and showed, that asRNA transcription does not repress sense transcription *per se*. First reports, that identified asRNA transcripts assumed a repressive function on sense gene transcription (Xu et al., 2011). Since asRNAs are mostly present on non-transcribed genes, asRNA transcription was thought to interfere with sense transcription. This was verified by Huber and colleagues who used a global approach to shut down asRNA transcription by adding a unidirectional transcription termination side (TTS) in front of 188 asRNAs while adding a GFP-tag to the corresponding sense gene. With repression of asRNA transcription, the protein amounts raised under wild typic conditions (Huber et al., 2016). Therefore, a nuclear function of asRNAs by repressing sense leakage or general transcription under non-inducing conditions was the explanation of their widespread existence.

To identify the influence of asRNA transcripts on mRNA localization, we overexpressed *asPHO85* from a vector. The existence of the asRNA did not change the overall level of *PHO85* mRNA (Figure 9). Thus, we did not identify a repression of *PHO85* transcription in the presence of its asRNA. However, it has been suggested that not the asRNA itself, but the act of antisense transcription interferes with sense transcription. Still, the transcription of the SRAT *asSEG2* also did not interfere with the mRNA level of *SEG2* in the *set2Δ* mutant (Figure 18c), but increased it slightly, which contradicts a repressive role. Also, on a global level, the upraised SRATs did not show a decrease of their mRNA levels in the RNA-seq experiment in *set2Δ* (Venkatesh et al., 2016; Figure 19a). The authors did not find an alteration of sense transcript levels upon SRAT transcription compared to wild type. This is furthermore supported by the example of *SUT719*, which is antisense to the so far uncharacterized *SUR7* gene. Sense and antisense are both highly expressed at growth under galactose. Interestingly, upon  $\alpha$ -factor pheromone stimulation, transcription of *SUR7* is shut down (Roberts et al., 2000), whereas *SUT719* stays highly expressed. If transcription of *SUT719* is inhibited during the  $\alpha$ -factor pheromone stimulation, the *SUR7* mRNA is raised about 4.5-fold. (Xu et al., 2011) Therefore, *SUT719* transcription does not repress the actively transcribed *SUR7* at growth under galactose, but its leakage at a repressive state during  $\alpha$ -factor pheromone stimulation. The active and high transcription of genes seems to overwrite a possible transcription inhibition of asRNAs. Strikingly, at an active state of transcription, asRNAs could even improve their sense transcription (Cloutier et al., 2016) and furthermore their export, as we show here. Thus, asRNAs and mRNAs can be simultaneously transcribed to form dsRNA structures.

#### **5.4 asRNAs are localized to the cytoplasm**

Previously, the localization of asRNAs and lncRNAs has been discussed based on their understood functionality or degradation pathways (van Dijk et al., 2011; Wery et al., 2016; Xu et al., 2011). In *S. cerevisiae*, it is assumed that lncRNAs function in transcription repression of their sense gene (Huber et al., 2016). The localization of other RNAs, like snoRNA and rRNA, is based on their place of function, which has resulted in the perception, that asRNAs are mostly nuclear localized. However, the majority of asRNA have been shown to be degraded by cytoplasmic Xrn1 in the process of NMD during translation, indicating that asRNAs are often exported (Wery et al., 2016). Thus, the understood functionality suggests a nuclear

localization, but the main degradation pathway was suggested to be cytoplasmic – a fact that so far has not been explained.

Our data clearly showed, that asRNAs are localized in the cytoplasm. Nearly 70 % of all asRNA even showed an enrichment in the cytoplasm compared to the whole cell lysate, which clearly surpasses mRNAs (~25 % of them showed a cytoplasmic enrichment) (Figure 6a). The cytoplasmic localization of asRNAs thus indicated a gap of knowledge regarding the function of asRNAs since an export only for degradation seemed like a waste of cellular resources. In human cells, the cytoplasmic localization of lncRNAs was already discovered. In the leukemia cell line K562 ~54 % and in the adenocarcinoma colon cell line LS-174 T ~68% of expressed lncRNAs are localized to the cytoplasm, of which ~70 % and ~80% are ribosome associated, respectively (Carlevaro-Fita et al., 2016; van Heesch et al., 2014). However, even *MALAT1* and *NEAT1*, which are involved in nuclear speckle and paraspeckle maintenance have been found in polysome fractions (Hutchinson et al., 2007; Tripathi et al., 2010b; Yamazaki et al., 2018). Their extensive studied nuclear function raises the question whether lncRNAs could also be exported for degradation. For other nuclear ncRNAs like snRNAs and *TLC1* it is known that they are exported for maturation followed by a nuclear reimport, separating their place of mRNP assembly and function (Becker et al., 2019; Hirsch et al., 2021). The shuttling process prevents the incorporation of possible faulty RNAs in the nuclear mRNP. This might also be applicable for the human *MALAT1* and *NEAT1*. Their association with the ribosomal fraction could be due to a cytoplasmic maturation step, where faulty RNAs could be degraded by translation dependent pathways. Thus, the presence of a lncRNA in the cytoplasm itself does not imply a cytoplasmic function. There might be a cytoplasmic phase of maturation for several lncRNAs, which can lead to cytoplasmic degradation if faulty. For others, the cytoplasmic localization is indeed connected to their functionality. The clear enrichment of a great number of asRNAs in the cytoplasm supports their function in export or cytoplasmic processes, as we propose. With the model of preferential mRNA export mediated by asRNAs and dsRNA formation we were able to close this gap, connecting asRNA localization and degradation pathway with their function (Figure 27). This is supported by J2-Immunofluorescence experiments, which showed the cytoplasmic localization of dsRNAs, thus, verifying the cytoplasmic localization of dsRNA associated asRNAs (Figure 13a).

### 5.5 The relevance and commonness of dsRNA formation

We were able to identify the modulation of the nucleo-cytoplasmic distribution of mRNAs by their asRNA. First, in our analysis of the cytoplasmic RNA fraction by RNA-seq, it was evident that if the asRNA was similar expressed as their mRNA, both were on average enriched in the cytoplasm (Figure 8a). Second, the exogenous transcription of *asPHO85* and the transcription of *asSEG2* in *set2Δ* resulted in a cytoplasmic shift of their corresponding mRNA *PHO85* and *SEG2* (Figure 9; Figure 17). Thus, the previously identified cytoplasmic localization of asRNAs was transferable onto their mRNA counterparts. With the introduction of RNAi in *S. cerevisiae* followed by RNA-seq, Wery and colleagues were able to identify dsRNA targets (Drinnenberg et al., 2009; Wery et al., 2016). Based on the log<sub>2</sub> fold change of the degradation products in the RNAi strain compared to wild type we established a probability of RNAs to form dsRNAs. With a higher probability to form dsRNA, RNAs showed on average a more cytoplasmic distribution (Figure 8b). Therefore, we suggest that the cytoplasmic localization of asRNAs and their mRNAs is caused by dsRNA formation. Indeed, we were able to verify previously identified dsRNAs with the J2-immunoprecipitation experiments (Figure 12a) and showed that these targets leave the nucleus preferentially (Figure 14). Our findings indicate the widespread existence and relevance of eukaryotic dsRNAs, thereby, further challenging the idea that eukaryotic RNA exists as a single strand contrary to genomic DNA and viral RNA. Previous studies in multi-cellular organisms have unraveled the possibility of asRNA and mRNA to form dsRNA, by which the antisense modulated senseRNA translation (Carrieri et al., 2012; Simone et al., 2021). However, in *S. cerevisiae*, asRNA function on their sense genes could so far not be connected to dsRNA formation.

The prevalent lower expression of asRNAs compared to their mRNAs is stated to disagree with their relevance in posttranscriptional gene regulation (Huber et al., 2016; Hüttenhofer et al., 2005). According to our model, dsRNA formation is used to establish the gene expression faster. For this fast adaptation, only the first transcribed and exported mRNAs must be double stranded and preferentially exported. A stable expressed gene only benefits from preferential export for fine-tuning of its expression, which again only needs partial dsRNA formation. In both cases, the low expression of asRNAs is not contradicting to our model but rather is intended.

In conclusion, regarding our model, mRNAs of one gene should be found as single strand and double strand at different time points or between different cells, depending on the



requirement of fine-tuning of gene expression or fast establishment of certain expression programs. The differentiation between the single stranded and the double stranded content of mRNAs of one gene is still challenging. Current methods like qPCR and RNA-seq only measure the complete quantities of mRNAs. The J2-immunoprecipitation is able to enrich dsRNAs but leaves the ssRNA content unattended. Thereby, the improvement of these methods to distinguish ssRNA and dsRNA of a mRNA is needed to further unravel the relevance and existence of dsRNA formation.

### 5.6 dsRNA formation and biogenesis

In many studies, the biogenesis and processing of mRNAs or lncRNAs and asRNAs have been studied separately (Tuck & Tollervey, 2013). Although it is possible to transfer the gained knowledge to dsRNA biogenesis, direct proof that they are processed like mRNAs is largely missing. We have shown for the first time that parts of the dsRNA biogenesis are very similar to that of ss mRNA, including the direct involvement of Mex67, Xpo1 and different RBPs. First, through the development of a J2-immunofluorescence protocol, we showed the nuclear accumulation of dsRNA after an export block in the double mutant *mex67-5 xpo1-1* (Figure 13a). Thereby, we identified that dsRNAs are formed in the nucleus and that they require Mex67 and Xpo1 for their nuclear export. In fact, the nuclear formation is supported by the lethality of cells expressing the *E. coli* dsRNase RNaseIII in the nucleus. This can only be explained through the nuclear dsRNA formation (Figure 16a).

Until now, reports that have unraveled functions of asRNAs in mRNA expression have taken their dsRNA formation as given (Carrieri et al., 2012; Simone et al., 2021; Villegas & Zaphiropoulos, 2015). Here, we have shown that the helicase Dbp2 is responsible for the cellular dsRNA formation. First, with the J2-immunoprecipitation we identified the binding of Dbp2 to dsRNA (Figure 21a). Secondly, in J2-immunofluorescence, the deletion of *DBP2* led to a loss of dsRNA (Figure 21b). Further, the overexpression of *asPHO85*, that led to a cytoplasmic shift of its mRNA *PHO85*, had no effect in *dbp2Δ* (Figure 22). Recently, it was assumed, that Dbp2 and Mtr4 are rather involved in resolving nuclear dsRNA before export, as their deletion led to an increase of asRNAs (Wery et al., 2016). Indeed, in an *MTR4* mutant strain, dsRNA accumulates in the nucleus (data not shown). However, Mtr4 as part of the TRAMP complex is most likely needed to resolve dsRNAs of faulty transcripts before degradation by the exosome. In the case of Dbp2, it is more plausible, that asRNAs increase because of the

opposite. Since asRNAs are not hybridized with their mRNAs in *dbp2Δ*, they accumulate in the nucleus as single strands, like seen in the poly(A)<sup>+</sup> FISH (Figure 20c). This is supported by RNA-seq in *dbp2Δ* and the specific dsRNA pair *FRE5-SUT802*. Upon deletion of *DBP2*, *FRE5* mRNA decreases and *SUT802* increases, probably because they fail to hybridize without Dbp2 (Figure 23b). These cases show that helicases are involved in dsRNA processing, even beyond their helicase activity. We have gained evidence *in vivo* that Dbp2 can function in opposite directions. It can unwind and form dsRNA structures, which makes this enzyme distinctive and helicases an interesting study object in dsRNA biogenesis.

In addition, the J2-Immunofluorescence in the translational mutants *rpl10(G161D)* and *nmd3Δ* identified the act of translation as the process that dissolves cytoplasmic dsRNAs, as dsRNA levels increased in these mutants (Figure 13a). Hereinafter, the mRNA gets translated and the asRNA degraded by NMD. While staying with the mRNA until reaching the ribosomes, asRNAs are also able to modulate their translation, as shown for SINEUPs and MIR-NATs (Carrieri et al., 2012; Simone et al., 2021). Afterwards, the asRNA gets degraded via NMD, as they accumulate in *upf1Δ* and *xrn1Δ* strains (Wery et al., 2016). Further studies are needed to find out whether dsRNAs might recruit translation factors faster than ssRNAs in *S. cerevisiae*.

### 5.7 Hybridization of dsRNA in the nucleus is accomplished by Dbp2 and Yra1

Dbp2 mediated dsRNA formation has been shown to be dependent on Yra1, which inhibits Dbp2 helicase activity and establishes its dsRNA binding (Ma et al., 2013). Interestingly, the first identification of *YRA1* (yeast RNA annealing protein) was based on its assumed ability to form or support dsRNA formation, which was not followed (Portman et al., 1997). With our findings, it is assumable that Yra1 indeed plays a crucial role in dsRNA formation, but most likely in cooperation with Dbp2. We propose the early co-transcriptional loading of Dbp2 onto mRNAs and asRNAs, where it initially dissolves secondary structures. With the binding of Yra1 to Dbp2, Dbp2 loses its helicase activity, which leads to the domination of its dsRNA binding activity. Thus, the complex of Dbp2 and Yra1 supports dsRNA formation. Previous *in vitro* studies have shown that the relative amounts between Yra1 and Dbp2 are important for their function in dsRNA formation. With increasing amounts of Yra1 compared to Dbp2, their dsRNA formation activity increases (Ma et al., 2016). In wild type cells, the Yra1 amount doubles the one of Dbp2, creating a condition for preferred dsRNA formation (Ho et al., 2017). As their relative amounts seem to be important for dsRNA formation, cells could have evolved

mechanisms, that secure these. Interestingly, both mRNAs have been shown to be regulated post transcriptionally via splicing interference and intron retention, which leads to the degradation of the mRNA (Kilchert et al., 2015; Rodríguez-Navarro et al., 2002). This mechanism could play an important role in maintaining stable Yra1 and Dbp2 levels, and thereby dsRNA formation, and would thus be a promising future study object.

### **5.8 Mex67-Mtr2 binding mediates the preferential export**

dsRNAs are preferentially exported, mediated by the export heterodimer Mex67-Mtr2. Our EMSA experiments showed that the capacity of dsRNA for the RNA binding heterodimer Mex67-Mtr2 is roughly doubled compared to ssRNAs (Figure 15b). Whereas the ssRNA was completely shifted at 2-molar excess of Mex67-Mtr2 and saturated at about 5-molar excess, the dsRNA showed a complete shift at about 3-molar excess and a saturation at 10-molar excess of added Mex67-Mtr2. Strikingly, dsRNAs additionally showed a higher affinity for Mex67-Mtr2, as it was the superior competitor in the competition assay (Figure 15c). We assume, that the higher capacity and affinity of dsRNA for Mex67-Mtr2 compared to ssRNA are key elements for the preferential export of dsRNAs. This is supported by a computational, agent-based modeling (ABM) approach of Azimi and colleagues, that has predicted several factors which influence RNA export (Azimi et al., 2014). Their approach showed reliable predictions of previous results regarding the RNA export mechanism. They have additionally observed that the density and the amount in which an export receptor binds to an RNA increases export efficiency and probability. This is applicable to our results, showing the higher amounts of Mex67-Mtr2 on dsRNA certainly can lead to faster export. Furthermore, the length of an mRNA represents a factor that decides about the possible amount of bound Mex67-Mtr2. Indeed, cytoplasmic fractionation RNA-seq showed an increasing cytoplasmic distribution with increasing length of transcripts (Figure 10e). Thus, this could rely on a similarly increased binding of Mex67-Mtr2 based on the length of a transcript. It was already shown for human cells, that the length of transcripts positively correlates with their cytoplasmic localization. Of course, this could be due to an extended translation time, but may also rely on export. In addition, Azimi and colleagues have predicted that the distribution and density of bound export receptor can be decisive for a successful export (Azimi et al., 2014). In this case, it is conceivable that dsRNAs have an advantage over ssRNAs. As Mex67-Mtr2

may bind on both strands of the dsRNA, it may cause a higher density of export receptors on the mRNP.

The export release assay showed that dsRNAs leave the nucleus and bind to the ribosomes before ssRNAs (Figure 14b). We initially blocked the nuclear export in the *mex67-5* mutant by shifting cells to its permissive temperature of 37 °C, which leads to the misallocation of the protein to the cytoplasm (Segref et al., 1997). After shifting back to its permissive temperature of 25 °C, Mex67 becomes functional again and is reimported into the nucleus. While reentering the nucleus higher amounts of Mex67 bind to dsRNA, because of its higher affinity as shown in the competition EMSA (Figure 15c). Therefore, the assembly of the export ready dsRNPs is faster than of the ssRNPs. This is transferable to the wild type situation. After mediating the export of an RNA, Mex67 is removed from the cytoplasmic RNP by Dbp5 and reimported into the nucleus. Here, it again binds to newly transcribed and quality controlled RNAs, preferable to dsRNAs like shown in our experiments, leading to their preferential export. This could be true for several RBPs involved in nuclear RNP assembly and could be similarly studied with an EMSA as we did for Mex67.

### **5.9 Export is the key factor for the nucleo-cytoplasmic distribution and half-life of RNAs**

The binding activity of Mex67 leads to a preferential nuclear export of dsRNA. On the one hand, the higher affinity of Mex67 to dsRNA finishes its RNP assembly faster, on the other hand, the higher capacity and the dense coverage of the export receptor on dsRNA is advantageous for export (Figure 15). This advantage is most likely not based on a faster channeling of the RNA through the NPC. With MS2-GFP tagging of *ACT1* mRNA and tracing in live cell microscopy, Grunwald and Singer showed, that the export process through the NPC takes about ~180 ms in mammalian cells. Docking on the nuclear side and release on the cytoplasmic side takes up to ~160 ms while the transport through the pore only takes ~5-20 ms (Grünwald & Singer, 2010). In yeast, a comparable time of ~200 ms for export has been discovered (Smith et al., 2015), thus showing a similar time scale in mammalian cells and yeast. However, accelerating a process of 200 ms would not explain the explicit cytoplasmic enrichment of dsRNAs. Grunwald and Singer have further described that an average mRNA stays in the nucleoplasm for several minutes before export. As soon as it randomly reaches an NPC, the export is initiated after successful docking of the mRNP to the NPC. However, the export of RNAs is a transient mechanism and does not show a 100% export efficiency of

correct RNAs. Grunewald and Singer traced 765 RNAs and saw only 115 transport events, resulting in an efficiency of about 15%. An optimal configuration helps to dock at the NPC and overcome its hydrophobic barrier. Thus, a compact formation is preferential for export and can accelerate the rate of export. This could be an advantage of dsRNAs: By binding export receptors at a higher density, dsRNA export is initiated more efficiently. Thus, it is more likely that the export of a dsRNA is initiated than the export of a ssRNA. Further, the coverage with export receptors of the mRNA, especially at its 5' and 3' end, is required for successful export. In *in vivo* experiments it has been shown that the 5' end leads the mRNA through the nuclear pore (Mehlin et al., 1992; Visa et al., 1996). For dsRNA, both ends are thus able to initiate export.

### **5.10 A longer cytoplasmic lifespan of dsRNAs could be implicated**

The cytoplasmic enrichment of dsRNAs can be explained by their preferential export. Still, we wondered whether the cytoplasmic enrichment could be due to a higher stability and therefore a longer lifetime of RNAs. Stabilization effects of intramolecular dsRNAs have already been described, making it to a comprehensible suggestion for the broad group of dsRNAs (Geisberg et al., 2014). To investigate such a possible stabilization, we consulted the data of Chan and colleagues, who measured the half-life of RNAs by pseudo uridylation and RNA-seq (Chan et al., 2018). Comparing the half-life with their cytoplasmic distribution based on our cytoplasmic fractionation and RNA-seq experiment, first a general stabilization effect for dsRNAs could not be suggested (Figure 10a). However, under certain circumstances like in the case of *FRE5* and *SUT802*, asRNA can lead to a verifiable stabilization (Figure 23). At high iron level when *Fre5* is not needed but rather toxic for cells, *SUT802* prevents *FRE5* translation by recruiting Hek2 (Figure 25; Figure 26). This translational inhibitor leads to a stabilization and storage of the bound dsRNA in the cytoplasm (Figure 23a). It must be noted that this stabilization only takes place under repressive conditions.

However, under wild typic conditions, a cytoplasmic stabilization could also be argued for. We showed, that dsRNAs are preferentially exported, which in the end leads to a shorter nuclear lifetime. Such a noticeable shorter nuclear lifespan should lead to an equivalent shorter half-life of dsRNA. Still, ssRNA and dsRNA did show a similar half-life, potentially implicating a longer cytoplasmic phase of dsRNA (Figure 28).

## DISCUSSION

Unlike in the specific case of *SUT802* and *FRE5* dsRNA, the potentially longer cytoplasmic lifetime of dsRNA cannot be explained by translation inhibition and storage. Cytoplasmic stored mRNAs enrich in the cytoplasm after an mRNA export block like we have identified for mRNAs involved in cell division and establishing daughter cell integrity (Figure 11b). A stabilization because of storage can thus be excluded. Chan et al. have found several correlations in their analysis that influenced the half-life and thus stabilizes mRNAs (Chan et al., 2018). One of them is the coverage of mRNAs with ribosomes and the associated efficient translation of these mRNAs. This might fit into our model. mRNAs which are incorporated into dsRNA structures could have a longer half-life in the cytoplasm because of a more efficient translation. In human and mice, SIENUP asRNA have been identified, that increase translation of their mRNA counterparts by recruiting additional ribosomes to their mRNA (Carrieri et al., 2012). Regarding the findings of Chan et al., this should lead to the stabilization of the mRNA in the cytoplasm. A similar process could be conceivable for yeast asRNAs. The faster export and thus shorter nuclear lifetime of dsRNAs is followed by an elongated cytoplasmic lifetime mediated by increased binding of ribosomes. This might result in a similar overall half-life compared to ssRNAs. This theory could expand the asRNA mediated preferential gene expression.

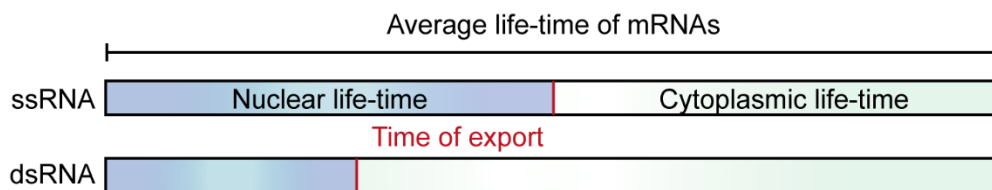


**Figure 28** ssRNAs and dsRNAs spend different amounts of time in the nucleus and in the cytoplasm. The export of dsRNAs occurs earlier in their lifetime compared to ssRNAs. If the time of export differs between ssRNA and dsRNA by equivalent half-life, the nuclear lifetime as well as the cytoplasmic lifetime is different between both.

### 5.11 dsRNAs are involved in stress response

Our new model of asRNA mediated fast adaptation and gene expression change is particularly vital in extreme situations when cells are exposed to stress. Indeed, our analysis of the RNA-seq data of cells exposed to 0.6 M NaCl showed a great increase of asRNA transcripts in addition to stress responsive genes (Lahtvee et al., 2016; Figure 19a). This increase indicates the great importance of asRNAs in stress response, most likely by modulating their sense gene expression. On the one hand, they form dsRNA with their upregulated mRNA to accelerate the export of the mRNA. Thereby, these asRNAs are not degraded but exported, which extends

## DISCUSSION

their lifetime and increases their cellular amounts. On the other hand, it is also likely that the amount of some asRNAs increases because the transcription of their sense gene is turned off, for instance in the case of genes associated with biomass production. Here, it would be plausible, that a similar repressive function takes over to prevent leakage of not needed genes, as seen for stress responsive genes under normal growth conditions (Xu et al., 2011). It can be assumed that both mechanisms take place, since ~70 % of asRNA levels increase upon stress response.

The J2-immunofluorescence after addition of 0.7 M NaCl and 10 % EtOH showed a great increase in dsRNA amounts in the cytoplasm and supports the idea of increased dsRNA formation upon stress induction (Figure 19b). The increase was already visible after 5 min of the applied stress condition and was continuously high after 10 min. This shows the direct involvement of dsRNAs in stress response. The immediate response to stress occurs in a time frame of a few minutes. During osmotic shock, even within less than one minute, the glycerol export channel is rapidly closed, preventing glycerol leakage that would follow the drastic osmotic change in the environment (Duskova et al., 2015). Additionally, the expression pattern must change to accelerate the production of the osmolyte glycerol or to arrest the cell cycle. This fast change does benefit from the dsRNA mediated preferential export. Consequentially, the degradation of dsRNA was toxic for cells (Figure 16a). Under stress conditions, the mild expression of the *E. coli* dsRNase *RNaseIII-NES*, which was expressed from the strong and steady *ADH1* promoter, already impaired the accurate stress response and lead to growth defects (Figure 20b). J2-immunofluorescence revealed the dissolution of the cytoplasmic dsRNA content upon *RNaseIII-NES* expression compared to the high amounts visible in wild type cells in response to stress. It is striking how essential this mechanism seems to be for cells, but the faster a cell can turn up its defence mechanism, the less damage will occur from extreme environmental changes.

The involvement of lncRNAs in osmotic stress response has been identified earlier, where 173 and 216 lncRNAs were directly upregulated by Hog1 after addition of 0.4 M NaCl and 1.2 M NaCl, respectively (Nadal-Ribelles et al., 2014). It has been shown that 37% of genes correlated positively with a simultaneous expression of stress induced lncRNA. Astonishingly, if the transcription of the stress induced asRNA of *CDC28* is inhibited, the induction of *CDC28* upon osmotic stress itself is impaired. *Cdc28* has been shown to be needed for cells to re-enter the cell cycle after its arrest during stress response. Cells without the *asCDC28* re-enter the cell

cycle approximately 20 min later upon stress. (Nadal-Ribelles et al., 2014) The re-entry the cell cycle is no immediate response to osmotic stress, but rather shows that not only the immediate response is asRNA mediated but also the tight regulation afterwards needs asRNA regulation.

Environment-dependent genes and stress responsive genes have in common that their expression is executed in a switch-like manner. asRNAs seem to be key factors in these processes. At the repressed state of genes, asRNAs prevent the basal transcription of stress response genes, whereas in the moment of the “on switch” they mediate a fast establishment of gene expression.

### **5.12 dsRNA formation and preferential expression could be a reason for cancer**

dsRNAs are essential for *S. cerevisiae*. They are already found in wild type cells under normal laboratory conditions and their nuclear degradation is lethal for cells (Figure 13a; Figure 16a). This shows, that dsRNAs fulfil functions beyond the rapid response to stress conditions. Probably, cells adjust their gene expression with asRNAs even in supposedly stable conditions. Since lncRNAs are involved in diverse regulatory mechanisms of gene expression, their malfunction leads to failed development, neurogenerative diseases and cancer (Batista & Chang, 2013). Thus, lncRNAs have become a focus in oncology (Slack & Chinnaiyan, 2019). Many studies exist, which show the diverse mis-regulation of lncRNAs in cancer in mammals. Especially, the powerful tool of preferential gene expression could be the reason for diseases if mis-regulated. Recently, microarrays have identified the asRNA *TTN-AS1* being upregulated in skin cutaneous melanoma (Lin et al., 2017). Further investigations showed that the increase of *TTN-AS1* correlates positively with an increase of its mRNA *TTN* and tumour progression. Most interestingly, the exogenous expression of *TTN-AS1* leads to a cytoplasmic enrichment of *TTN* mRNA, as we showed for *asPHO85* and *PHO85* mRNA (Figure 9c), suggesting that *TTN-AS1* leads to the preferential export and gene expression of *TTN*. Consequently, the knock-down of *TTN-AS1* markedly reduced mRNA and protein level of *TTN* and tumour growth (Wang et al., 2020). This highlights the importance of the discovered preferential gene expression mechanism discovered in this study.



### 5.13 *SUT802* inhibits *FRE5* translation under high iron levels and thus highlights the multifunctional properties of asRNAs

The main finding of asRNA mediated preferential export in this study is expanded by the additional and most likely specific function of *SUT802* in *FRE5* translation, demonstrating the multifunctional property of asRNAs. *FRE5* is a member of the iron reductase *FRE* family involved in iron homeostasis, regulating the cellular level of the bioactive  $\text{Fe}^{2+}$  (Dancis, 1998). While the expression of other asRNAs such as *asPHO85* (*SUT412*) and *asSEG2* did not show an increase in their corresponding mRNA level (Figure 9c, Figure 18c), the overexpression of *SUT802* led to an ~4.5-fold increase of *FRE5* mRNA (Figure 23a). This increase in mRNA level indicated an additional role of *SUT802* in *FRE5* stability. Most likely, the stabilization effect is based on a repressive function. Under high iron levels, *FRE5* transcription is reduced by the transcription factor Aft1 to prevent the excessive reduction of  $\text{Fe}^{3+}$  to  $\text{Fe}^{2+}$  (Figure 24b), which is toxic for cells. Overexpression of *FRE5* from the *GAL1* promoter led to cell death due to elevated  $\text{Fe}^{2+}$  levels (Figure 25). The additional overexpression of *SUT802* rescued the phenotype. Thus, *SUT802* can prevent *FRE5* expression under repressive conditions (Figure 29).

By consulting the data of Tuck and Tollervey, we further noticed that Hek2 (Khd1) binds to the asRNA *SUT802* (Tuck & Tollervey, 2013). Hek2 is part of the She-complex, the cytoplasmic transport machinery. It prevents translation initiation until mRNAs have reached their destination (Denisenko & Bomsztyk, 2002; K et al., 2002). In the case of *ASH1* mRNA, it has been shown that upon arrival at the plasma membrane the casein kinase Yck1 phosphorylates Hek2, leading to its dissociation and subsequent translation of *ASH1* mRNA. We suggest, that *SUT802* recruits Hek2 to its dsRNA with *FRE5* and thereby prevents translation, which leads to the storage and stabilization of *FRE5* mRNA in the cytoplasm. This would represent a unique and novel regulatory mechanism. The phosphorylation and release of Hek2 could be mediated by the cellular  $\text{Fe}^{2+}$  levels, thus, allowing the translation of *Fre5* under low iron conditions. The decrease of *SUT802* after addition of the iron chelator BPS (Figure 24a) indicates the degradation of the asRNA after the dsRNA is separated during translation. The degradation of *SUT802* is most likely mediated via NMD, as it increases in *upf1Δ*, *dcp2Δ* and *xrn1Δ* (Geisler et al., 2012; Wery et al., 2016).

Interestingly, if dsRNA formation is disabled in *dbp2Δ*, the *FRE5* mRNA level drops dramatically, while the *SUT802* level increases (Figure 23b). Thus, if *FRE5* is not hybridized with

*SUT802*, it gets rapidly degraded. *FRE5* possesses an unusually long 3'UTR of 1.2 kb, which is normally covered by *SUT802*. Without *SUT802*, *FRE5* mRNA could be targeted by NMD, leading to its degradation. This could be a mechanism to secure *FRE5* translation only if it was beforehand controlled and regulated by *SUT802*, making *SUT802* the multifunctional master regulator of *FRE5* expression.

Therefore, the asRNA *SUT802* can mediate preferential export and translation inhibition. As argued before, this shows the condition-dependent possibility of asRNAs to carry out different functions in the expression of their sense gene.

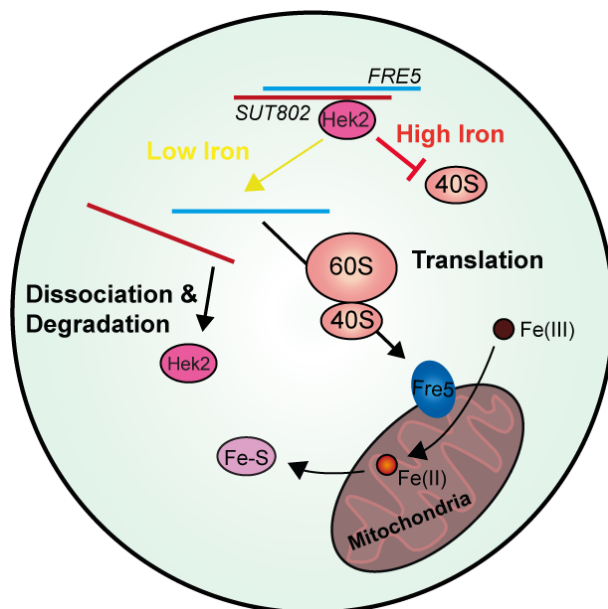


**Figure 29** *SUT802* prevents translation of its mRNA *FRE5* under high iron levels. *FRE5* mRNA and *SUT802* are exported as a dsRNA. In the cytoplasm, *SUT802* recruits Hek2. Under high iron levels, Hek2 prevents the translation initiation of *FRE5* mRNA. Under low iron conditions, Hek2 dissociates, allowing the translation of *FRE5* mRNA. During the process of translation, *SUT802* gets detached and degraded via NMD.

## 6. Concluding remarks

In the last decade, our knowledge of lncRNAs has increased tremendously. Still, every year new pioneering studies are published, helping us to understand the functional versatility and diversity of lncRNAs. However, regarding the indicated enormous landscape of lncRNAs, a lot of properties and characteristics in lncRNA biology are still hidden (Statello et al., 2020; Villegas & Zaphiropoulos, 2015). For instance, the dsRNA formation between asRNAs and their mRNA counterparts needs further detailed investigations.

In this study, we unraveled crucial steps in dsRNA biogenesis, like its nuclear formation, which is dependent on the helicase Dbp2 and Yra1. Through the dsRNA formation, asRNAs can accelerate the export of their mRNA by preferential Mex67 binding. This preferential export mechanism leads to a faster establishment of gene expression, which is essential for the adaptation of cells to new requirements and presents the possibility of fine-tuning of gene expression. Further, we suggest a multifunctional property for lncRNAs based on the specific lncRNA *SUT802*. In addition to the mediation of preferential export, *SUT802* prevents translation of its mRNA *FRE5* under repressive conditions.

The results in this study indicate a new cell biological mechanism and contribute to a better understanding of the complex posttranscriptional gene regulation. The decoding of the cellular and physiological functions of lncRNAs has led to an expanded knowledge of several diseases (Arun et al., 2016; Grelet et al., 2017; Huarte et al., 2010; Kim et al., 2015; Wei et al., 2018). lncRNAs can be used as biomarkers and as therapeutic targets with high specificity, like done in Alzheimer's patients with the *BACE1-AS* (Feng et al., 2018). Therefore, our findings could help to identify functional disorders in diseases, which represents an opportunity to take measures against those.

## 7. References

- Alepuz, P. M., Jovanovic, A., Reiser, V., & Ammerer, G. (2001). Stress-induced map kinase Hog1 is part of transcription activation complexes. *Molecular Cell*, 7(4), 767–777.
- Arun, G., Diermeier, S., Akerman, M., Chang, K. C., Wilkinson, J. E., Hearn, S., Kim, Y., MacLeod, A. R., Krainer, A. R., Norton, L., Brogi, E., Egeblad, M., & Spector, D. L. (2016). Differentiation of mammary tumors and reduction in metastasis upon Malat1 lncRNA loss. *Genes & Development*, 30(1), 34–51.
- Askwith, C., Eide, D., van Ho, A., Bernard, P. S., Li, L., Davis-Kaplan, S., Sipe, D. M., & Kaplan, J. (1994). The FET3 gene of *S. cerevisiae* encodes a multicopper oxidase required for ferrous iron uptake. *Cell*, 76(2), 403–410.
- Avalos, C. B., Brugmann, R., & Sprecher, S. G. (2019). Single cell transcriptome atlas of the drosophila larval brain. *ELife*, 8.
- Azimi, M., Bulat, E., Weis, K., & Mofrad, M. R. K. (2014). An agent-based model for mRNA export through the nuclear pore complex. *Molecular Biology of the Cell*, 25(22), 3643–3653.
- Baejen, C., Torkler, P., Gressel, S., Essig, K., Söding, J., & Cramer, P. (2014). Transcriptome maps of mRNP biogenesis factors define pre-mRNA recognition. *Molecular Cell*, 55(5), 745–757.
- Bahar Halpern, K., Caspi, I., Lemze, D., Levy, M., Landen, S., Elinav, E., Ulitsky, I., & Itzkovitz, S. (2015). Nuclear Retention of mRNA in Mammalian Tissues. *Cell Reports*, 13(12), 2653–2662.
- Baierlein, C., Hackmann, A., Gross, T., Henker, L., Hinz, F., & Krebber, H. (2013). Monosome Formation during Translation Initiation Requires the Serine/Arginine-Rich Protein Npl3. *Molecular and Cellular Biology*, 33(24), 4811.
- Batista, P. J., & Chang, H. Y. (2013). Long Noncoding RNAs: Cellular Address Codes in Development and Disease. *Cell*, 152(6), 1298–1307.
- Beck, Z. T., Cloutier, S. C., Schipma, M. J., Petell, C. J., Ma, W. K., & Tran, E. J. (2014). Regulation of glucose-dependent gene expression by the RNA helicase Dbp2 in *Saccharomyces cerevisiae*. *Genetics*, 198(3), 1001–1014.
- Beck, Z. T., Xing, Z., & Tran, E. J. (2016). LncRNAs: Bridging environmental sensing and gene expression. In *RNA Biology* (Vol. 13, Issue 12, pp. 1189–1196). Taylor and Francis Inc.
- Becker, D., Hirsch, A. G., Bender, L., Lingner, T., Salinas, G., & Krebber, H. (2019). Nuclear Pre-snRNA Export Is an Essential Quality Assurance Mechanism for Functional Spliceosomes. *Cell Reports*, 27(11), 3199–3214.e3.
- Beißel, C., Grosse, S., & Krebber, H. (2020). Dbp5/DDX19 between Translational Readthrough and Nonsense Mediated Decay. *International Journal of Molecular Sciences*, 21(3).
- Beißel, C., Neumann, B., Uhse, S., Hampe, I., Karki, P., & Krebber, H. (2019). Translation termination depends on the sequential ribosomal entry of eRF1 and eRF3. *Nucleic Acids Research*, 47(9), 4798–4813.
- Brogna, S., & Wen, J. (2009). Nonsense-mediated mRNA decay (NMD) mechanisms. *Nature Structural & Molecular Biology* 2009 16:2, 16(2), 107–113.

- Brown, C. J., Ballabio, A., Rupert, J. L., Lafreniere, R. G., Grompe, M., Tonlorenzi, R., & Willard, H. F. (1991). A gene from the region of the human X inactivation centre is expressed exclusively from the inactive X chromosome. *Nature*, *349*(6304), 38–44.
- Brune, C., Munchel, S. E., Fischer, N., Podtelejnikov, A. v., & Weis, K. (2005). Yeast poly(A)-binding protein Pab1 shuttles between the nucleus and the cytoplasm and functions in mRNA export. *RNA*, *11*(4), 517–531.
- Bucheli, M. E., & Buratowski, S. (2005). Npl3 is an antagonist of mRNA 3' end formation by RNA polymerase II. *The EMBO Journal*, *24*(12), 2150.
- Callahan, K. P., & Butler, J. S. (2010). TRAMP Complex Enhances RNA Degradation by the Nuclear Exosome Component Rrp6. *The Journal of Biological Chemistry*, *285*(6), 3540.
- Camblong, J., Iglesias, N., Fickentscher, C., Dieppois, G., & Stutz, F. (2007). Antisense RNA stabilization induces transcriptional gene silencing via histone deacetylation in *S. cerevisiae*. *Cell*, *131*(4), 706–717.
- Carlevaro-Fita, J., Rahim, A., Guigó, R., Vardy, L. A., & Johnson, R. (2016). Cytoplasmic long noncoding RNAs are frequently bound to and degraded at ribosomes in human cells. *RNA (New York, N.Y.)*, *22*(6), 867–882.
- Carninci, P., Kasukawa, T., Katayama, S., Gough, J., Frith, M. C., Maeda, N., Oyama, R., Ravasi, T., Lenhard, B., Wells, C., Kodzius, R., Shimokawa, K., Bajic, V. B., Brenner, S. E., Batalov, S., Forrest, A. R. R., Zavolan, M., Davis, M. J., Wilming, L. G., ... Hayashizaki, Y. (2005). The transcriptional landscape of the mammalian genome. *Science (New York, N.Y.)*, *309*(5740), 1559–1563.
- Carrieri, C., Cimatti, L., Biagioli, M., Beugnet, A., Zucchelli, S., Fedele, S., Pesce, E., Ferrer, I., Collavin, L., Santoro, C., Forrest, A. R. R., Carninci, P., Biffo, S., Stupka, E., & Gustincich, S. (2012). Long non-coding antisense RNA controls Uchl1 translation through an embedded SINEB2 repeat. *Nature*, *491*(7424), 454–457.
- Chan, L. Y., Mugler, C. F., Heinrich, S., Vallotton, P., & Weis, K. (2018). Non-invasive measurement of mRNA decay reveals translation initiation as the major determinant of mRNA stability. *ELife*, *7*.
- Chartrand, P., Singer, R. H., & Long, R. M. (2001). RNP localization and transport in yeast. *Annual Review of Cell and Developmental Biology*, *17*, 297–310.
- Cheng, E. chun, & Lin, H. (2013). Repressing the repressor: a lincRNA as a MicroRNA sponge in embryonic stem cell self-renewal. *Developmental Cell*, *25*(1), 1–2.
- Chlebowski, A., Lubas, M., Jensen, T. H., & Dziembowski, A. (2013). RNA decay machines: The exosome. *Biochimica et Biophysica Acta - Gene Regulatory Mechanisms*, *1829*(6–7), 552–560.
- Cloutier, S. C., Ma, W. K., Nguyen, L. T., & Tran, E. J. (2012). The DEAD-box RNA helicase Dbp2 connects RNA quality control with repression of aberrant transcription. *Journal of Biological Chemistry*, *287*(31), 26155–26166.
- Cloutier, S. C., Wang, S., Ma, W. K., al Husini, N., Dhoondia, Z., Ansari, A., Pascuzzi, P. E., & Tran, E. J. (2016). Regulated Formation of lncRNA-DNA Hybrids Enables Faster Transcriptional Induction and Environmental Adaptation. *Molecular Cell*, *61*(3), 393–404.

- Colognori, D., Sunwoo, H., Kriz, A. J., Wang, C. Y., & Lee, J. T. (2019). Xist Deletional Analysis Reveals an Interdependency between Xist RNA and Polycomb Complexes for Spreading along the Inactive X. *Molecular Cell*, *74*(1), 101-117.e10.
- Comings, D. E. (1972). The structure and function of chromatin. *Advances in Human Genetics*, *3*, 237-431.
- Cramer, P., Armache, K. J., Baumli, S., Benkert, S., Brueckner, F., Buchen, C., Damsma, G. E., Dengl, S., Geiger, S. R., Jasiak, A. J., Jawhari, A., Jennebach, S., Kamenski, T., Kettenberger, H., Kuhn, C. D., Lehmann, E., Leike, K., Sydow, J. F., & Vannini, A. (2008). Structure of Eukaryotic RNA Polymerases. [Http://Dx.Doi.Org/10.1146/Annurev.Biophys.37.032807.130008](http://Dx.Doi.Org/10.1146/Annurev.Biophys.37.032807.130008), *37*, 337-352.
- Dancis, A. (1998). Genetic analysis of iron uptake in the yeast *Saccharomyces cerevisiae*. *The Journal of Pediatrics*, *132*(3 Pt 2).
- Das, S., Sarkar, D., & Das, B. (2017). The interplay between transcription and mRNA degradation in *Saccharomyces cerevisiae*. *Microbial Cell*, *4*(7), 212.
- David, L., Huber, W., Granovskaia, M., Toedling, J., Palm, C. J., Bofkin, L., Jones, T., Davis, R. W., & Steinmetz, L. M. (2006). A high-resolution map of transcription in the yeast genome. *Proceedings of the National Academy of Sciences of the United States of America*, *103*(14), 5320-5325.
- Davis, C. A., Grate, L., Spingola, M., & Ares, M. (2000). Test of intron predictions reveals novel splice sites, alternatively spliced mRNAs and new introns in meiotically regulated genes of yeast. *Nucleic Acids Research*, *28*(8), 1700.
- de Andres-Pablo, A., Morillon, A., & Wery, M. (2017). LncRNAs, lost in translation or licence to regulate? *Current Genetics*, *63*(1), 29-33.
- de Nadal, E., Ammerer, G., & Posas, F. (2011). *Controlling gene expression in response to stress*.
- Dehecq, M., Decourty, L., Namane, A., Proux, C., Kanaan, J., le Hir, H., Jacquier, A., & Saveanu, C. (2018). Nonsense-mediated mRNA decay involves two distinct Upf1-bound complexes. *The EMBO Journal*, *37*(21).
- Denisenko, O., & Bomsztyk, K. (2002). Yeast hnRNP K-like genes are involved in regulation of the telomeric position effect and telomere length. *Molecular and Cellular Biology*, *22*(1), 286-297.
- Denzler, R., Agarwal, V., Stefano, J., Bartel, D. P., & Stoffel, M. (2014). Assessing the ceRNA hypothesis with quantitative measurements of miRNA and target abundance. *Molecular Cell*, *54*(5), 766-776.
- Dobin, A., Davis, C. A., Schlesinger, F., Drenkow, J., Zaleski, C., Jha, S., Batut, P., Chaisson, M., & Gingeras, T. R. (2013). STAR: ultrafast universal RNA-seq aligner. *Bioinformatics (Oxford, England)*, *29*(1), 15-21.
- Drinnenberg, I. A., Weinberg, D. E., Xie, K. T., Mower, J. P., Wolfe, K. H., Fink, G. R., & Bartel, D. P. (2009). RNAi in Budding Yeast. *Science*, *326*(5952), 544-550.
- Dupuis-Sandoval, F., Poirier, M., & Scott, M. S. (2015). The emerging landscape of small nucleolar RNAs in cell biology. *Wiley Interdisciplinary Reviews: RNA*, *6*(4), 381-397.

- Duskova, M., Borovikova, D., Herynkova, P., Rapoport, A., & Sychrova, H. (2015). The role of glycerol transporters in yeast cells in various physiological and stress conditions. *FEMS Microbiology Letters*, *362*(3), 1–8.
- Faghihi, M. A., Modarresi, F., Khalil, A. M., Wood, D. E., Sahagan, B. G., Morgan, T. E., Finch, C. E., St-Laurent, G., Kenny, P. J., & Wahlestedt, C. (2008). Expression of a noncoding RNA is elevated in Alzheimer's disease and drives rapid feed-forward regulation of beta-secretase. *Nature Medicine*, *14*(7), 723–730.
- Faghihi, M. A., Zhang, M., Huang, J., Modarresi, F., van der Brug, M. P., Nalls, M. A., Cookson, M. R., St-Laurent, G., & Wahlestedt, C. (2010). Evidence for natural antisense transcript-mediated inhibition of microRNA function. *Genome Biology*, *11*(5).
- Falk, S., Weir, J. R., Hentschel, J., Reichelt, P., Bonneau, F., & Conti, E. (2014). The Molecular Architecture of the TRAMP Complex Reveals the Organization and Interplay of Its Two Catalytic Activities. *Molecular Cell*, *55*(6), 856–867.
- Fang, S., Zhang, L., Guo, J., Niu, Y., Wu, Y., Li, H., Zhao, L., Li, X., Teng, X., Sun, X., Sun, L., Zhang, M. Q., Chen, R., & Zhao, Y. (2018). NONCODEV5: a comprehensive annotation database for long non-coding RNAs. *Nucleic Acids Research*, *46*(D1), D308–D314.
- Feng, L., Liao, Y. T., He, J. C., Xie, C. L., Chen, S. Y., Fan, H. H., Su, Z. P., & Wang, Z. (2018). Plasma long non-coding RNA BACE1 as a novel biomarker for diagnosis of Alzheimer disease. *BMC Neurology*, *18*(1).
- Fernández-Pevida, A., Kressler, D., & de la Cruz, J. (2015). Processing of preribosomal RNA in *Saccharomyces cerevisiae*. *Wiley Interdisciplinary Reviews: RNA*, *6*(2), 191–209.
- Gadal, O., Strauß, D., Kessl, J., Trumpower, B., Tollervey, D., & Hurt, E. (2001). Nuclear Export of 60S Ribosomal Subunits Depends on Xpo1p and Requires a Nuclear Export Sequence-Containing Factor, Nmd3p, that Associates with the Large Subunit Protein Rpl10p. *Molecular and Cellular Biology*, *21*(10), 3405.
- Geisberg, J. v., Moqtaderi, Z., Fan, X., Oszolak, F., & Struhl, K. (2014). Global analysis of mRNA isoform half-lives reveals stabilizing and destabilizing elements in yeast. *Cell*, *156*(4), 812–824.
- Geisler, S., Lojek, L., Khalil, A. M., Baker, K. E., & Collier, J. (2012). Decapping of Long Noncoding RNAs Regulates Inducible Genes. *Molecular Cell*, *45*(3), 279–291.
- González-Aguilera, C., Tous, C., Babiano, R., de La Cruz, J., Luna, R., & Aguilera, A. (2011). Nab2 functions in the metabolism of RNA driven by polymerases II and III. *Molecular Biology of the Cell*, *22*(15), 2729–2740.
- Goss, D. J., & Kleiman, F. E. (2013). Poly(A) binding proteins: are they all created equal? *Wiley Interdisciplinary Reviews: RNA*, *4*(2), 167–179.
- Granovskaia, M. v., Jensen, L. J., Ritchie, M. E., Toedling, J., Ning, Y., Bork, P., Huber, W., & Steinmetz, L. M. (2010). High-resolution transcription atlas of the mitotic cell cycle in budding yeast. *Genome Biology*, *11*(3).
- Grelet, S., Link, L. A., Howley, B., Obellianne, C., Palanisamy, V., Gangaraju, V. K., Diehl, J. A., & Howe, P. H. (2017). A regulated PNUTS mRNA to lncRNA splice switch mediates EMT and tumour progression. *Nature Cell Biology*, *19*(9), 1105–1115.

- Gromadzka, A. M., Steckelberg, A. L., Singh, K. K., Hofmann, K., & Gehring, N. H. (2016). A short conserved motif in ALYREF directs cap- and EJC-dependent assembly of export complexes on spliced mRNAs. *Nucleic Acids Research*, *44*(5), 2348–2361.
- Grosse, S., Lu, Y.-Y., Coban, I., Neumann, B., & Krebber, H. (2021). Nuclear SR-protein mediated mRNA quality control is continued in cytoplasmic nonsense-mediated decay. <https://doi.org/10.1080/15476286.2020.1851506>, *18*(10), 1390–1407.
- Grünwald, D., & Singer, R. H. (2010). In vivo imaging of labelled endogenous  $\beta$ -actin mRNA during nucleocytoplasmic transport. *Nature* *2010* *467*:7315, *467*(7315), 604–607.
- Guerra-Almeida, D., & Nunes-da-Fonseca, R. (2020). Small Open Reading Frames: How Important Are They for Molecular Evolution? *Frontiers in Genetics*, *11*, 1102.
- Guo, C. J., Ma, X. K., Xing, Y. H., Zheng, C. C., Xu, Y. F., Shan, L., Zhang, J., Wang, S., Wang, Y., Carmichael, G. G., Yang, L., & Chen, L. L. (2020). Distinct Processing of lncRNAs Contributes to Non-conserved Functions in Stem Cells. *Cell*, *181*(3), 621-636.e22.
- Häcker, S., & Krebber, P. (2004). Differential Export Requirements for Shuttling Serine/Arginine-type mRNA-binding Proteins \*. *Journal of Biological Chemistry*, *279*(7), 5049–5052.
- Hackmann, A., Wu, H., Schneider, U. M., Meyer, K., Jung, K., & Krebber, H. (2014). Quality control of spliced mRNAs requires the shuttling SR proteins Gbp2 and Hrb1. *Nature Communications*, *5*, 3123.
- Haimovich, G., Medina, D. A., Causse, S. Z., Garber, M., Millán-Zambrano, G., Barkai, O., Chávez, S., Pérez-Ortín, J. E., Darzacq, X., & Choder, M. (2013). XGene expression is circular: Factors for mRNA degradation also foster mRNA synthesis. *Cell*, *153*(5), 1000–1011.
- He, F., Li, X., Spatrick, P., Casillo, R., Dong, S., & Jacobson, A. (2003). Genome-wide analysis of mRNAs regulated by the nonsense-mediated and 5' to 3' mRNA decay pathways in yeast. *Molecular Cell*, *12*(6), 1439–1452.
- Hedges, J., West, M., & Johnson, A. W. (2005). Release of the export adapter, Nmd3p, from the 60S ribosomal subunit requires Rpl10p and the cytoplasmic GTPase Lsg1p. *The EMBO Journal*, *24*(3), 567–579.
- Hirsch, A. G., Becker, D., Lamping, J. P., & Krebber, H. (2021). Unraveling the stepwise maturation of the yeast telomerase including a Cse1 and Mtr10 mediated quality control checkpoint. *Scientific Reports* *2021* *11*:1, *11*(1), 1–18.
- Ho, B., Baryshnikova, A., Brown Correspondence, G. W., Ch, C., Sh, O. O. O., Oh, H. O., & Brown, G. W. (2017). Unification of Protein Abundance Datasets Yields a Quantitative *Saccharomyces cerevisiae* Proteome Differential regulation Mass Spectrometry GFP-Microscopy TAP-Immunoblot Protein abundance in molecules per cell RNA-seq Stress protein abundance Ribosome profiling Ribosome Protein R N A Tag-affected proteins Stress abundance changes Article Unification of Protein Abundance Datasets Yields a Quantitative *Saccharomyces cerevisiae* Proteome. *Cell Systems*, *6*, 1–14.
- Ho, J. H. N., Kallstrom, G., & Johnson, A. W. (2000). Nmd3p is a Crm1p-dependent adapter protein for nuclear export of the large ribosomal subunit. *The Journal of Cell Biology*, *151*(5), 1057–1066.



- Hocine, S., Singer, R. H., & Grünwald, D. (2010). RNA Processing and Export. *Cold Spring Harbor Perspectives in Biology*, 2(12), a000752.
- Hodge, C. A., Colot, H. v., Stafford, P., & Cole, C. N. (1999). Rat8p/Dbp5p is a shuttling transport factor that interacts with Rat7p/Nup159p and Gle1p and suppresses the mRNA export defect of xpo1-1 cells. *The EMBO Journal*, 18(20), 5778–5788.
- Holmes, R. K., Tuck, A. C., Zhu, C., Dunn-Davies, H. R., Kudla, G., Clauder-Munster, S., Granneman, S., Steinmetz, L. M., Guthrie, C., & Tollervey, D. (2015). Loss of the Yeast SR Protein Npl3 Alters Gene Expression Due to Transcription Readthrough. *PLoS Genetics*, 11(12).
- Hongay, C. F., Grisafi, P. L., Galitski, T., & Fink, G. R. (2006). Antisense Transcription Controls Cell Fate in *Saccharomyces cerevisiae*. *Cell*, 127(4), 735–745.
- Houseley, J., LaCava, J., & Tollervey, D. (2006). RNA-quality control by the exosome. *Nature Reviews Molecular Cell Biology* 2006 7:7, 7(7), 529–539.
- Houseley, J., Rubbi, L., Grunstein, M., Tollervey, D., & Vogelauer, M. (2008). A ncRNA modulates histone modification and mRNA induction in the yeast GAL gene cluster. *Molecular Cell*, 32(5), 685–695.
- Hsin, J. P., & Manley, J. L. (2012). The RNA polymerase II CTD coordinates transcription and RNA processing. *Genes & Development*, 26(19), 2119–2137.
- Huang, Y., & Steitz, J. A. (2005). SRprises along a messenger's journey. *Molecular Cell*, 17(5), 613–615.
- Huarte, M., Guttman, M., Feldser, D., Garber, M., Koziol, M. J., Kenzelmann-Broz, D., Khalil, A. M., Zuk, O., Amit, I., Rabani, M., Attardi, L. D., Regev, A., Lander, E. S., Jacks, T., & Rinn, J. L. (2010). A large intergenic noncoding RNA induced by p53 mediates global gene repression in the p53 response. *Cell*, 142(3), 409–419.
- Huber, F., Bunina, D., Gupta, I., Khmelinskii, A., Meurer, M., Theer, P., Steinmetz, L. M., & Knop, M. (2016). Protein Abundance Control by Non-coding Antisense Transcription. *Cell Reports*, 15(12), 2625–2636.
- Hurt, E., Luo, M. J., Röther, S., Reed, R., & Sträßer, K. (2004). Cotranscriptional recruitment of the serine-arginine-rich (SR)-like proteins Gbp2 and Hrb1 to nascent mRNA via the TREX complex. *Proceedings of the National Academy of Sciences of the United States of America*, 101(7), 1858–1862.
- Hutchinson, J. N., Ensminger, A. W., Clemson, C. M., Lynch, C. R., Lawrence, J. B., & Chess, A. (2007). A screen for nuclear transcripts identifies two linked noncoding RNAs associated with SC35 splicing domains. *BMC Genomics*, 8.
- Hüttenhofer, A., Schattner, P., & Polacek, N. (2005). Non-coding RNAs: hope or hype? *Trends in Genetics : TIG*, 21(5), 289–297.
- Jensen, T. H., Boulay, J., Rosbash, M., & Libri, D. (2001). The DECD box putative ATPase Sub2p is an early mRNA export factor. *Current Biology*, 11(21), 1711–1715.
- Jensen, T. H., Patricio, K., McCarthy, T., & Rosbash, M. (2001). A block to mRNA nuclear export in *S. cerevisiae* leads to hyperadenylation of transcripts that accumulate at the site of transcription. *Molecular Cell*, 7(4), 887–898.
- Ji, X. (2008). The mechanism of RNase III action: how dicer dices. *Current Topics in Microbiology and Immunology*, 320, 99–116.

- Jiang, C., Li, Y., Zhao, Z., Lu, J., Chen, H., Ding, N., Wang, G., Xu, J., & Li, X. (2016). Identifying and functionally characterizing tissue-specific and ubiquitously expressed human lncRNAs. *Oncotarget*, 7(6), 7120.
- Jiao, X., Xiang, S., Oh, C., Martin, C. E., Tong, L., & Kiledjian, M. (2010). Identification of a quality-control mechanism for mRNA 5'-end capping. *Nature* 2010 467:7315, 467(7315), 608–611.
- Johnston, M., Flick, J. S., & Pextont, T. (1994). Multiple mechanisms provide rapid and stringent glucose repression of GAL gene expression in *Saccharomyces cerevisiae*. *Molecular and Cellular Biology*, 14(6), 3834.
- K, I., T, T., PA, T., RD, V., K, M., & I, H. (2002). The Khd1 protein, which has three KH RNA-binding motifs, is required for proper localization of ASH1 mRNA in yeast. *The EMBO Journal*, 21(5), 1158–1167.
- Kapranov, P., Willingham, A. T., & Gingeras, T. R. (2007). Genome-wide transcription and the implications for genomic organization. *Nature Reviews Genetics* 2007 8:6, 8(6), 413–423.
- Kebaara, B. W., & Atkin, A. L. (2009). Long 3'-UTRs target wild-type mRNAs for nonsense-mediated mRNA decay in *Saccharomyces cerevisiae*. *Nucleic Acids Research*, 37(9), 2771.
- Kilchert, C., Wittmann, S., Passoni, M., Shah, S., Granneman, S., & Vasiljeva, L. (2015). Regulation of mRNA Levels by Decay-Promoting Introns that Recruit the Exosome Specificity Factor Mmi1. *Cell Reports*, 13(11), 2504–2515.
- Kim, T., Jeon, Y. J., Cui, R., Lee, J. H., Peng, Y., Kim, S. H., Tili, E., Alder, H., & Croce, C. M. (2015). Role of MYC-regulated long noncoding RNAs in cell cycle regulation and tumorigenesis. *Journal of the National Cancer Institute*, 107(4).
- Kress, T. L., Krogan, N. J., & Guthrie, C. (2008). A Single SR-like Protein, Npl3, Promotes Pre-mRNA Splicing in Budding Yeast. *Molecular Cell*, 32(5), 727–734.
- Kung, J. T. Y., Colognori, D., & Lee, J. T. (2013). Long Noncoding RNAs: Past, Present, and Future. *Genetics*, 193(3), 651.
- Kurosaki, T., Popp, M. W., & Maquat, L. E. (2019). Quality and quantity control of gene expression by nonsense-mediated mRNA decay. *Nature Reviews. Molecular Cell Biology*, 20(7), 406–420.
- LaCava, J., Houseley, J., Saveanu, C., Petfalski, E., Thompson, E., Jacquier, A., & Tollervey, D. (2005). RNA degradation by the exosome is promoted by a nuclear polyadenylation complex. *Cell*, 121(5), 713–724.
- Lahtvee, P.-J., Kumar, R., Hallström, B. M., & Nielsen, J. (2016). Adaptation to different types of stress converge on mitochondrial metabolism. *Molecular Biology of the Cell*, 27(15), 2505–2514.
- Lemay, J. F., Lemieux, C., St-André, O., & Bachand, F. (2010). Crossing the borders: Poly(A)-binding proteins working on both sides of the fence. [Http://Dx.Doi.Org/10.4161/Rna.7.3.11649](http://Dx.Doi.Org/10.4161/Rna.7.3.11649), 7(3), 291–295.
- Lenstra, T. L., Coulon, A., Chow, C. C., & Larson, D. R. (2015). Single-Molecule Imaging Reveals a Switch between Spurious and Functional ncRNA Transcription. *Molecular Cell*, 60(4), 597–610.

- Li, B., Howe, L. A., Anderson, S., Yates, J. R., & Workman, J. L. (2003). The Set2 histone methyltransferase functions through the phosphorylated carboxyl-terminal domain of RNA polymerase II. *The Journal of Biological Chemistry*, 278(11), 8897–8903.
- Li, L., Wang, X., Stolc, V., Li, X., Zhang, D., Su, N., Tongprasit, W., Li, S., Cheng, Z., Wang, J., & Xing, W. D. (2006). Genome-wide transcription analyses in rice using tiling microarrays. *Nature Genetics*, 38(1), 124–129.
- Liao, Y., Smyth, G. K., & Shi, W. (2014). featureCounts: an efficient general purpose program for assigning sequence reads to genomic features. *Bioinformatics (Oxford, England)*, 30(7), 923–930.
- Lindahl, P. A. (2019). A comprehensive mechanistic model of iron metabolism in *Saccharomyces cerevisiae*. *Metallomics : Integrated Biometal Science*, 11(11), 1779–1799.
- Liu, S., Trapnell, C., Institutet, K., Linnarsson Stockholm, S., Craig Venter Institute, J., & Roger Lasken Jolla, L. S. (2016). Single-cell transcriptome sequencing: recent advances and remaining challenges. *F1000Research 2016 5:182*, 5, 182.
- Long, J. C., & Caceres, J. F. (2009). The SR protein family of splicing factors: master regulators of gene expression. *The Biochemical Journal*, 417(1), 15–27.
- Long, R. M., Gu, W., Lorimer, E., Singer, R. H., & Chartrand, P. (2000). She2p is a novel RNA-binding protein that recruits the Myo4p–She3p complex to ASH1 mRNA. *The EMBO Journal*, 19(23), 6592–6601.
- Love, M. I., Huber, W., & Anders, S. (2014). Moderated estimation of fold change and dispersion for RNA-seq data with DESeq2. *Genome Biology*, 15(12), 1–21.
- Lund, M. K., & Guthrie, C. (2005). The DEAD-box protein Dbp5p is required to dissociate Mex67p from exported mRNPs at the nuclear rim. *Molecular Cell*, 20(4), 645–651.
- Lykke-Andersen, J., & Bennett, E. J. (2014). Protecting the proteome: Eukaryotic cotranslational quality control pathways. *The Journal of Cell Biology*, 204(4), 467–476.
- Ma, W. K., Cloutier, S. C., & Tran, E. J. (2013). The DEAD-box protein Dbp2 functions with the RNA-binding protein Yra1 to promote mRNP assembly. *Journal of Molecular Biology*, 425(20), 3824–3838.
- Ma, W. K., Paudel, B. P., Xing, Z., Sabath, I. G., Rueda, D., & Tran, E. J. (2016). Recruitment, Duplex Unwinding and Protein-Mediated Inhibition of the Dead-Box RNA Helicase Dbp2 at Actively Transcribed Chromatin. *Journal of Molecular Biology*, 428(6), 1091–1106.
- Maquat, L. E., & Serin, G. (2001). Nonsense-mediated mRNA decay: insights into mechanism from the cellular abundance of human Upf1, Upf2, Upf3, and Upf3X proteins. *Cold Spring Harbor Symposia on Quantitative Biology*, 66, 313–320.
- Martínez-Lumbreras, S., Taverniti, V., Zorrilla, S., Séraphin, B., & Pérez-Cañadillas, J. M. (2016). Gbp2 interacts with THO/TREX through a novel type of RRM domain. *Nucleic Acids Research*, 44(1), 437–448.
- Martinez-Rucobo, F. W., Kohler, R., van de Waterbeemd, M., Heck, A. J. R., Hemann, M., Herzog, F., Stark, H., & Cramer, P. (2015). Molecular Basis of Transcription-Coupled Pre-mRNA Capping. *Molecular Cell*, 58(6), 1079–1089.

- Mehlin, H., Daneholt, B., & Skoglund, U. (1992). Translocation of a specific pre-messenger ribonucleoprotein particle through the nuclear pore studied with electron microscope tomography. *Cell*, *69*(4), 605–613.
- Melé, M., Mattioli, K., Mallard, W., Shechner, D. M., Gerhardinger, C., & Rinn, J. L. (2017). Chromatin environment, transcriptional regulation, and splicing distinguish lincRNAs and mRNAs. *Genome Research*, *27*(1), 27–37.
- Milkereit, P., Strauss, D., Bassler, J., Gadad, O., Kühn, H., Schütz, S., Gas, N., Lechner, J., Hurt, E., & Tschöchner, H. (2003). A Noc Complex Specifically Involved in the Formation and Nuclear Export of Ribosomal 40 S Subunits \*. *Journal of Biological Chemistry*, *278*(6), 4072–4081.
- Miller, C., Schwalb, B., Maier, K., Schulz, D., Dümcke, S., Zacher, B., Mayer, A., Sydow, J., Marcinowski, L., Dölken, L., Martin, D. E., Tresch, A., & Cramer, P. (2011). Dynamic transcriptome analysis measures rates of mRNA synthesis and decay in yeast. *Molecular Systems Biology*, *7*(458).
- Murtha, K., Hwang, M., Peccarelli, M. C., Scott, T. D., & Kebaara, B. W. (2019). The nonsense-mediated mRNA decay (NMD) pathway differentially regulates COX17, COX19 and COX23 mRNAs. *Current Genetics*, *65*(2), 507–521.
- Nadal-Ribelles, M., Conde, N., Flores, O., González-Vallinas, J., Eyra, E., Orozco, M., de Nadal, E., & Posas, F. (2012). Hog1 bypasses stress-mediated down-regulation of transcription by RNA polymerase II redistribution and chromatin remodeling. *Genome Biology*, *13*(11), 1–11.
- Nadal-Ribelles, M., Solé, C., Xu, Z., Steinmetz, L. M., deNadal, E., & Posas, F. (2014). Control of Cdc28 CDK1 by a Stress-Induced lncRNA. *Molecular Cell*, *53*(4), 549–561.
- Nagalakshmi, U., Wang, Z., Waern, K., Shou, C., Raha, D., Gerstein, M., & Snyder, M. (2008). The transcriptional landscape of the yeast genome defined by RNA sequencing. *Science (New York, N.Y.)*, *320*(5881), 1344–1349.
- Niño, C. A., Hérisant, L., Babour, A., & Dargemont, C. (2013). mRNA nuclear export in yeast. *Chemical Reviews*, *113*(11), 8523–8545.
- Ohno, S. (1972). So much “junk” DNA in our genome. *Brookhaven Symp Biol.*, *23*, 366–370.
- Peccarelli, M., & Kebaara, B. W. (2014). Measurement of mRNA decay rates in *Saccharomyces cerevisiae* using *rpb1-1* strains. *Journal of Visualized Experiments*, *94*, 52240.
- Peccarelli, M., Scott, T. D., & Kebaara, B. W. (2019). Nonsense-mediated mRNA decay of the ferric and cupric reductase mRNAs FRE1 and FRE2 in *Saccharomyces cerevisiae*. *FEBS Letters*, *593*(22), 3228–3238.
- Peccarelli, M., Scott, T. D., Steele, M., & Kebaara, B. W. (2016). mRNAs involved in copper homeostasis are regulated by the nonsense-mediated mRNA decay pathway depending on environmental conditions. *Fungal Genetics and Biology : FG & B*, *86*, 81–90.
- Pelechano, V., & Steinmetz, L. M. (2013). Gene regulation by antisense transcription. *Nature Reviews Genetics* *2013 14:12*, *14*(12), 880–893.
- Pintacuda, G., Wei, G., Roustan, C., Kirmizitas, B. A., Solcan, N., Cerase, A., Castello, A., Mohammed, S., Moindrot, B., Nesterova, T. B., & Brockdorff, N. (2017). hnRNP

- Recruits PCGF3/5-PRC1 to the Xist RNA B-Repeat to Establish Polycomb-Mediated Chromosomal Silencing. *Molecular Cell*, 68(5), 955-969.e10.
- Porrúa, O., & Libri, D. (2013). RNA quality control in the nucleus: The Angels' share of RNA. *Biochimica et Biophysica Acta (BBA) - Gene Regulatory Mechanisms*, 1829(6–7), 604–611.
- Porrúa, O., & Libri, D. (2015). Transcription termination and the control of the transcriptome: why, where and how to stop. *Nature Reviews. Molecular Cell Biology*, 16(3), 190–202.
- Portman, D. S., O'Connor, J. P., & Dreyfuss, G. (1997). YRA1, an essential *Saccharomyces cerevisiae* gene, encodes a novel nuclear protein with RNA annealing activity. *RNA*, 3(5), 527. /pmc/articles/PMC1369502/?report=abstract
- Preker, P., Nielsen, J., Kammler, S., Lykke-Andersen, S., Christensen, M. S., Mapendano, C. K., Schierup, M. H., & Jensen, T. H. (2008). RNA exosome depletion reveals transcription upstream of active human promoters. *Science (New York, N.Y.)*, 322(5909), 1851–1854.
- Presnyak, V., Alhusaini, N., Chen, Y. H., Martin, S., Morris, N., Kline, N., Olson, S., Weinberg, D., Baker, K. E., Graveley, B. R., & Collier, J. (2015). Codon optimality is a major determinant of mRNA stability. *Cell*, 160(6), 1111–1124.
- Proft, M., & Struhl, K. (2004). MAP kinase-mediated stress relief that precedes and regulates the timing of transcriptional induction. *Cell*, 118(3), 351–361.
- Pueyo, J. I., & Couso, J. P. (2008). The 11-aminoacid long Tarsal-less peptides trigger a cell signal in *Drosophila* leg development. *Developmental Biology*, 324(2), 192–201.
- Putnam, A. A., & Jankowsky, E. (2013). DEAD-box helicases as integrators of RNA, nucleotide and protein binding. *Biochimica et Biophysica Acta*, 1829(8), 884–893.
- Quinlan, A. R., & Hall, I. M. (2010). BEDTools: a flexible suite of utilities for comparing genomic features. *Bioinformatics (Oxford, England)*, 26(6), 841–842.
- Quinn, J. J., Zhang, Q. C., Georgiev, P., Ilik, I. A., Akhtar, A., & Chang, H. Y. (2016). Rapid evolutionary turnover underlies conserved lncRNA–genome interactions. *Genes & Development*, 30(2), 191–207.
- Quinodoz, S., & Guttman, M. (2014). Long noncoding RNAs: An emerging link between gene regulation and nuclear organization. *Trends in Cell Biology*, 24(11), 651–663.
- Ramos-Alonso, L., Romero, A. M., Martínez-Pastor, M. T., & Puig, S. (2020). Iron Regulatory Mechanisms in *Saccharomyces cerevisiae*. *Frontiers in Microbiology*, 11, 2222.
- Roberts, C. J., Nelson, B., Marton, M. J., Stoughton, R., Meyer, M. R., Bennett, H. A., He, Y. D., Dai, H., Walker, W. L., Hughes, T. R., Tyers, M., Boone, C., & Friend, S. H. (2000). Signaling and circuitry of multiple MAPK pathways revealed by a matrix of global gene expression profiles. *Science (New York, N.Y.)*, 287(5454), 873–880.
- Rodríguez-Navarro, S., Sträßer, K., & Hurt, E. (2002). An intron in the YRA1 gene is required to control Yra1 protein expression and mRNA export in yeast. *EMBO Reports*, 3(5), 438.
- Rose, M. D., Winston, F. M., & Heiter, P. (1990). *Methods in yeast genetics: a laboratory course manual*.
- Rutherford, J. C., Jaron, S., & Winge, D. R. (2003). Aft1p and Aft2p mediate iron-responsive gene expression in yeast through related promoter elements. *The Journal of Biological Chemistry*, 278(30), 27636–27643.

- Saito, H., & Posas, F. (2012). Response to hyperosmotic stress. *Genetics*, *192*(2), 289–318.
- Schein, A., Zucchelli, S., Kauppinen, S., Gustincich, S., & Carninci, P. (2016). Identification of antisense long noncoding RNAs that function as SINEUPs in human cells. *Scientific Reports* *2016* *6*:1, *6*(1), 1–8.
- Schmid, M., Olszewski, P., Pelechano, V., Gupta, I., Steinmetz, L. M., & Jensen, T. H. (2015). The Nuclear PolyA-Binding Protein Nab2p Is Essential for mRNA Production. *Cell Reports*, *12*(1), 128–139.
- Schonborn, J., Oberstraß, J., Breyel, E., Tittgen, J., Schumacher, J., & Lukacs, N. (1991). Monoclonal antibodies to double-stranded RNA as probes of RNA structure in crude nucleic acid extracts. *Nucleic Acids Research*, *19*(11), 2993.
- Schulz, D., Schwalb, B., Kiesel, A., Baejen, C., Torkler, P., Gagneur, J., Soeding, J., & Cramer, P. (2013). Transcriptome surveillance by selective termination of noncoding RNA synthesis. *Cell*, *155*(5), 1075.
- Schwer, B., Mao, X., & Shuman, S. (1998). Accelerated mRNA decay in conditional mutants of yeast mRNA capping enzyme. *Nucleic Acids Research*, *26*(9), 2050–2057.
- Segref, A., Sharma, K., Doye, V., Hellwig, A., Huber, J., Lührmann, R., & Hurt, E. (1997). Mex67p, a novel factor for nuclear mRNA export, binds to both poly(A)<sup>+</sup> RNA and nuclear pores. *The EMBO Journal*, *16*(11), 3256–3271.
- Shen, E. C., Stage-Zimmermann, T., Chui, P., & Silver, P. A. (2000). The Yeast mRNA-binding Protein Npl3p Interacts with the Cap-binding Complex \*. *Journal of Biological Chemistry*, *275*(31), 23718–23724.
- Sherman, F., & Hicks, J. (1991). Micromanipulation and dissection of asci. *Methods in Enzymology*, *194*(C), 21–37.
- Sickmann, A., Reinders, J., Wagner, Y., Joppich, C., Zahedi, R., Meyer, H. E., Schönfisch, B., Perschil, I., Chacinska, A., Guiard, B., Rehling, P., Pfanner, N., & Meisinger, C. (2003). The proteome of *Saccharomyces cerevisiae* mitochondria. *Proceedings of the National Academy of Sciences of the United States of America*, *100*(23), 13207–13212.
- Sigel, A., & Sigel, H. (1998). Metal ions in biological systems, volume 35: iron transport and storage microorganisms, plants, and animals. *Metal-Based Drugs*, *5*(5), 262–262.
- Sikorski, R. S., & Hieter, P. (1989). A system of shuttle vectors and yeast host strains designed for efficient manipulation of DNA in *Saccharomyces cerevisiae*. *Genetics*, *122*(1), 19–27.
- Simone, R., Javad, F., Emmett, W., Wilkins, O. G., Almeida, F. L., Barahona-Torres, N., Zareba-Paslawska, J., Ehteramy, M., Zuccotti, P., Modelska, A., Siva, K., Viridi, G. S., Mitchell, J. S., Harley, J., Kay, V. A., Hondhamuni, G., Trabzuni, D., Ryten, M., Wray, S., ... de Silva, R. (2021). MIR-NATs repress MAPT translation and aid proteostasis in neurodegeneration. *Nature* *2021* *594*:7861, *594*(7861), 117–123.
- Sinturel, F., Navickas, A., Wery, M., Descrimes, M., Morillon, A., Torchet, C., & Benard, L. (2015). Cytoplasmic Control of Sense-Antisense mRNA Pairs. *Cell Reports*, *12*(11), 1853–1864.
- Slack, F. J., & Chinnaiyan, A. M. (2019). The Role of Non-coding RNAs in Oncology. *Cell*, *179*(5), 1033–1055.
- Smith, C., Lari, A., Derrer, C. P., Ouwehand, A., Rossouw, A., Huisman, M., Dange, T., Hopman, M., Joseph, A., Zenklusen, D., Weis, K., Grunwald, D., & Montpetit, B. (2015).

- In vivo single-particle imaging of nuclear mRNA export in budding yeast demonstrates an essential role for Mex67p. *Journal of Cell Biology*, 211(6), 1121–1130.
- Smith, J. E., Alvarez-Dominguez, J. R., Kline, N., Huynh, N. J., Geisler, S., Hu, W., Coller, J., & Baker, K. E. (2014). Translation of Small Open Reading Frames within Unannotated RNA Transcripts in *Saccharomyces cerevisiae*. *Cell Reports*, 7(6), 1858–1866.
- Soheilypour, M., & Mofrad, M. R. K. (2018). Quality control of mRNAs at the entry of the nuclear pore: Cooperation in a complex molecular system. <https://doi.org/10.1080/19491034.2018.1439304>, 9(1), 202–211.
- Spingola, M., Grate, L., Haussler, D., & Manuel, A. (1999). Genome-wide bioinformatic and molecular analysis of introns in *Saccharomyces cerevisiae*. *RNA (New York, N.Y.)*, 5(2), 221–234.
- Stamm, S. (2008). Regulation of alternative splicing by reversible protein phosphorylation. *Journal of Biological Chemistry*, 283(3), 1223–1227.
- Statello, L., Guo, C. J., Chen, L. L., & Huarte, M. (2020). Gene regulation by long non-coding RNAs and its biological functions. *Nature Reviews Molecular Cell Biology* 2020 22:2, 22(2), 96–118.
- Stearman, R., Yuan, D. S., Yamaguchi-Iwai, Y., Klausner, R. D., & Dancis, A. (1996). A permease-oxidase complex involved in high-affinity iron uptake in yeast. *Science (New York, N.Y.)*, 271(5255), 1552–1557.
- Steinmetz, E. J., Conrad, N. K., Brow, D. A., & Corden, J. L. (2001). RNA-binding protein Nrd1 directs poly(A)-independent 3'-end formation of RNA polymerase II transcripts. *Nature*, 413(6853), 327–331.
- Stolc, V., Gauhar, Z., Mason, C., Halasz, G., van Batenburg, M. F., Rifkin, S. A., Hua, S., Herreman, T., Tongprasit, W., Barbano, P. E., Bussemaker, H. J., & White, K. P. (2004). A gene expression map for the euchromatic genome of *Drosophila melanogaster*. *Science (New York, N.Y.)*, 306(5696), 655–660.
- Struhl, K. (2007). Transcriptional noise and the fidelity of initiation by RNA polymerase II. *Nature Structural & Molecular Biology*, 14(2), 103–105.
- Sun, M., Schwalb, B., Pirkl, N., Maier, K. C., Schenk, A., Failmezger, H., Tresch, A., & Cramer, P. (2013). Global analysis of Eukaryotic mRNA degradation reveals Xrn1-dependent buffering of transcript levels. *Molecular Cell*, 52(1), 52–62.
- Szachnowski, U., Andus, S., Foretek, D., Morillon, A., & Wery, M. (2019). Endogenous RNAi pathway evolutionarily shapes the destiny of the antisense lncRNAs transcriptome. *Life Science Alliance*, 2(5), 1–12.
- Tran, E. J., Zhou, Y., Corbett, A. H., & Wenthe, S. R. (2007). The DEAD-box protein Dbp5 controls mRNA export by triggering specific RNA:protein remodeling events. *Molecular Cell*, 28(5), 850–859.
- Traven, A., Jelicic, B., & Sopta, M. (2006). Yeast Gal4: a transcriptional paradigm revisited. *EMBO Reports*, 7(5), 496–499.
- Tripathi, V., Ellis, J. D., Shen, Z., Song, D. Y., Pan, Q., Watt, A. T., Freier, S. M., Bennett, C. F., Sharma, A., Bubulya, P. A., Blencowe, B. J., Prasanth, S. G., & Prasanth, K. v. (2010a). The nuclear-retained noncoding RNA MALAT1 regulates alternative splicing by modulating SR splicing factor phosphorylation. *Molecular Cell*, 39(6), 925–938.

- Tripathi, V., Ellis, J. D., Shen, Z., Song, D. Y., Pan, Q., Watt, A. T., Freier, S. M., Bennett, C. F., Sharma, A., Bubulya, P. A., Blencowe, B. J., Prasanth, S. G., & Prasanth, K. v. (2010b). The nuclear-retained noncoding RNA MALAT1 regulates alternative splicing by modulating SR splicing factor phosphorylation. *Molecular Cell*, *39*(6), 925–938.
- Tuck, A. C., & Tollervey, D. (2013). A transcriptome-wide atlas of RNP composition reveals diverse classes of mRNAs and lncRNAs. *Cell*, *154*(5), 996–1009.
- Tudek, A., Schmid, M., Makaras, M., Barrass, J. D., Beggs, J. D., & Jensen, T. H. (2018). A Nuclear Export Block Triggers the Decay of Newly Synthesized Polyadenylated RNA. *Cell Reports*, *24*(9), 2457–2467.e7.
- Tutucci, E., & Stutz, F. (2011). Keeping mRNPs in check during assembly and nuclear export. *Nature Reviews Molecular Cell Biology* 2011 12:6, *12*(6), 377–384.
- Uszczynska-Ratajczak, B., Lagarde, J., Frankish, A., Guigó, R., & Johnson, R. (2018). Towards a complete map of the human long non-coding RNA transcriptome. *Nature Reviews Genetics* 2018 19:9, *19*(9), 535–548.
- Vadkertiová, R., Molnárová, J., Vránová, D., & Sláviková, E. (2012). Yeasts and yeast-like organisms associated with fruits and blossoms of different fruit trees. *Canadian Journal of Microbiology*, *58*(12), 1344–1352.
- van Dijk, E. L., Chen, C. L., Daubenton-Carafa, Y., Gourvennec, S., Kwapisz, M., Roche, V., Bertrand, C., Silvain, M., Legoix-Ne, P., Loeillet, S., Nicolas, A., Thermes, C., & Morillon, A. (2011). XUTs are a class of Xrn1-sensitive antisense regulatory non-coding RNA in yeast. *Nature*, *475*(7354), 114–119.
- van Heesch, S., van Iterson, M., Jacobi, J., Boymans, S., Essers, P. B., de Bruijn, E., Hao, W., MacInnes, A. W., Cuppen, E., & Simonis, M. (2014). Extensive localization of long noncoding RNAs to the cytosol and mono- and polyribosomal complexes. *Genome Biology*, *15*(1).
- Vargas, D. Y., Raj, A., Marras, S. A. E., Kramer, F. R., & Tyagi, S. (2005). Mechanism of mRNA transport in the nucleus. *Proceedings of the National Academy of Sciences of the United States of America*, *102*(47), 17008–17013.
- Venkatesh, S., Li, H., Gogol, M. M., & Workman, J. L. (2016). Selective suppression of antisense transcription by Set2-mediated H3K36 methylation. *Nature Communications*, *7*(1), 1–14.
- Villegas, V. E., & Zaphiropoulos, P. G. (2015). Neighboring gene regulation by antisense long Non-Coding RNAs. *International Journal of Molecular Sciences*, *16*(2), 3251–3266.
- Visa, N., Izaurralde, E., Ferreira, J., Daneholt, B., & Mattaj, I. W. (1996). A nuclear cap-binding complex binds Balbiani ring pre-mRNA cotranscriptionally and accompanies the ribonucleoprotein particle during nuclear export. *The Journal of Cell Biology*, *133*(1), 5–14.
- Wahl, M. C., Will, C. L., & Lührmann, R. (2009). The spliceosome: design principles of a dynamic RNP machine. *Cell*, *136*(4), 701–718.
- Wang, Y., Li, D., Lu, J., Chen, L., Zhang, S., Qi, W., Li, W., & Xu, H. (2020). Long noncoding RNA TTN-AS1 facilitates tumorigenesis and metastasis by maintaining TTN expression in skin cutaneous melanoma. *Cell Death and Disease*, *11*(8), 1–13.



- Wei, C. W., Luo, T., Zou, S. S., & Wu, A. S. (2018). The Role of Long Noncoding RNAs in Central Nervous System and Neurodegenerative Diseases. *Frontiers in Behavioral Neuroscience*, *12*, 175.
- Wente, S. R., & Rout, M. P. (2010). The nuclear pore complex and nuclear transport. *Cold Spring Harbor Perspectives in Biology*, *2*(10).
- Wery, M., Describes, M., Vogt, N., Dallongeville, A. S., Gautheret, D., & Morillon, A. (2016). Nonsense-Mediated Decay Restricts LncRNA Levels in Yeast Unless Blocked by Double-Stranded RNA Structure. *Molecular Cell*, *61*(3), 379–392.
- Windgassen, M., Sturm, D., Cajigas, I. J., González, C. I., Sedorf, M., Bastians, H., & Krebber, H. (2004). Yeast Shuttling SR Proteins Npl3p, Gbp2p, and Hrb1p Are Part of the Translating mRNPs, and Npl3p Can Function as a Translational Repressor. *Molecular and Cellular Biology*, *24*(23), 10479–10491.
- Wong, C. M., Tang, H. M. V., Kong, K. Y. E., Wong, G. W. O., Qiu, H., Jin, D. Y., & Hinnebusch, A. G. (2010). Yeast arginine methyltransferase Hmt1p regulates transcription elongation and termination by methylating Npl3p. *Nucleic Acids Research*, *38*(7), 2217–2228.
- Wu, H., Becker, D., & Krebber, H. (2014). Telomerase RNA TLC1 shuttling to the cytoplasm requires mRNA export factors and is important for telomere maintenance. *Cell Reports*, *8*(6), 1630–1638.
- Wutz, A., Rasmussen, T. P., & Jaenisch, R. (2002). Chromosomal silencing and localization are mediated by different domains of Xist RNA. *Nature Genetics* *2002* *30*:2, *30*(2), 167–174.
- Wyers, F., Rougemaille, M., Badis, G., Rousselle, J. C., Dufour, M. E., Boulay, J., Régnault, B., Devaux, F., Namane, A., Séraphin, B., Libri, D., & Jacquier, A. (2005). Cryptic Pol II transcripts are degraded by a nuclear quality control pathway involving a new poly(A) polymerase. *Cell*, *121*(5), 725–737.
- Xie, B., Becker, E., Stuparevic, I., Wery, M., Szachnowski, U., Morillon, A., & Primig, M. (2019). The anti-cancer drug 5-fluorouracil affects cell cycle regulators and potential regulatory long non-coding RNAs in yeast. *RNA Biology*, *16*(6), 727–741.
- Xu, Z., Wei, W., Gagneur, J., Clauder-Münster, S., Smolik, M., Huber, W., & Steinmetz, L. M. (2011). Antisense expression increases gene expression variability and locus interdependency. *Molecular Systems Biology*, *7*(1), 468.
- Xu, Z., Wei, W., Gagneur, J., Perocchi, F., Clauder-Münster, S., Camblong, J., Guffanti, E., Stutz, F., Huber, W., & Steinmetz, L. M. (2009). Bidirectional promoters generate pervasive transcription in yeast. *Nature*, *457*(7232), 1033–1037.
- Yamazaki, T., Souquere, S., Chujo, T., Kobelke, S., Chong, Y. S., Fox, A. H., Bond, C. S., Nakagawa, S., Pierron, G., & Hirose, T. (2018). Functional Domains of NEAT1 Architectural lncRNA Induce Paraspeckle Assembly through Phase Separation. *Molecular Cell*, *70*(6), 1038-1053.e7.
- Yassour, M., Pfiffner, J., Levin, J. Z., Adiconis, X., Gnirke, A., Nusbaum, C., Thompson, D. A., Friedman, N., & Regev, A. (2010). Strand-specific RNA sequencing reveals extensive regulated long antisense transcripts that are conserved across yeast species. *Genome Biology*, *11*(8).

- Yun, C. W., Bauler, M., Moore, R. E., Klebba, P. E., & Philpott, C. C. (2001). The Role of the FRE Family of Plasma Membrane Reductases in the Uptake of Siderophore-Iron in *Saccharomyces cerevisiae*. *Journal of Biological Chemistry*, 276(13), 10218–10223.
- Zaman, S., Lippman, S. I., Zhao, X., & Broach, J. R. (2008). How *Saccharomyces* responds to nutrients. *Annual Review of Genetics*, 42, 27–81.
- Zander, G., Hackmann, A., Bender, L., Becker, D., Lingner, T., Salinas, G., & Krebber, H. (2016). mRNA quality control is bypassed for immediate export of stress-responsive transcripts. *Nature*, 540(7634), 593–596.
- Zenklusen, D., Vinciguerra, P., Wyss, J.-C., & Stutz, F. (2002). Stable mRNP Formation and Export Require Cotranscriptional Recruitment of the mRNA Export Factors Yra1p and Sub2p by Hpr1p. *Molecular and Cellular Biology*, 22(23), 8241–8253.
- Zhou, H., & Winston, F. (2001). NRG1 is required for glucose repression of the SUC2 and GAL genes of *Saccharomyces cerevisiae*. *BMC Genetics*, 2(5), 5.  
<http://www.biomedcentral.com/1471-2156/2/5>
- Zucchelli, S., Cotella, D., Takahashi, H., Carrieri, C., Cimatti, L., Fasolo, F., Jones, M. H., Sblattero, D., Sanges, R., Santoro, C., Persichetti, F., Carninci, P., & Gustincich, S. (2015). SINEUPs: A new class of natural and synthetic antisense long non-coding RNAs that activate translation. *RNA Biology*, 12(8), 771–779.
- Zuckerman, B., Ron, M., Mikl, M., Segal, E., & Ulitsky, I. (2020). Gene Architecture and Sequence Composition Underpin Selective Dependency of Nuclear Export of Long RNAs on NXF1 and the TREX Complex. *Molecular Cell*, 79(2), 251-267.e6.
- Zuckerman, B., & Ulitsky, I. (2019). Predictive models of subcellular localization of long RNAs. *RNA*, 25(5), rna.068288.118.

## 8. Acknowledgement - Danksagung

An dieser Stelle will ich mich gerne bei allen bedanken, die zum Gelingen dieser Arbeit beigetragen haben und mich über den Zeitraum der letzten vier Jahre unterstützt haben.

Vor allem danke ich Prof. Dr. Heike Krebber, die mir ermöglicht hat an diesem spannenden Thema zu arbeiten. Zum einen danke ich ihr für die Freiräume zur Verfolgung eigener Interessen und damit verbunden für das Vertrauen und die anregenden Diskussionen. Zum anderen danke ich ihr dafür, mir immer wieder den roten Faden dieser Arbeit in die Hand gedrückt zu haben, der mich zu einem erfolgreichen Abschluss geführt hat. Weiterhin bedanke ich mich bei den Mitgliedern meines *Thesis Committees* Prof. Dr. Jörg Großhans und Prof. Dr. Ralf Ficner, die mich mit wertvollen Ratschlägen begleitet haben.

Außerdem möchte ich mich bei den aktuellen und ehemaligen Mitgliedern der AG Krebber und AG Bastians für eine unterstützende und angenehme Arbeitsatmosphäre bedanken. Für die Zusammenarbeit und einen Beitrag zu dieser Arbeit bedanke ich mich herzlich bei Anna Greta Hirsch. Ihr anfänglicher Beitrag war eine große Hilfe für den weiteren Verlauf meiner Arbeit. Ebenso danke ich auch Judith Aylin Weyergraf und Sarah Wasilewski für die großartige Zusammenarbeit. Außerdem danke ich Dr. Wilfried Kramer für seine kritischen Fragen und Anekdoten beim Mittagessen. Besonders will ich mich noch für die schöne Zeit innerhalb und außerhalb des Labors bedanken, bei allen die daran mitgewirkt haben.

Für das Korrekturlesen dieser Arbeit bedanke ich mich bei Prof. Dr. Heike Krebber, Anna Greta Hirsch, Jan-Phillip Lamping, Theresa Binder, Anne-Sophie Lindemann, Markus Röder und Sarah Wasilewski.

Zu guter Letzt bedanke ich mich bei meiner Familie und Freunden für die durchgehende Unterstützung und die schönen Erlebnisse in dieser Zeit. Ganz besonderer Dank gilt dabei meiner Mutter Ingrid und meiner Schwester Alev!

## 9. Curriculum Vitae

### Personal Information

Name	Cesur Ivo Coban
Date of birth	15.01.1989
Place of birth	Berlin

### Education and training

Dates	October 2017 – present
Position	PhD student in the group of Prof. Dr. Heike Krebber, department of Molecular Genetics, Institute for Microbiology and Genetics
Name and type of Organization	Georg-August University Göttingen
Dates	April 2013 – March 2015
Title of qualification awarded	Master of Science “Biology”
	Master thesis in the group of Prof. Dr. Gerd Technau, Department of Developmental Neurobiology
	“Creating a link between embryonic and postembryonic neuroblast lineages in the VNS of <i>Drosophila melanogaster</i> ”
Name and type of Organization	Johannes Gutenberg – University Mainz
Dates	April 2009 – March 2013
Title of qualification awarded	Bachelor of Science „Biology“
	Bachelor thesis in the group of Prof. Dr. Gerd Technau, Department of Developmental Neurobiology
	“Localisation of a <i>Antennapedia</i> -mutation in <i>Drosophila melanogaster</i> with the help of complementation analysis”
Name and type of Organization	Johannes Gutenberg – University Mainz
Dates	October 2008 – March 2009
Title of qualification awarded	Bachelor of Science „Naturwissenschaften in der Informationsgesellschaft“
Name and type of Organization	Technical University of Berlin
Dates	August 2001 – June 2008
Title of qualification awarded	German “Abitur“(equivalent of “A” Levels)
Name and type of Organization	Sophie-Charlotte-Oberschule Berlin